

Aus der Medizinischen Klinik und Poliklinik IV
Klinik der Ludwig-Maximilians-Universität München
Direktor: Prof. Dr. med. Martin Reincke

**Extracellular DNA contributes to
cholesterol crystal embolism-induced clot formation,
acute kidney injury, and tissue infarction**

Dissertation
zum Erwerb des Doktorgrades der Humanbiologie
an der Medizinischen Fakultät der
Ludwig-Maximilians-Universität München

vorgelegt von
Chongxu Shi
aus Henan, China
2021

**Mit Genehmigung der Medizinischen Fakultät
der Universität München**

Berichterstatter: Prof. Dr. med. Hans-Joachim Anders

Mitberichterstatter: Prof. Dr. med. Susanna Hofmann

Prof. Dr. med. Federico Tatò

Prof. Dr. med. Peter Weyrich

Dekan: Prof. Dr. med. dent. Reinhard Hickel

Tag der mündlichen Prüfung: 20.04.2021

Contents

Declaration	iii
Zusammenfassung	iv
Summary	vii
1. Introduction	1
1.1 Cholesterol crystal embolism	1
1.1.1 Pathophysiology of cholesterol crystal embolism.....	3
1.1.2 Cholesterol crystal embolism in the kidney	4
1.2 Acute kidney injury and acute kidney disease	8
1.2.1 The pathophysiology of ischemic AKI.....	11
1.2.2 Therapies for acute kidney injury.....	18
1.3 Kidney infarction	20
2. Research hypotheses	22
3. Material and methods	23
3.1 Materials.....	23
3.2 Experimental procedures	28
3.2.1 Animals	28
3.2.2 Animal models.....	28
3.2.3 Basic experimental design of the cholesterol crystal-induced AKI model	29
3.3 Preparing of cholesterol crystal stock solution	35
3.4 Primary and secondary endpoints.....	35
3.5 Immunostainings	36
3.6 Periodic acid Schiff (PAS) staining	37
3.6.1 PAS staining for kidney injury scoring	37
3.7 Feulgen staining and TUNEL staining	38
3.8 Immunohistochemistry in human tissue.....	38
3.9 Micro-computed tomography (μ CT) imaging.....	38
3.10 Flow cytometry.....	39
3.11 In vitro studies	39
3.11.1 Human neutrophil isolation	39
3.11.2 Formation of the neutrophil extracellular trap (NET) and cell death	39
3.11.3 Human and mouse endothelial cell culture	40
3.11.4 Endothelial cell death detection and extracellular DNA quantification.....	40
3.11.5 Confocal imaging	41
3.11.6 Human platelet studies	41

3.12 Statistical analysis.....	42
4. Results	43
4.1 A new mouse model of cholesterol crystal-embolism.....	43
4.1.1 Cholesterol crystal injection-induced acute kidney failure and kidney infarction.....	43
4.1.2 Crystal clots-induced kidney injury, inflammation and vascular injury at 24 h.....	44
4.1.3 Crystal clots obstruct intrarenal arteries at 24 h.....	47
4.1.4 Time-dependent intravascular crystal clot formation.....	48
4.1.5 The influence of gender on cholesterol crystal embolism.....	50
4.1.6 Cholesterol crystal embolism-induced acute kidney disease.....	52
4.2 Role of plasmatic coagulation in crystal clot formation.....	53
4.3 Role of platelets in crystal clot formation.....	57
4.4 Role of neutrophils in crystal clots formation.....	59
4.5 Role of necroinflammation in CCE-induced kidney injury.....	63
4.5.1 Necroptosis inhibition improved CCE-related kidney infarction but not AKI.....	64
4.5.2 Inflammasome inhibition protected from CCE-related kidney infarction but not AKI.....	66
4.6 Role of extracellular DNA in crystal clots formation.....	68
4.7.1 Recombinant DNase I inhibited CC injection-mediated pathological processes in the kidney by preventing crystal clot formation.....	69
4.7.2 In vitro studies to identify the origin of extracellular DNA.....	70
4.8 A two-step strategy to prevent CCE-related outcomes.....	73
4.8.1 The window of opportunity to improve CCE-related outcomes by DNase I.....	73
4.8.2 Nec-1s combined with DNase I treatment prevents CCE-related outcomes.....	75
5. Discussion	78
6. References	88
7. Abbreviations	108
8. Acknowledgement	109

Declaration

Hereby I declare that all of the present work embodied in this thesis was carried out by myself from 12/2016 until 02/2020 under the supervision of Prof. Dr. Hans Joachim Anders, Nephrologisches Zentrum, Medizinische Klinik und Poliklinik IV, Innenstadt Klinikum der Universität München. This work has not been submitted in part or full to any other university or institute for any degree or diploma.

Part of the work was supported by others, as follows:

Prof. Dr. Peter Boor and Prof. Twan Lammers, RWTH Aachen University Hospital, Germany, and their teams helped with the *ex vivo* studies of 3D- μ CT to show CCE-induced vascular rarefaction and obstruction in mouse kidney. The data are presented in the results part section 4.1 of this thesis.

Prof. Paola Romagnani, University of Florence, Italy, and her team performed the 3D *in vitro* studies of cholesterol crystal-stimulated DNA release and cell death of HUVEC. The data are presented in the results part section 4.7.2 of this thesis.

Parts of this work were accepted for publication in the journal of Circulation Research (2020 Feb 24. doi: 10.1161/CIRCRESAHA.119.315625).

Date:

Signature:

Place: Munich, Germany

Chongxu Shi

Zusammenfassung

Atherosklerose ist weltweit eine der Hauptursachen für Morbidität und Mortalität. Bei fortgeschrittener Atherosklerose ist die Cholesterinkristallembolie (CCE) eine potenziell lebensbedrohliche Komplikation mit einer durchschnittlichen Mortalität von 62,8%. Autopsien oder Gewebebiopsien zeigen Cholesterinkristalle (CC) im arteriellen Lumen, umgeben von einer fibrotischen Matrix, die das Gefäßlumen verschließt. Über die genauen zellulären und molekularen Mechanismen nach CCE ist wenig bekannt, was teilweise auf das Fehlen eines Tiermodells zurückzuführen ist. Wir stellten daher die Hypothese auf, dass die Entwicklung eines reproduzierbaren Mausmodells der CCE zur Nachahmung der morphologischen und funktionellen Eigenschaften der CCE beim Menschen dazu beitragen würde, die molekularen Mechanismen des CC-gesteuerten arteriellen Verschlusses, des Gewebeinfarkts und des Organversagens zu untersuchen.

CCE wurden in C57BL/6J-Mäusen durch Injektion von CC über einen minimal-invasiven Eingriff in die linke Nierenarterie induziert. Primärer Endpunkt war die glomeruläre Filtrationsrate (GFR), die am wachen und frei beweglichen Tier gemessen wurde, um den Abfall der exkretorischen Nierenfunktion als Marker eines akuten Nierenversagens zu bestimmen. Die Größe des Niereninfarkts wurde, wie bei Myokardinfarkt oder Schlaganfallmodellen etabliert, per TTC-Färbung von Nierenschnitten und Planimetrie quantifiziert.

Injektion von CC verursachte einen dosis-abhängigen Abfall der GFR und Territorialinfarkte der Niere. Ursache waren Verschlüsse präglomerulärer Arterien und Arteriolen. Der Kristallanteil am Gefäßverschluss war gering, stattdessen fanden sich Fibrin+ Thrombusmaterial um die Kristalle, die das arterielle Lumen ausfüllten. Wir nannten diese Strukturen "Kristallthrombosen". Im Vergleich zum GFR Abfall, war das Ausmaß der Infarktgrößen variabler. 3D Rekonstruktionen von Angio- μ CTs zeigte partielle und vollständige arterielle Verschlüsse und Rarefizierung der arteriellen Blutgefäße. Histologisch fand sich nach 24 h ein deutliches perilesionales Neutrophileninfiltrat. Somit imitiert unser Modell periphere CCE mit arteriellen Verschlüssen, die akute territoriale Infarkte, perilesionale Entzündung und fiunktionelles Organversagen. Das Blockieren der Nekroinflammation/Infarzierung in mixed lineage kinase domain-like (*Mkl*)-defizienten Mäusen oder mit dem Inhibitor Nec-1s bzw. einem NLRP3-Inhibitor reduzierte signifikant die Infarktgröße und Infiltration von Neutrophilen im Vergleich zu Kontrollen. Keine dieser Interventionen hatte jedoch

Auswirkungen auf den durch CCE verursachten GFR-Verlust (=Organversagen), weil keine der Interventionen Einfluss auf die arteriellen Verschlüsse hatte. Da in der Niere die Funktion zu allererst von der glomerulären Perfusion abhängt, verhindert die Hemmung der ischämischen Nekrose alleine noch nicht das Nierenversagen. Somit war klar, dass die Kristallthrombosen das entscheidende Therapietarget bei CCE darstellen.

Histologisch bestanden die Kristallthrombosen aus Erythrozyten, Plättchen, Neutrophile, Fibrin, und extrazelluläre DNA (ecDNA). Zunächst haben wir Neutrophile mit einem depletierenden Antikörper selektiv entfernt, bzw. die Bildung von neutrophil extracellular traps (NETs) mit einem Inhibitor gehemmt. Beide Interventionen verringerten die Größe des Niereninfarkts im Vergleich zur Kontrollgruppe, dies hatte jedoch keinen signifikanten Einfluss auf die arteriellen Verschlüsse bzw. den GFR-Verlust. Im Gegensatz dazu schützte der Thrombozyten-P2Y₁₂-Rezeptorantagonist Clopidogrel Mäuse vollständig vor Kristallthrombosen, GFR-Abfall und Niereninfarkt. Daher sind Blutplättchen, jedoch nicht neutrophile Granulozyten, von zentraler Bedeutung für CCE-induzierte Kristallthrombosen und ihre Folgen. Als Nächstes testeten wir die Wirkung von Heparin und des Fibrinolytikums Urokinase. Nach 24 Stunden reduzierten sowohl Heparin als auch Urokinase die Anzahl der arteriellen Verschlüsse signifikant. Niereninfarkt, Nierenverletzung, Infiltration von Neutrophilen, Gefäßverletzung sowie tubuläre Nekrose waren nahezu vollständig abwesend. Beide Behandlungen hatten im Vergleich zu mit Vehikel-behandelten Mäusen einen vollständigen Schutz vor GFR-Abfall. Zusammenfassend lässt sich sagen, dass nicht die Kristalle an sich, sondern die Kristallthrombosen arterielle Obstruktion, Gewebeinfarkt und Organversagen verursachen.

Um die Bedeutung der ecDNA zu untersuchen, gaben wir rekombinante DNase I, die ecDNA degradiert. Tatsächlich war 24 h nach DNase I Gabe in den Arterien keine ecDNA mehr nachweisbar und, überraschenderweise, traten auch Kristallthrombosen nicht mehr auf. Die Verhinderung von arteriellen Verschlüssen war mit einem vollständigen Schutz vor GFR-Abfall, einer signifikanten Verringerung der Niereninfarktgröße verbunden. Somit ist ecDNA eine weitere nicht-redundante Komponente der CCE-bedingten arteriellen Obstruktion, des Gewebeinfarkts und des Organversagens. Da Herz- oder Aortenoperationen die Verwendung von Antikoagulanzen oder Fibrinolytika ausschließen, betrachteten wir rekombinante DNase I als mögliche Alternative zur Abschwächung der CC-Gerinnselbildung durch Hemmung der

Fibrinbildung und der ecDNA-Akkumulation. Zuerst testeten wir das therapeutische Zeitfenster und stellten fest, dass die DNase I-Behandlung, die 3 Stunden nach der CCE verabreicht wurde, immer noch einen Trend zu verbesserten Ergebnissen im Vergleich zu 6 und 12 Stunden zeigte. Um die Ergebnisse bei der Einstellung einer CCE im Zusammenhang mit kardiovaskulären Eingriffen weiter zu optimieren, haben wir ein Regime getestet, das eine präventive Einzeldosis des Nekroptosehemmers Nec-1s mit therapeutischer Gabe von rekombinanter DNase 1 3 Stunden nach Kristallinjektion kombiniert. Hierunter kam es zu einer vollständigen Protektion von Kristallthrombosen Organversagen und Infarkt, was eine neue Behandlungsoption bei elektiven Eingriffen bei Hochrisikopatienten aufzeigen könnte. Mechanistische *in vitro* Untersuchungen im Organ-Chip Modell, zeigten wie Cholesterin-Kristalle zu Endothelschäden führen, dass ecDNA v.a. aus Endothel und Neutrophilen freigesetzt wird. Thrombozyten setzen nur wenig mitochondriale DNA frei. DNase I inhibiert die CC-induzierte Thrombozytenaktivierung, möglicherweise durch Abbau von ADP.

Zusammengenommen präsentieren wir erstmals ein Mausmodell einer CCE mit Organversagen und Infarkt, das pathophysiologische Studien gestattet. Nicht der Infarkt an sich, sondern die Kristallthrombosen sind für das Organversagen entscheidend. Endothelschädigung mit Freisetzung von ecDNA und Plättchenaktivierung führen zur Bildung der Kristallthrombosen und bieten alte und neue Therapietargets. Eine prophylaktische Einmalgabe eines Zelltodinhitors und die Gabe von DNase I im postinterventionellen Zeitfenster von 3 h (bei der Maus) könnten helfen, die Prognose von Patienten mit Prozedur-assoziiertes CCE zu verbessern.

Summary

Atherosclerosis is a leading cause of global morbidity and mortality. In advanced atherosclerosis, cholesterol crystal (CC) embolism (CCE) is a potentially life-threatening complication with an average mortality of 62.8 %. Autopsies or tissue biopsies reveal CC inside the arterial lumen surrounded by an undefined biological matrix obstructing the vessel lumen. Little is known about the precise cellular and molecular mechanisms following CCE, in part due to the lack of animal models. Therefore, I hypothesized that developing a reproducible mouse model of CCE to mimic the morphological and functional characteristics of CCE in humans would be instrumental to dissect the molecular mechanisms of CC-driven arterial occlusion, tissue infarction, and organ failure.

To induce CCE, different doses of CC were injected into the left kidney artery of C57BL/6J mice. Acute kidney failure was evaluated by kidney function (i.e. GFR), kidney infarction was quantified using the TTC method. CC caused crystal clots occluding intrarenal arteries and a dose-dependent drop in GFR. In contrast, the extent of kidney infarction was more variable. 3D μ CT showed partial and complete arterial occlusions, blood vessel rarefaction, and volume change. The macroscopic analysis revealed kidney swelling and territorial infarctions, tubular necrosis, interstitial edema, neutrophil infiltrates, and loss of CD31. Thus, intraarterial CC injection induces arterial occlusions causing acute territorial infarctions, perilesional inflammation, and organ failure. Blocking necroptosis with *Mkl-/-* mice or *Nec-1s*, and the NLRP3 inhibitor significantly reduced infarct size, kidney injury, and neutrophil infiltration at 24 h compared to WT controls. However, none of these interventions affected CCE-related GFR loss. Consistently, necroinflammation is involved in kidney infarction but not in arterial occlusions as an upstream event. Thus, as nephron perfusion is ultimately required for kidney function, inhibiting infarction alone does not prevent acute kidney failure.

Immunostaining revealed that crystal clots involved platelets, neutrophils, fibrin, and extracellular DNA (ecDNA). Therefore, I depleted neutrophils or inhibited NET formation before CC injection. Neutrophil depletion or NET inhibition significantly decreased kidney infarction compared to the control groups, but this had no significant effect on arterial obstructions or GFR loss, maybe because mononuclear cells had partially replaced neutrophils inside crystal clots as a source of ecDNA. In contrast, the platelet P2Y₁₂ receptor antagonist clopidogrel completely protected mice from intravascular obstructions, GFR loss, kidney infarction, and perilesional neutrophil infiltrate. Therefore, CC occlude arteries by forming

crystal clots consisting of fibrin, platelets, and neutrophils. Thus, platelets but not neutrophils are central for CCE-related arterial occlusion, organ failure, and tissue infarction. Next, I tested the effects of the anticoagulant heparin and the fibrinolytic agent urokinase. At 24h both heparin and urokinase significantly reduced the arterial occlusions number, kidney infarction, kidney injury, neutrophils infiltration, vascular injury as well as tubular necrosis. Both treatments had complete protection from GFR loss compared to vehicle-treated mice. Conclusively, not the crystals per se but rather crystal clots cause arterial obstruction, tissue infarction, and organ failure.

In the DNase I treatment group, I noticed a significant reduction in the percentage of CC clots with ecDNA. After 24h of DNase I treatment intraarterial ecDNA had disappeared and the number of arterial occlusions was significantly reduced. Preventing arterial occlusions was associated with complete protection from GFR loss, a significant reduction in kidney infarct size as well as kidney cell death, neutrophil infiltrates, and vascular rarefaction. Thus, ecDNA is another non-redundant component of CCE-related arterial obstruction, tissue infarction, and organ failure. As cardiac or aorta surgeries preclude the use of anticoagulants or fibrinolytic agents, I considered recombinant DNase I as a possible alternative to attenuate CC clot formation by inhibiting fibrin formation and ecDNA accumulation. First, I tested the therapeutic window-of-opportunity and found that DNase I treatment given 3 h after CCE showed trends towards improved outcomes compared to 6 h and 12 h. To further optimize outcomes in the setting of a cardiovascular procedure-related CCE I tested a regimen combining a pre-emptive single dose of the necroptosis inhibitor Nec-1s with therapeutic recombinant DNase I given 3 h after intraarterial CC injection. This approach could be feasible as prophylaxis given to all patients at risk, while DNase I would be only given to those with signs of CCE into the kidney, e.g. an early decline of urinary output. This dual strategy resulted in significant protection from GFR loss and kidney infarction in almost all animals together with a significant reduction in vascular occlusions by crystal clots.

In my *in vitro* studies, platelets were exposed to thrombin with or without CC and found that CC enhances fibrinogen release from platelet alpha (α)-granules, which further promotes fibrin clot formation. CC exposure also induced ATP secretion from dense (δ)-granules, but co-incubation with DNase I strongly reduced these extracellular ATP releases. Next, I stimulated platelets with thrombin and collagen-related peptide and indicated DNase I can inhibit

fibrinogen and ATP secretion and subsequent fibrin formation and P2Y₁₂ receptor signaling, respectively. To model this process *in vitro*, I tested collagen-driven platelet aggregation with or without CC. Indeed, collagen I triggered massive platelet aggregation within 5 min with CC, DNase I treatment normalized this accelerated aggregation response. Endothelial cells and neutrophils studies showed that CC did not directly induce plasmatic coagulation but induced NET formation and DNA release mainly from kidney endothelial cells, neutrophils, and few from platelets. Thus, the *in vitro* studies support that CC and platelet dependent ecDNA release from neutrophils and endothelial cells, and DNase I can attenuate CC-induced platelet activation, aggregation, and fibrin clot formation.

In summary, not CC by itself but the fibrin clots forming around CC obstruct peripheral arteries causing tissue infarction and organ failure. Hence, crystal clots represent the primary target for therapeutic interventions. Among the possible molecular targets in thrombosis and haemostasis, especially enhancing fibrinolysis or inhibiting platelet purinergic signaling could reduce arterial occlusions, infarction, and organ failure albeit with a relatively short window-of-opportunity up to 3 h. My results suggest that prophylactic necroptosis inhibition with a combination of DNase I therapy could have a synergistic effect on CC induced clot formation in mice and might be a feasible two-step prophylactic/therapeutic approach in human patients with a risk for procedure-related CCE.

1. Introduction

1.1 Cholesterol crystal embolism

Cholesterol crystal embolism (CCE) is a unique version of arterio-arterial embolization. CCE occurs upon the rupture of an atherosclerotic plaque of a large artery (usually the aorta) when CC mobilize from the plaque material into the bloodstream. Taken to smaller arteries these CCs get stuck at some point and trigger biological processes leading to mechanical obstruction of arteries, ultimately resulting in tissue ischemia and organ failure (1). This process is similar to arterio-arterial thromboembolism, where a thrombus built-up on an atheromatous plaque mobilizes and gets flushed to a distal artery causing acute ischemic pain and injury (2). CCE is somewhat different. In contrast, the release of CC emboli in CCE can affect numerous arteries and organs and occur repeatedly over a while (3). CCE is a complication of advanced atherosclerosis (4). Clinical symptoms of CCE mostly relate to the location of the atheromatous plaque and the affected arterial beds. CC emboli release from the descending thoracic aorta may cause kidney failure, kidney infarction, mesenteric ischemia, while plaque rupture in the ascending aorta may also affect the brain and cause stroke-like symptoms (Fig. 1). Besides, fever, malaise, hypereosinophilia, and elevated serum levels of inflammatory markers, for example, increased erythrocyte sedimentation rate and C-reactive protein, are also typical systemic signs and symptoms of CCE (5).

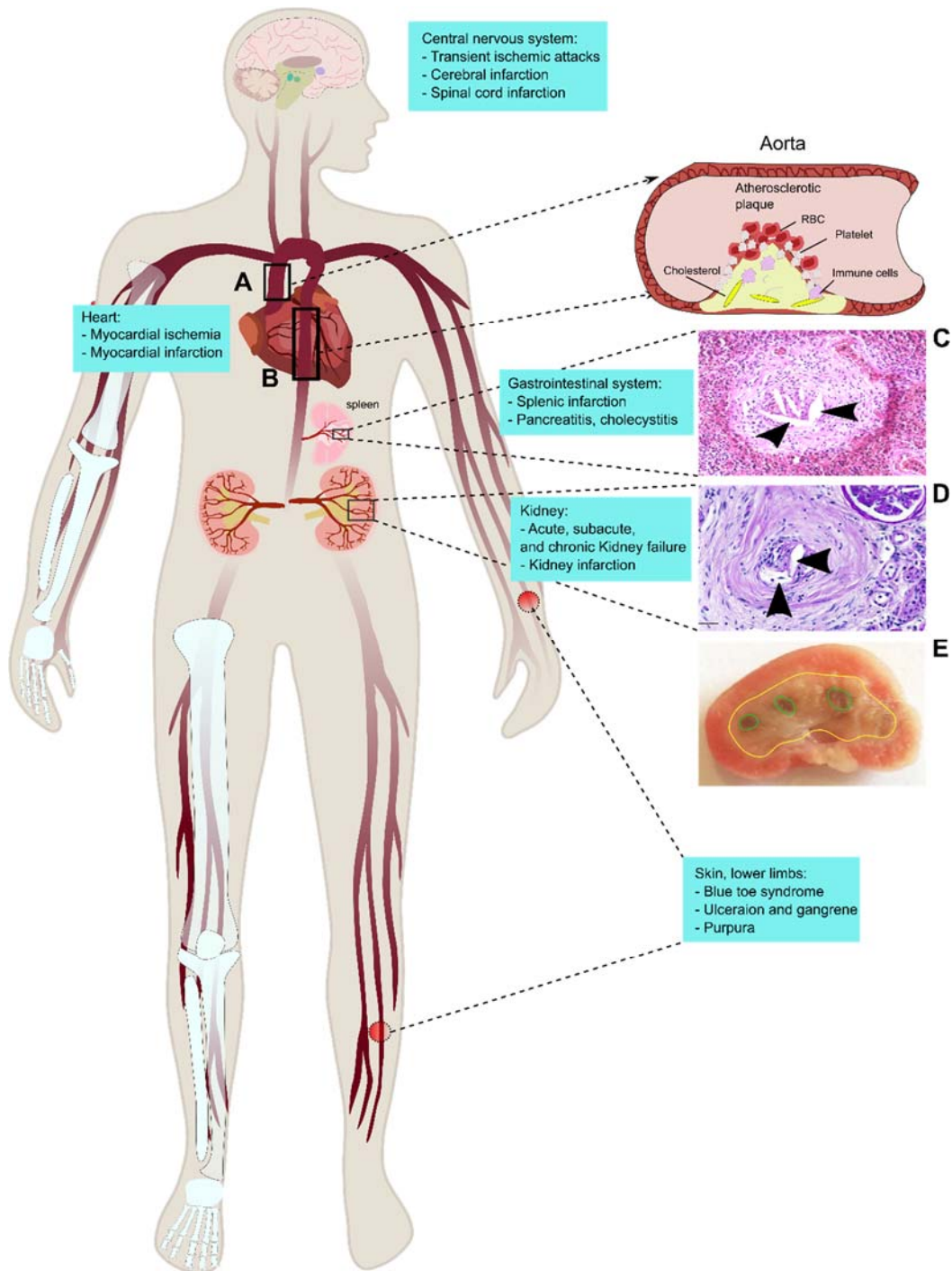


Figure 1. Cholesterol crystal embolism in multiple organs. A: Rupture of advanced atherosclerotic plaques in the ascending aorta can cause a shower of CC into arteries of the brain and the upper limbs. In the brain, the CC will lead to cerebral or spinal cord infarction and transient ischemic attacks. In the limbs, it will cause *livedo reticularis* and blue toe syndrome. B: When an advanced atherosclerotic plaque of descending aorta ruptures, which is the most common case it can induce CCE in multiple organs, such as the kidney, the gastrointestinal system, and the lower limbs. Skin lesions in the lower limbs are the most common complication of CCE. C: CCE in the human spleen, arrows indicate cholesterol clefts. The kidneys are the second vulnerable organ to plaque-induced CCE. Fig. D shows CCE in the human kidney, around the CCE obstructed kidney artery are ischemic necrotic tubular cells. Arrows indicate cholesterol clefts. CCE-induced ischemia can cause acute kidney infarction, as shown in Fig. E: CCE-induced tissue infarction in mouse kidney. The green circles indicate ischemic cores, and inside the yellow circle is infarcted kidney.

1.1.1 Pathophysiology of cholesterol crystal embolism

Six key elements are involved in the pathophysiology of CCE: 1. The atherosclerotic plaque present in the proximal large artery; 2. Plaque rupture; 3. CC mobilization; 4. Lodging of CC showers to distal small arteries; 5. CC emboli triggering biological responses; 6. End-organ injury.

Atherosclerotic plaque in the proximal artery. It is the premise for CCE development that an advanced atherosclerotic plaque is present in a large artery usually the aorta (6). Similar to atherosclerosis, kidney CCE normally affects males with diabetes and/or hypertension with a history of smoking and an age > 60 (7). The plaque is the main pathological manifestation of atherosclerosis. As a typical feature, the fibrous cap of the atherosclerotic plaque covers a necrotic core consisting of necrotic cell debris, foam cells, and CCs. Many risk factors can destabilize plaques and render them prone to erosion and rupture (8). CCE is initiated and propagated by deprivation of the fibrous cap, following segments break off from the core and approaching toward small arteries (9,10).

Plaque rupture. The rupture of atherosclerotic plaques can occur spontaneous, traumatic, or be related to thrombolytic and anticoagulation therapy. Plaque vulnerability relates to factors such as adhesion molecule expression, local cytokine release, monocyte and macrophage activation, endothelial cell dysfunction, and the activity of proteolytic enzymes (11). Autopsy studies revealed an incidence of spontaneous CCE ranging from 1 % to 3.4 % (9,12). Blunt trauma, catheterization, and cardiovascular surgery also cause traumatic plaque rupture. CCE is a relatively uncommon complication of cardiac catheterization even though plaque debris has been found in more than 50 % of guiding catheters (13). The incidence of clinically recognized CCE is less than 2 % of all catheter procedures (14). The occurrence of CCE in patients undergoing cardiac surgery is broadly dependent on the extent of atherosclerosis in the ascending aorta. Coronary revascularizations have a higher incidence of CCE in patients compared to valvular surgeries (15). Traditional cardiopulmonary bypass surgeries may provoke more microembolization events compared to off-pump cardiovascular procedures (16). Traditional carotid endarterectomy as well as carotid stenting both can generate CC emboli. Although CC emboli may affect multiple organs, the brain is considered as the most vulnerable site to CC emboli. Several clinical cases have been reported that thrombolytic therapy management for acute coronary syndrome and deep vein thrombosis can trigger CCE

(17). Nonetheless, controversy still exists regarding the correlation between thrombolytic therapy (18). As such anticoagulants have not been established as routine therapy for CCE as it is in atheroembolism. To date, no randomized clinical trials to specifically address the link between anticoagulation therapy and CCE.

Embolization of plaque components. CCE is characterized by multiple microemboli composed of CCs and plaque debris mobilized to various end-organ arteries often over some time. CCE becomes clinically evident once the manifestation of end-organ damage is apparent.

Lodging of cholesterol crystal emboli in distal small arteries. Showers of CC lodge into small arteries with a diameter of mostly between 100 and 200 μm . Within the lumen of obstructed vessels, classic ovoid, or needle-shaped clefts are observed not CC themselves in conventional biopsy specimens as CCs have washed away during processing (5). However, CC is visible in cryofixed biopsy specimens under polarized light (19).

The inflammatory response to cholesterol emboli. CC emboli are thought to not only directly restrict blood flow but also provoke a local inflammatory response. Histopathological lesions suggest that a series of reactions ultimately lead to a classical foreign body reaction. Generally, polymorphonuclear cells and eosinophils infiltrate the affected small arterial walls first. Following that mononuclear cells arrive and transform into giant cells, attempting to phagocytose CCs, followed by proliferation of endothelial cells and formation of intimal fibrosis. Ultimately, the result is a partial or complete occlusion of the arterial lumen and signs of tissue ischemia (20).

End-organ damage. End-organ damage may involve both, the mechanical obstruction of arteries and the local *response*. CCE can impair the function of any organ, in particular the brain, kidneys, gastrointestinal tract, skin, and the lower limbs are the most frequently affected by CCE.

1.1.2 Cholesterol crystal embolism in the kidney

CCE affecting the kidney is also known as atheroembolic kidney disease. Kidney CCE shows a pattern of acute kidney failure related to diffuse thrombosis occlusion of intrarenal arteries, arterioles, and glomerular capillaries with CC emboli originating from atheromatic plaques of the major arteries such as the aorta. Kidney CCE frequently occurs together with signs and symptoms of CCE in the skin, gastrointestinal system, lower limbs, and brain (6,9,10,21).

Kidney CCE is a serious complication of prevalent atherosclerosis in adult men and over 60 years of age (22,23). While the incidence of the disorder is still unknown because of the reported prevalence is diverse and in different clinical series, probably because of recognition bias. Random autopsy studies reported that the prevalence of kidney CCE ranging from 0.31 % to 2.4 % (12,24). Other autopsy studies reported higher incidences of the disease ranging from 12 % to 77 %, a high variability because these autopsy samples included elderly patients who died upon aortic surgery or aortography (21,23,24). Two large kidney biopsy studies reported a prevalence of 1 %, and 4 % to 6.5 % in elderly people (> 60) (25,26). Clinical studies estimated that CCE is supposed to account for 5-10 % of AKI in all cases (27). Regarding ICU patients, 3 % of those patients were diagnosed with CCE.

Pathophysiology of kidney cholesterol crystal embolism

Currently, 76-77 % of kidney CCE is considered iatrogenic, probably because of the increased use of vascular surgeries, anticoagulation, or thrombolysis (10,23,28,29). CCE was first observed as a complication of plaque disruption caused by vascular surgery (21). Any vascular procedure (including endovascular surgery, coronary artery bypass surgery, etc) has a risk of developing CCE (23,30). Angiography accounts for up to 80 % of CCE cases that is the most prevalent iatrogenic trigger (22,28). Anticoagulants or after thrombolytic therapy rarely leads to kidney CCE in patients (6,10,22,27,31). Thrombi have a stabilizing protective effect on ulcerated plaques, while anticoagulants may impair plaque sealing and account for repetitive CC showers into the periphery (32). In studies of patients with kidney CCE, anticoagulation was thought as an accelerating factor accounting for 13-76 % of cases (10,22,23,27,28,31). However, only 7 % of patients who had preceding invasive vascular surgeries developed CCE in the kidney after anticoagulant treatment (33).

On histology analysis, CC emboli are observed in the lumen of arcuate and interlobular arteries of the kidney, small CCs rarely embed in the afferent arterioles and glomerular capillaries (34). On paraffin sections, CCs appear as empty clefts of fusiform and needle-shaped because the CCs were washed away with ethanol treatment during specimen processing with paraffin. CC emboli usually provoke variable tissue injury (7). Tissue ischemia is the predominant cause for tissue atrophy and interstitial fibrosis, and acute tubular necrosis areas can be identified during the early stages (35).

Clinical features of kidney cholesterol crystal embolism

Many factors affect the clinical manifestations of kidney CCE, including the size and location of atheromatous plaques, lodging sites, amount of mobilized material, and the frequency of plaque rupture. CC emboli shuttle to the cerebral and retinal arteries are mainly derived from the ascending aorta and proximal aortic arch (9). Emboli mobilizing to arteries of the kidneys and lower limbs (leg and feet) can also originate from the descending thoracic and abdominal aorta (10,21,31). Although severe CCE can lead to a sudden illness due to pain and dysfunction of multiple organs, subclinical or mild episodes of the disease are frequent (22,23,27–29).

CCE in kidney impairs kidney function in various progressive ways, acute, subacute, or slowly progressive (22,23,27–30). Acute onset occurs within one week of a clear causal event of atheroembolism and presents as loss of excretory kidney function in 20-30 % of patients (30). This incident of AKI indicates diffuse intrarenal CCE. In most cases, gastrointestinal and cutaneous systems are also affected (36). Subacute kidney disease, as the most frequent form of CCE, with accelerating kidney function loss arising progressively during several weeks after a provoking condition. The mean time to diagnosis of the disorder was 5.3 weeks after an arteriographic procedure (35). This long gap between the causing event and the clinical evidence of kidney insufficiency indicates recurrent CC emboli showers and related inflammatory responses play a causal role in the disease process. Another presentation is the moderately increasing CKD that is usually attributed to nephroangiosclerosis or ischaemic nephropathy that mostly accompanies CCE events (37). The chronic presentation is a gent low-grade process accompanied by additional symptoms of other organs, therefore the CCE is clinically silent and usually underdiagnosed because kidney biopsy is not routinely performed. The progression of CKD is highly variable. 28-61 % of patients at acute or subacute stages need kidney replacement therapy, and partial recovery of kidney function occurs in 20-30 % of those patients after a variable period of dialysis (22,27,28). Recovery of kidney function is associated with reduced inflammatory response and resolution of concurrent acute tubular necrosis in ischaemic areas. Moreover, kidney CCE also associates with severe, uncontrolled hypertension. Kidney infarction is a unique outcome of CCE (38).

Therapies for kidney cholesterol crystal embolism

Regarding treatments for patients with CCE in the kidney, the primary purpose is to limit

ischaemic injury and to inhibit recurrent embolization. No reliable treatment option could be established so far and currently, interventions focus mostly on prevention and supportive therapy (8,23,29). Pre-emptive measures focus on restricting the exposure to trigger factors, such as re-evaluating the indication for anticoagulant therapy and avoidance of unnecessary vascular procedures or surgeries. In established cases, medical intervention mostly targets symptoms of this disease. Cardiac dysfunction and hypertension are aggressively treated. Therefore, future interventions should also aim to address the current gaps in preventing organ failure and injury.

Although no randomized clinical trials for patients with kidney CCE have been conducted so far, uncontrolled studies suggest the potential effects of statins and steroids.

Steroids. Small studies suggest possible benefits of steroids on kidney CCE (39,40). Low-dose administration of steroid (0.3 mg/kg) ameliorated symptoms and nutritional intake in 18 patients with recurrence disease (28). Other series imply that high doses of steroids could have beneficial effects, while other studies found little or insignificant effects of steroid treatment (10). A prospective study of 354 patients with kidney CCE, steroids had no effects on kidney function or other patient conditions (41). Hence, the use of steroids is still controversial, although it could have a role in patients with multi-system involvement, periodic and progressive disease, and systemic inflammation.

Statins. It has been reported that intermittent cases of kidney CCE respond to statins. In a prognostic study, the administration of a statin reduced the risk of developing ESKD in 12 patients. This finding was supported by a large prospective study (41). Moreover, statins had a promising effect on disease progression even the therapy was started after the diagnosis of CCE. Plaque stabilization and regression through lipid-lowering and anti-inflammatory activities could be the potential mechanisms of action of statins in this setting (42). Plaque stabilization might reduce the risk of further embolization. Nonetheless, the effects of statins do not address the acute setting. Despite these limitations, the early use of statins could be justifiable.

Besides, other successful therapies in small numbers of patients have also been reported, including iloprost, pentoxifylline, and LDL apheresis, although these approaches have yet to be tested in controlled studies (23,30). Removal by surgery or sealing the ruptured plaque with a covered stent could be another option, although is not easy to identify the embolic

source in each patient. Moreover, surgical treatment is usually not feasible for all patients and is associated with fundamental morbidity. Particularly, patients with CCE in kidney usually have a poor general condition to perform major surgery. Notably, the procedures of surgery would induce major risk for recurrence emboli due to the necessary aortic clamping.

Anyway, primary prevention of kidney CCE is important, e.g. restricting unnecessary angiographies and surgical procedures in patients at risk. The non-invasive diagnostic can help to avoid the risk of catheter-induced embolization, for instance, MR angiography or computer-assisted tomographic angiography. Application of the appropriate and cautious techniques to avoid direct damage to the atheromatous vessel wall during endovascular surgeries might also reduce embolization risk. Finally, the potential application of embolic protection devices could maximum reduce the risk of embolization by removing atheromatous debris.

1.2 Acute kidney injury and acute kidney disease

Acute kidney injury (AKI) is characterized by a rapid decline of kidney function, also referred to as “Acute kidney failure” (43). AKI normally happens within a few hours or a few days, kidney function is measured by serum creatinine and urine output in the clinic. The Kidney Disease Improving Global Outcomes (KDIGO) committee categorizes the AKI into three stages (Tab. 1) based on the serum creatinine and urine output (44).

Table 1: Stages of AKI based on current KDIGO definition

Stage of AKI	International consensus criteria
Stage I	Serum creatinine ≥ 1.5 times baseline or increase of ≥ 0.3 mg/dl within any 48 h period, or urine volume < 0.5 ml/kg for 6-12 h, or both.
Stage II	Serum creatinine ≥ 2.0 times baseline or urine volume < 0.5 ml/kg for ≥ 12 h.
Stage III	Serum creatinine ≥ 3.0 times baseline or increase to ≥ 4.0 mg/dl, or acute dialysis, or urine volume < 0.3 ml/kg for ≥ 24 h.

AKI is associated with high mortality and morbidity and is therefore a global health concern. In the hospital, AKI is an important complication that affects approximately 10-15 % hospitalized patients (45,46), in particular in ICU patients, the prevalence of AKI is higher than 50 %, and 4-5 % of those patients require kidney replacement therapy (47,48). Additionally,

AKI impacts about 13.3 million patients and accounts for about 1.7 million deaths worldwide that cause an enormous economic burden to families and national health care systems every year (45,46,49). While the incidence of AKI is highly variable in different regions that are described in Tab. 2.

Table. 2: Regional incidence rate of AKI according to the KDIGO-equivalent definition

	Region	AKI incidence rate (%)
Europe	Eastern Europe	22
	Western Europe	20.1
	Southern Europe	31.5
	Northern Europe	14.7
Asia	Eastern Asia	14.7
	Western Asia	20.1
	Southern Asia	23.7
	Australia and New Zealand	24.4
America	North American	24.5
	South America	29.6

Even though the high prevalence and huge economic costs of AKI, pharmacological cures, or therapeutic interventions for AKI have not yet been developed (50). According to epidemiologic investigations, AKI is a major risk factor of ESKD as kidney infarction involves an irreversible loss, i.e. CKD (49,51). Recently, the definition of acute kidney disease (AKD) has been added to the spectrum of kidney diseases and covers the gap between AKI and CKD, i.e. kidney injury lasting for more than 7 days up to 3 months (52). Accordingly, the early and rapid diagnosis and treatment of AKI is essential to generally manage patients with various potential syndromes of AKI. Meanwhile, the administration of the original disorder might help to resolve the secondary AKI condition in some cases.

In general, kidney disease is a silent condition. In a healthy individual, the glomerular filtration rate (GFR) loss must be nearly 50 % when the change of serum creatinine is detectable, thereby the levels of serum creatinine do not well indicate early impairments of kidney function (53). Even though changes in urine output might be more sensitive, the urinary output is hardly quantified outside ICU. In some particular AKI conditions, disability of tubular

urine concentration can result in polyuria (54). However, changes in serum creatinine or urinary output are neither sensitive nor specific for AKI in those situations. Currently, serum creatinine remains the standard approach to the diagnosis of AKI (55). In the research labs, the GFR can be precisely measured, but the available technology is time-consuming. AKI is also often induced by other diseases, for example, heart attack, liver injury, and sepsis (56–58). The major challenge for diagnosis is that AKI is normally accompanied by other specific syndromes (Fig. 2), which make it more complicated to categorize the severity of AKI and predict the short-term and long-term outcomes.

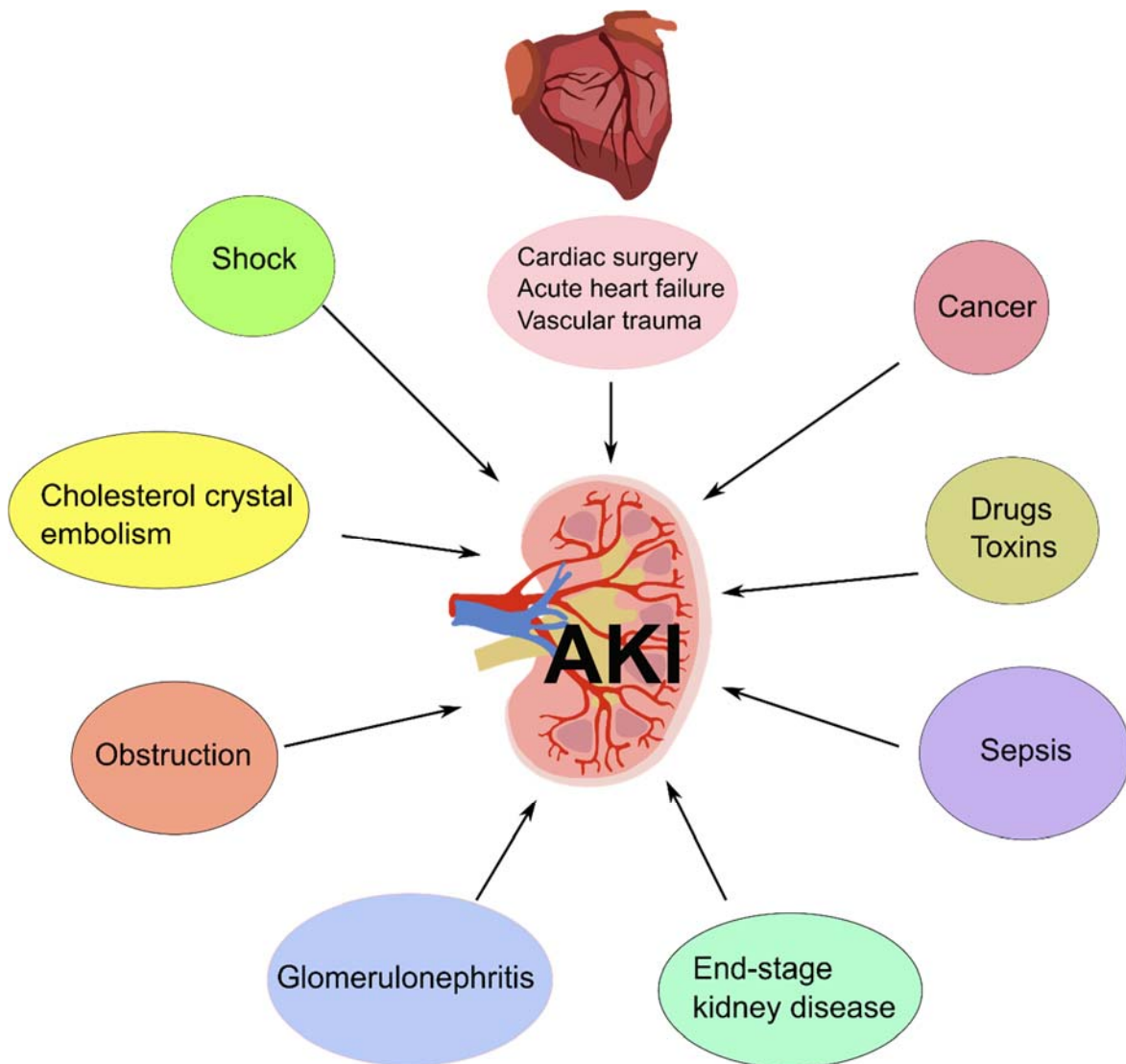


Figure 2. Causes and comorbidities of acute kidney injury (AKI). AKI can develop as a consequence of other pathological disorders, such as injury-related inflammation, oxidative stress, vascular trauma, and haemolysis. Acute heart failure decreases kidney perfusion pressure. Cholesterol crystal embolism, sepsis, and thrombosis-induced vascular obstruction. When these diseases cause death, AKI may be missed as a diagnosis.

Ischemia-reperfusion injury (IRI) is a major cause of AKI among many others (59). Kidney IRI also occurs in clinical conditions that can interrupt kidney blood flow (ischemia) and follow by the subsequent reperfusion, such as surgeries of major vascular and cardiac, kidney transplantation, shock, sepsis, trauma (59,60). IRI triggers an imbalance between the supply and demand of oxygen and nutrients in the perfused tissue. Damaged kidney cells will consecutively release toxic by-products (e.g., proinflammatory cytokines and DAMPs) that initiate injury to the surrounding tubular epithelial and endothelial cells injury resulting in a decline of kidney function (61). Various pathophysiological mechanisms, including tubular epithelial cell apoptosis, necrosis, and inflammation contribute to ischemic AKI.

1.2.1 The pathophysiology of ischemic AKI

Evidence from human and animal studies revealed that normal or even periodic decreased kidney blood flow can cause AKI, in terms of these situations, dysfunction of the intrarenal microcirculation plays a more important role in the pathophysiology of AKI (62). The kidney consists of two vascular compartments, the glomeruli and peritubular microcirculatory systems that both largely contribute to the progress and propagation of AKI (63). While the disruption of glomerular blood flow will consequently affect peritubular perfusion as the peritubular vessels are derived from the efferent glomerular arterioles, even when global kidney blood flow is unaffected or increased (64). Moreover, the arteriolar vasoconstriction can reduce local blood flow to the outer medulla that further leads to local edema.

The endothelium forms a natural barrier between intravascular and extravascular spaces and plays a decisive role in maintaining homeostasis and intactness of the endothelial barrier (65). The endothelium can produce prostacyclin, nitric oxide, and other vasoactive substances to regulate vascular tone, leukocyte activity, platelet aggregation, and smooth muscle response under steady condition, thereby it also influences the microcirculation and glomerular filtration (66). There are many additional pathways involved in endothelial cell function that contribute to the pathology of ischemic AKI. Under disease conditions, the activated coagulation cascade loop together with endothelial-leukocyte connections results in enhanced vasoconstriction and small-vessel occlusion that lead to interruption of local microcirculation related regional ischemia, especially in the outer medulla.

Tubule injury in ischemic AKI

Histological analysis shows that the presence of necrotic tubule segments is the typical pathological feature of ischemic AKI, also referred to as acute tubular necrosis (47,59). The kidney is highly susceptible to ischemic injury, in particular the proximal tubule of the S3 segment in the outer medulla, a site of intense metabolic activity and oxygen demand (67).

Necroptosis pathway in ischemic AKI. In ischemic AKI, regulated necrosis has been widely studied by using different animal models (68–70). Necrosis is induced by cytoplasmic and mitochondrial swelling, followed by cell membrane rupture and release of DAMPs (for example DNA, histone, ATP), resulting in inflammation and immune activation. Necroptosis is the most widely investigated regulated necrosis pathway. It is substantially regulated by the cytoplasmic molecules RIPK1, RIPK3 (receptor-interacting protein kinase 1, 3), and MLKL (mixed lineage kinase domain-like protein) (71,72) (Fig. 3). Necroptosis plays a vital role in ischemic AKI has been proved by animal studies that using gene deficiency mice or pharmacological inhibitors for necroptosis major mediators (RIPK1, RIPK3, and MLKL). Evidence from gene deficiency mice studies has demonstrated that necroptosis contributes to ischemic tubular injury. In severe 43-minute ischemia, *RIPK3* deficient group has a modest survival advantage (73). In the 30-minute standard ischemia, *RIPK3*^{-/-} and *Mkl1*^{-/-} mice both modestly improved kidney function compared to WT controls (73). A study from other groups confirmed the findings that *RIPK3*^{-/-} and *RIPK1*^{-/-} both markedly improved survival and protected mice from 30-minute standard ischemia injury (74). However, in the *Mkl1*^{-/-} group was no significant difference compared to WT groups in overall survival at 24 h (74). While other studies showed *Mkl1*^{-/-} mice were protected from ischemic injury at 48 and 72 h after reperfusion, but not at 24 h (75). *RIPK3*^{-/-} or *Mkl1*^{-/-} mice kidneys show less ischemic injury compared to WT (76). Additionally, *RIPK3* deficiency also protects mice from tubular injury in a sepsis-induced kidney disease model while *Mkl1* deficiency mice not (77). On the contrary, *RIPK3* deficiency does not show protection in inflammation models but *Mkl1* deficiency mice do (74). This discrepancy may be due to *RIPK3* also inducing oxidative stress and mitochondrial dysfunction and thereby promoting kidney tubular injury (77).

Necrostatin-1s (Nec-1s) is a RIPK1 inhibitor that has been tested in *in vivo* and *in vitro* studies. In *in vitro* studies, Nec-1s protected rat and human tubular cells from TNF- α -induced injury (78). An *in vivo* study using the standard kidney IRI model demonstrated that administration

of Nec-1s either 15 min pre-ischemia or 15 min postreperfusion significantly prevented kidney function loss and protected mice from tubular injury at 48 h (79). Furthermore, the administration of Nec-1s also significantly protects mice from more severe ischemic injury and improved survival (79). Another pharmacologic strategy to prevent necroptosis is blocking MLKL which is the most informative way, currently (80). Necrosulfonamide is an inhibitor specific for human MLKL. Therefore, the administration of necrosulfonamide reduces necroptosis of human cells *in vitro* although it does not show protection in mice *in vivo* (81). GW806742X and SYN1215 both specifically target the pseudokinase domain of mouse MLKL (82). It has been shown that both protect mouse fibroblasts from necroptosis *in vitro* (80), while the *in vivo* effect of GW806742X and SYN1215 in IRI remains unclear.

Necroinflammation. The process of necroptosis takes at least 3 h from induction until cell membrane rupture according to *in vitro* studies (83,84). Necroptotic cells can release DAMPs and cytokines that trigger inflammation in a variety of pathways (85). Necroptotic cells release intracellular constituents, including nucleic acids, histones, HMGB1, and ATP, which act as DAMPs with predominantly proinflammatory properties (86). Also, necroptotic cells release numerous inflammatory cytokines directly leading to more necroptosis, which in turn promotes inflammation and forms a self-amplification loop, which is called “necroinflammation” (87). While uncontrolled necroinflammation will continually release DAMPs triggering a systemic inflammatory response leading to tissue damage and ultimately organ failure. In certain types of AKI, necroptosis seems to represent the second wave of cell death caused by inflammatory cytokines released from the primary necrotic cells. In a model of folic acid-induced AKI, the authors observed upregulated expression of *RIPK3* and *Mkl1* in the early phase, while inhibition of necroptosis did not show protection at 48 h (88), which suggested that the kidney is sensitive to necroptosis in ongoing AKI, whereas necroptosis may not be involved in the primary injury. The above concept was supported by the finding that necroptosis inhibition shows protection at 96 h but not earlier, the inflammatory response determines the secondary injury during AKI (89).

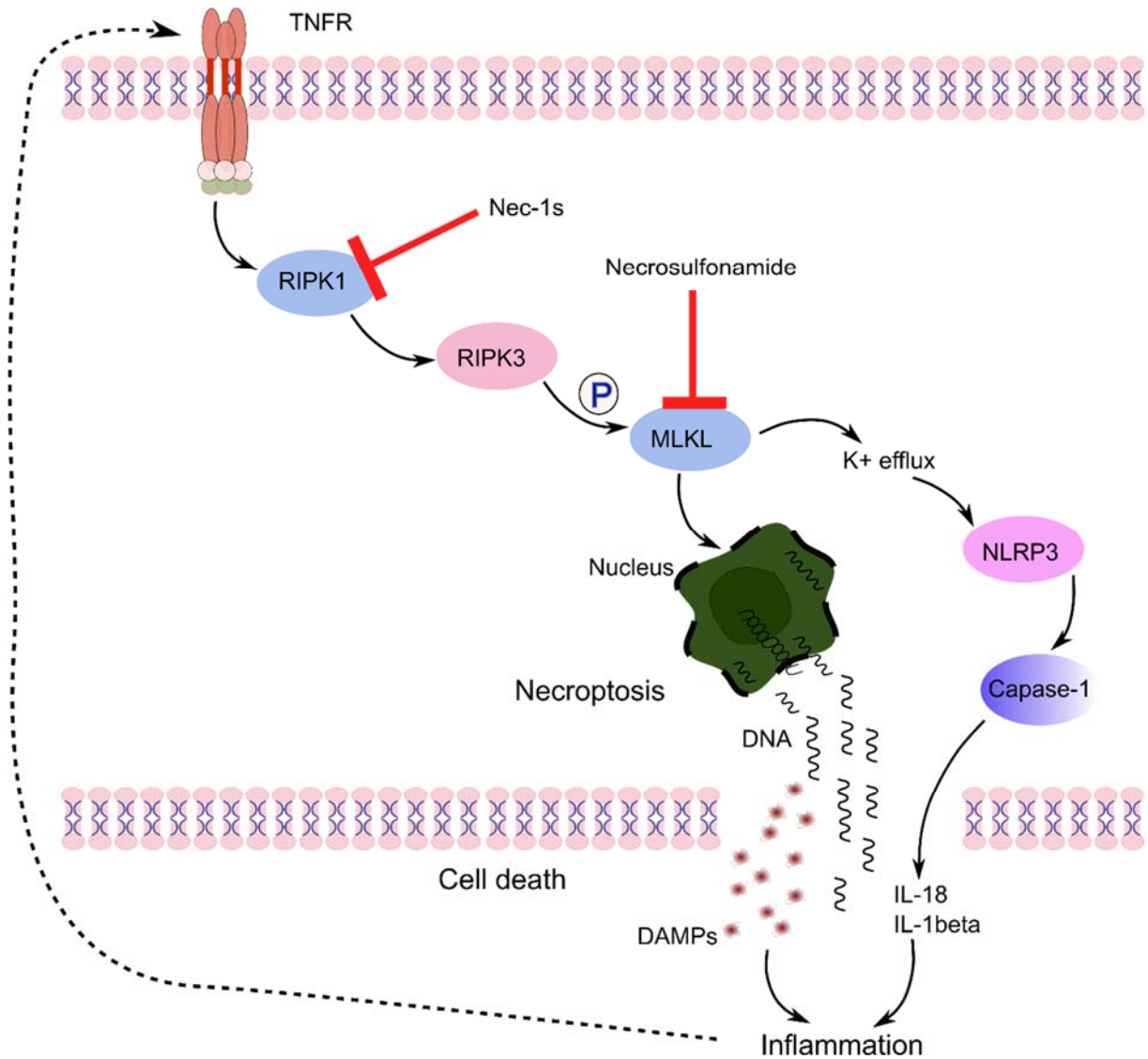


Figure 3. Necroptosis pathway initiation and related inflammation. Necroptosis is triggered by TNF α through binding to TNF α receptor. Subsequently, forms the complex of RIPK1 and RIPK3, which can phosphorylate MLKL. Phospho-MLKL causes lysis of the nuclear and plasma membranes leading to DNA, chromatin, and DAMPs release to extracellular space. Extracellular DNA and DAMPs result in inflammation. On the other way, phospho-MLKL also activates the NLRP3 inflammasome causing secretion of IL-1 β and IL-18, which also trigger inflammation. Small molecule inhibitors such as Nec-1s and necrosulfonamide can inhibit RIPK1 or MLKL and hence suppress cell death.

Role of immune cells in ischemic acute kidney injury

Accumulating studies demonstrate that both the innate and the adaptive immune systems contribute to the pathogenesis of ischemic AKI. The first immune response is initiated by endothelial cell injury, leukocytes activation together with the crosstalk of endothelial and leukocytes (47). In IRI, activated endothelial cells highly express a variety of adhesion molecules, those adhesion molecules act as the binding sites of activated leukocytes and guide

them to infiltrate into the interstitial space. Many studies support that blocking or genetic depletion of endothelial adhesion molecules protects mouse kidneys from IRI (90). Meanwhile, activated leukocytes, in turn, promote endothelial cell injury resulting in increased permeability of the endothelial barrier (91). Additionally, kidney epithelial cells can also secrete proinflammatory cytokines and chemokines contributing to the inflammation during IRI (92). Not only that, but tubular epithelial cells also express TLRs, complement factors and their receptors, and costimulatory molecules of T lymphocytes thereby facilitating cytokine secretion (93).

Neutrophils. Neutrophils are the most abundant leukocytes in the blood, they can rapidly infiltrate into the kidney and accumulated in the inflamed sites during the initial period of kidney IRI. Neutrophils will release ROS, proteinases, elastases, MPO, and cationic peptides that mainly contribute to necroinflammation in the kidney (94). To engage and activate more neutrophils, activated neutrophils can form a positive feedback loop by producing proinflammatory cytokines and chemokines. Upon kidney IRI, not only neutrophils, but other leukocytes also involve kidney injury, including natural killer cells, monocytes, and macrophages (95,96). In particular, the kidney resident dendritic cells can release TNF- α , IL-6, monocyte chemoattractant protein-1, RANTES, macrophage inflammatory protein-2 initiating an effective chemotactic gradient which is crucial for neutrophil recruitment to the kidney (94). Neutrophil has been considered as the therapeutic target to prevent ischemic AKI, although the effect of blocking neutrophil infiltration to prevent kidney injury has been controversial. Studies using an animal model of ischemic AKI showed that neutrophil inhibition can protect mice from kidney injury (97), but these results were not confirmed by others (98). Recently, it is been proposed that NETs formation could potentially explain how neutrophils cause tissue damage during ischemic AKI. The authors showed that *PAD4*^{-/-} displayed the modest protection of kidney function compared to WT control groups after IRI (99). As studies have demonstrated that blocking ICAM-1, p-selectins, or CD11a/11b effectively protected mice from ischemic AKI, the above studies suggest that not only neutrophil but also other leukocytes involve in ischemic AKI via synergistic interaction (100).

Macrophages. Macrophages are another critical leukocyte subtype contributing to the inflammatory response during the injury phase of kidney IRI. Macrophages can present at different functional states or phenotypes with, in part, opposite functions, but the initial phase

of IRI mostly involves a pro-inflammatory, so-called M1 macrophage phenotype. *In vivo* studies using a mouse model of IRI observed that the infiltration of macrophages is significantly increased at 48 h and persists over 7 days (101). Activated M1 macrophages, similar to neutrophils, can produce sufficient ROS and proinflammatory cytokines that can activate other leukocytes driving more tubular injury (102). Macrophage depletion from kidney and spleen before kidney IRI exhibit markedly reduced AKI, whereas adoptive transfer of macrophages displayed similar ischemic AKI (103). On the other hand, macrophage depletion performed later also abated tubular cell proliferation and impaired tubular repair because of M2 macrophages contribute to the repair process after kidney IRI (104).

Role of inflammasomes in ischemic acute kidney injury

The NLRP3 inflammasomes are a critical component of the innate immune system and contribute to many forms of sterile inflammation. A variety of cytosolic stimuli can initiate inflammasome, for example, DAMPs released from damaged host cells or microbe-derived PAMPs (105). The inflammasome forms as a cytosolic multiprotein complex that is typically categorized into two distinct families according to their receptor: the NOD-like receptor (NLR) family and the pyrin (PYD) and HIN200 domain-containing protein (PYHIN) family (106). The NLRP3 inflammasome belongs to the NLR subfamily that has been most studied. Structurally, except for the specific NOD-like receptor protein (NLRP), the NLRP inflammasome also includes an adaptor protein of apoptosis-associated speck-like protein containing a CARD (ASC) together with a procaspase-1 (107). Generally, the NLRP3 inflammasome senses danger signals (i.e. PAMPs or DAMPs) and recognize them by PRRs that further initiate the NLRP3 inflammasome. The activated NLRP3 inflammasome can activate the proinflammatory cytokines IL-1 β and IL-18, which in turn trigger an inflammatory response and induce cell death (Fig. 4).

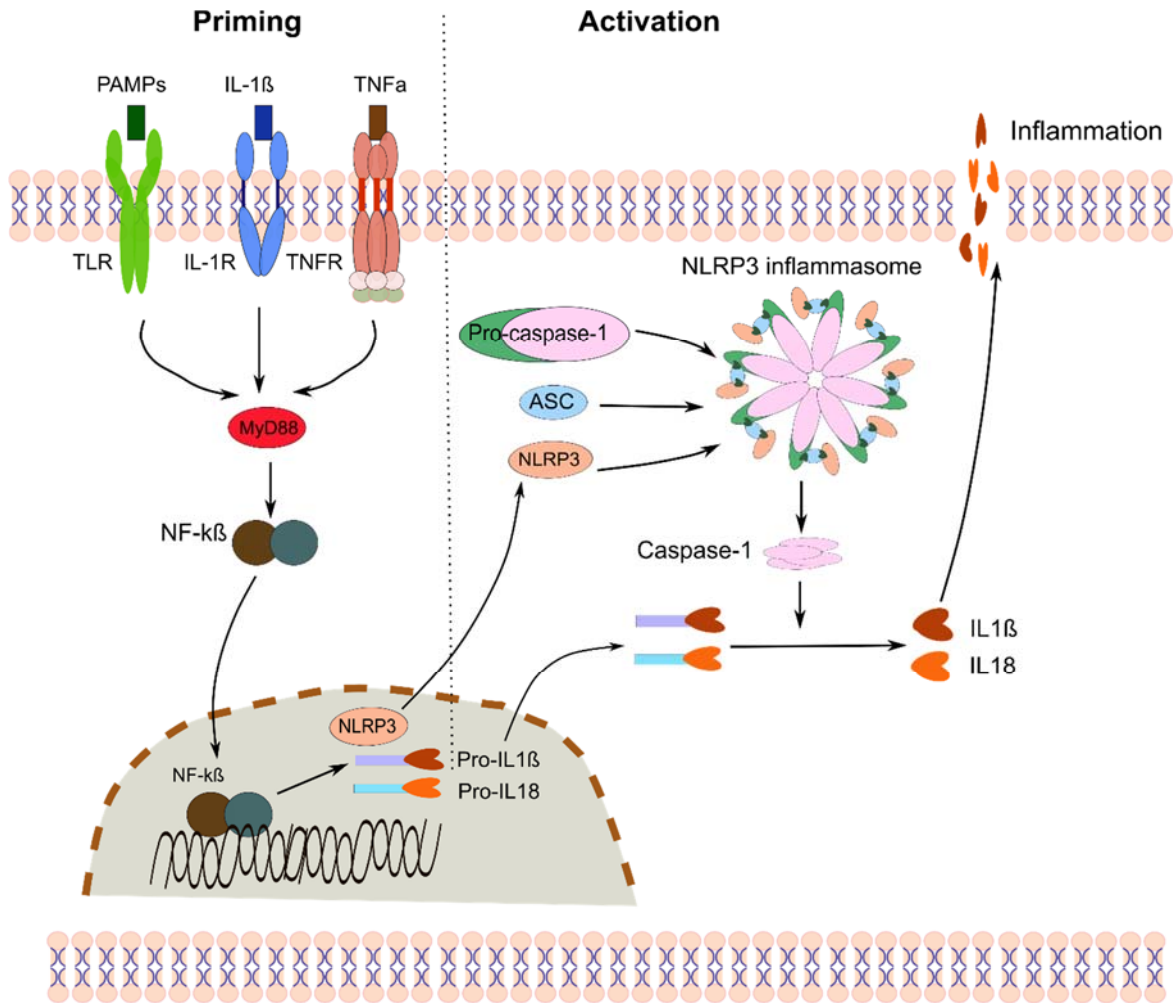


Figure 4. NLRP3 inflammasome activation. Upon the TLR is activated by PAMPs, the following is NF- κ B pathway mediated gene transcription of NLRP3, pro-IL-18, and pro-IL-1 β . NLRP3 together with ASC and pro-caspase-1 assemble and form the NLRP3-ASC inflammasome complex activating caspase-1. Activated caspase-1 cleaves pro-forms to mature IL-18 and IL-1 β , which are ultimately secreted to extracellular space. In the extracellular space, these cytokines trigger inflammation leading to more cell death.

In ischemic AKI, IL-1 β and IL-18 will trigger leukocyte recruitment and accelerate tubular injury (108). Moreover, the increased IL-1 β and/or IL-18 levels have been observed in kidney IRI model (109). Another study compared the effects of NLRP3 and ASC on mouse kidney IRI. *NLRP3*^{-/-} mice show less tubular injury at 24 h, as well as reduced IL-1 β levels in the kidney. These results are correlated to less neutrophil infiltration and decreased neutrophil chemoattractant levels of CXCL1 in the *NLRP3*^{-/-} mouse kidney (110). Interestingly, *ASC*^{-/-} has no significant effects on early kidney injury compared to WT, while 5 days later, *ASC*^{-/-} partially protects the kidney from ischemic injury, which is accompanied by decreased levels of CXCL1 and IL-1 β and fewer neutrophils in the kidney. IL-1 and IL-18 both account for the IRI-induced

AKI (111). *IL-1R*^{-/-} mice kidney displayed significantly reduced neutrophil infiltration and better kidney function in IRI compared to WT groups. Consistently, WT mice that are treated with IL-1R antagonists also exhibit reduced inflammation and kidney injury (111). It is already known urinary IL-18 is a biomarker that is used to assess tubular inflammation after AKI. *IL-18* deficiency or inhibition both protected mice from IRI by reducing macrophage infiltration to the post-ischemic kidney (112).

1.2.2 Therapies for acute kidney injury

The tight correlation between AKI with acute fatality as well as, in survivors, subsequent progressive CKD and ESKD finding appropriate treatments is a major unmet medical need in the fields of nephrology and critical care medicine (113–115). Using a variety of interventions to control AKI is required to avoid its unfortunate outcomes. Several pharmacological and non-pharmacological drugs have been tested in clinical trials and some with successful results in AKI prevention (Tab. 3).

Table 3: Therapies for AKI prevention

Treatment agents	Functional roles in the kidney	Clinical trials and outcomes	
		Trials	Outcomes
Alkaline phosphatase (AP)	Anti-inflammatory and detoxifying effects; reduce levels of plasma TNF- α and IL-6, and serum nitric oxide; improve kidney function after AKI (116,117).	Bovine intestinal AP (biAP): phase 2, sepsis, or septic shock patients, with or without AKI (118,119).	Overall, biAP improved kidney function and survival in the early phase of AKI.
		Human recombinant (hrAP): phase 2, acute and chronic studies (120).	hrAP no influence in the acute phase, improved kidney function, and survival rate in a chronic study.
Statin	Inhibit the activity of endothelial nitric oxide synthase, suppress inflammation (121).	Retrospective cohort study (136).	Statins reduced kidney complications after major surgery and improved patients' survival (123).
Prostaglandin E1 (PGE1)	A potent inhibitor of vasoconstriction and platelet aggregation (124).	Randomized controlled trials.	Contrary results on AKI protection (125,126).
Adenosine receptors	Adenosine can decrease GFR by modulating microcirculation (127).	Pentoxifylline in bone-marrow transplantation patients (128,129).	Contrary results on AKI protection.
Novel targets	Hypoxia-inducible factor (HIF), HIF pathway adaptively responds to the hypoxia condition of cells and tissue (130). Peroxisome proliferator-activated receptor- α (PPAR α), anti-inflammatory.	Ongoing clinical trial.	
		PPAR α protected animals from AKI by preventing proximal tubule cell death (131). No clinical trial.	
	Cell targeting therapies.	Infused mesenchymal stem cells and regulatory T cells showed protective effects on AKI in the animal model (132,133).	

Although some of the possible therapies for AKI as described in tab. 3, there is still no drug approved to treat or prevent AKI. Consequently, these critically ill patients only receive supportive care and kidney replacement is the final option. In addition, a single therapy may not be sufficient to prevent the progression of AKI because of the complex pathophysiology of kidney infarction. Most importantly, AKI establishes almost always before it is detected. Therefore, new biomarkers of AKI as well as drugs are needed.

1.3 Kidney infarction

Territorial kidney infarction is a rare condition resulting from the acute disruption of kidney blood flow by an obstruction of arterial blood supply. Classically, kidney infarction is a consequence of embolization from the heart or proximal aorta, abdominal trauma, or intrinsic pathology of the kidney arteries (134). Kidney infarction could present as a sudden decline in kidney function that also can develop in patients with precedent CKD. The infarct size predicts kidney function in the long run (135).

The frequency of infarction-related AKI ranges from 0 to 60 % in reports of different cohort studies. A clinical study of 100 kidney infarction patients reported 30 patients with AKI (136). Of those 30 AKI patients, 7 developed CKD and 6 died from complex complications. On the contrary, in another study, all 94 patients with kidney infarction survived the first 30 days after onset of the disease, but 5 % of patients required intermittent hemodialysis (137). According to another study, the initial GFR loss was around 30 % in patients with acute kidney infarction. Fortunately, their kidney functions gradually recovered to around 80 % of baseline values after one year (138). Another follow-up study assessed overall kidney function by serum creatinine and eGFR showing that kidney function of all patients maintained stable until the end of study albeit one developed ESKD. The kidney scintigraphy of the affected kidneys indicated some recovery after injury (139).

Kidney infarction is an uncommon disease but probably underdiagnosed. The early diagnosis of kidney infarction remains a challenge. Kidney infarction most commonly presents with abdominal pain, flank pain, nausea, vomiting, and occasionally, fever (140,141). According to the recent studies, the estimated prevalence maybe 0.013 %, while the diagnosed incidence is between 0.003 % and 0.004 % (141). Importantly, contrast-enhanced 3D-CT images of the

kidney artery can directly show artery defects making a precise diagnosis in time that will prevent long-term complications. It has been reported that typical radiologic evidence from CT, MRI, and/or radioisotope scans can diagnose and confirm kidney infarction (141). Therefore, comparing to other methods, using 3D-CT imaging to measure accurate volume will be a useful tool for predicting the degree of kidney function.

Kidney infarction normally occurs in patients with heart disease (cardiac embolism), diffuse atherosclerosis (atheroembolism or CCE), or vascular aneurysms (atheroembolism) (142). Risk factors for kidney infarction include kidney artery thrombosis, coagulopathy, ischemic heart disease, and atrial fibrillation (141,143). Among 438 patients with kidney infarction, a cardioembolic event accounted for 55.7 % of patients, atrial fibrillation accounted for 48.2 %, while kidney artery injury only accounted for 7.5 % (137,143). The prevalence of hypercoagulability-related kidney infarction ranged from 6.6 % to 16.6 % and mostly affected both kidneys (137,144). Antiphospholipid antibody syndrome and nephrotic syndrome are the most common causes of hypercoagulable states in kidney infarction.

Therapies for kidney infarction

Because kidney infarction is rare, only limited reports are available that information about clinical presentations, outcomes, and management (136,137,141–143). Management depends on the underlying cause and from the time between the onset of clinical symptoms and diagnosis. Treatment options include anticoagulation and endovascular therapy (145,146). In cardioembolic events, anticoagulation is used to prevent further episodes while in the acute phase anticoagulation may also foster revascularization of occluded intrarenal arteries. The combination of intravenous heparin followed by oral anticoagulants such as coumarins or direct thrombin inhibitors is the standard regimen (146). In CCE the role of anticoagulation is less clear, as the site of plaque rupture and the site of vascular obstruction might require opposite manipulation of the coagulation system.

2. Research hypotheses

Based on the above literature, I hypothesized that developing a reproducible mouse model of cholesterol crystal embolism would be instrumental to dissect the molecular mechanisms of CCE-driven arterial occlusion, tissue infarction, and organ failure.

Accordingly, the specific objectives based on the hypotheses were:

1. To establish a CCE model in mice by directly injecting CC through the renal artery. This model should be allowed to quantify thrombus obstruction and measure kidney function.
2. To investigate whether CC injection forms thrombi inside renal arteries and whether the thrombus formation is time-dependent or gender-related. Surgery was performed on both genders and kidneys were harvested at different time points after CC injection to quantify CC thrombus formation.
3. To investigate the role of plasmatic coagulation in CCE, antiplatelet, and fibrinolysis interventions were tested in this model, such as clopidogrel, urokinase, and heparin.
4. To investigate the potential contribution of neutrophils in CCE, neutrophils depletion by specific antibody or blockade of NETosis with inhibitor was applied in this study.
5. To investigate the potential contribution of necroinflammation in CCE-related tissue injury and infarction by using *Mkl1*^{-/-} mice or a Nec-1s inhibitor. The MCC950 inhibitor was used to block NLRP3-related inflammation.
6. To evaluate the role of ecDNA in CCE-related pathological process by using recombinant human DNase I.

3. Material and methods

3.1 Materials

Table 4: Instruments and devices

Instrument	Designation	Manufacturer
Balance	Analytic balance BP 110 S	Sartorius, Göttingen, DE
	Mettler PJ 3000	Mettler-Toledo, Greifensee, CH
Centrifuges	Centrifuge 5415 C	Eppendorf, Hamburg, DE
	Haraeus, Minifuge T	VWR Internation, Darmstadt, DE
	Haraeus, Sepatech Biofugue A	Heraeus Sepatech, Osterode, DE
Microscopes	Light microscope Leitz DM II	Leica Microsystems, Solms, DE
	Libra 120	Carl-Zeiss AG, Oberkochen, DE
	CCD-Camera	Tröndle, Moorenweis, DE
	Light microscope Zeiss AxioPlan 2	Carl-Zeiss AG, Oberkochen, DE
	Axiocam HR	Carl-Zeiss AG, Oberkochen, DE
Fluorescence microscope	Leica DMI8	Leica Microsystems, Cambridge, UK
	Olympus BX50	Olympus Microscopy, Hamburg, DE
	Zeiss observer microscope	Carl Zeiss AG, DE
Confocal microscopy	LSM 510 microscope	Carl Zeiss AG, DE
	Leica SP5 AOBS confocal microscope	Leica Microsystems, Wetzlar, DE
Scanning Electron Microscope (SEM)	Phenom XL Desktop SEM	ThermoFisher, USA
Cell culture		
Cell incubator	Heracell Type B5060 EC-CO2	Heraeus Sepatech, Osterode, DE
Cell counting chamber	Neubauer cell counting chamber	Roth, Karlsruhe, DE
Cell culture work bench	Sterile card hood class II, type A/B3	Baker Company, Stanford, ME, USA
Flow cytometry	FACS Canto II	BD, USA
	FACS Calibur	BD, USA
Tissue homogenizer	Ultra Turrax T 25	IKA GmbH, Staufen, DE
Microtome	Microtome HM 340 E	Microm, Heidelberg, DE

Instrument	Designation	Manufacturer
Cryomicrotome	Cryostat RM 2155	Leica Microsystems, Bensheim, DE
	Cryostat CM 3000	Leica Microsystems, Bensheim, DE
pH meter	pH meter WTW	WTW GmbH, Weilheim, DE
Thermomixer	Thermomixer 5436	Eppendorf AG, Hamburg, DE
	Thermocycler UNO II	Biometra, Göttingen, DE
Vortex mixer	Vortex Genie 2tm	Bender &Hobein, Zürich, CH
Workbench	Sterile workbench Microflow, biological safety cabinet class II	Nunc GmbH, Wiesbaden, DE
Rotary mixer	Heavy-duty rotator	Bachofer Laboratoriumsgeräte, Reutlingen, DE
Water bath	Water bath HI 1210	Leica Microsystems, Bensheim, DE
Manual pipette aid	Research Plus 30 - 300 µl	Eppendorf AG, Hamburg, DE
	Pipetman 2, 10, 20, 100, 200, 1000 µl	Gilson, Middleton, WI, USA
	Pipetus classic	Hirschmann Laborgeräte, Eberstadt, DE
Miniaturized imager device	For GFR measurement	Mannheim Pharma & Diagnostics GmbH
Miniaturized battery	For GFR imager device	Mannheim Pharma & Diagnostics GmbH
µCT system		SkyScan, Kontich, Belgium

Abb: SEM: Scanning electron microscope, FACS: Fluorescence-activated cell sorting, µCT: Micro-computed tomography.

Table 5: Disposable instruments

Instrument	Designation	Manufacturer
Eppendorf tubes	1.5, 2 ml	TPP Trasadingen, CH
Falcon tubes	15, 50 ml	BD, Heidelberg, DE
Serological pipettes	5, 10, 25 ml	BD Heidelberg, DE
Pipettes	Pipettes Pipetman	Gilson, Middleton, WI, USA
Pipette tips	10, 200, 1000 µl type Gilson	Peske, Aindling-Arnhofen, DE
	Pipette tips ep T.I.P.S	Eppendorf AG, Hamburg, DE
Embedding cassettes	Embedding cassettes "Biopsy"	ISOLAB, Wertheim, DE
Cell culture plates	6-, 12-, 96-well plate	TPP, Trasadingen, CH
8-well plate		Ibidi, Martinsried, DE
Two-lane OrganoPlate	400 µm × 220 µm channels	Mimetas BV, the Netherlands
Needles	20, 23, 25, 26, 30 Gauge	BD, Drogheda, IE
	33 Gauge	TSK Laboratory, Japan
Syringes	1, 2, 5, 10 ml	Becton Dickinson GmbH, Heidelberg, DE
Microscope slides	Super frost Plus	Menzel-Gläser, Braunschweig, DE
Cell culture dishes	10, 15 cm	TPP, Trasadingen, Switzerland

Table 6: Chemicals, reagents, and solutions

Product	Designation	Manufacturer
Ethanol		Merck, Darmstadt, DE
Formalin		Merck, Darmstadt, DE
HCl	Hydrogen chloride	Merck, Darmstadt, DE
NaCl		Merck, Darmstadt, DE
KCl		Merck, Darmstadt, DE
CaCl ₂		Merck, Darmstadt, DE
NaH ₂ PO ₄		Merck, Darmstadt, DE
NaHCO ₃		Merck, Darmstadt, DE
Glucose		Merck, Darmstadt, DE
Trisodium citrate		Merck, Darmstadt, DE
Tris-buffered saline		Merck, Darmstadt, DE
HEPES		Merck, Darmstadt, DE
Microfil injection compound		Flow-Tech, Carver, MA, USA
FITC-sinistrin		Mannheim Pharma & Diagnostics GmbH
Triton X-100	Tetramethylbutylphenyl-polyethylene glycol	Fluka, Chemie AG, Buchs, CH
TTC	2,3,5-Triphenyltetrazolium chloride	Merck, Darmstadt, DE
Cholesterol crystal		Merck, Darmstadt, DE
Cell death detection kit (TUNEL)	Terminal deoxynucleotidyl transferase dUTP nick end labeling	Roche, Mannheim, DE
SYTOX green assay	Extracellular DNA staining	Life Technologies, Eugene, OR, USA
Pico green double-strand (ds) DNA assay		Life Technologies, Eugene, OR, USA
LDH cytotoxicity assay	LDH: Lactate dehydrogenase	Roche, DE
Feulgen Stain Kit,	DNA staining	Abcam, DE

Table 7: Antibodies for immunohistology and others

Method	Name	Manufacturer
Immunohistology	CD31	Abcam, Cambridge, UK
	Ly6B2+	Serotec, Oxford, UK
	Alpha smooth muscle actin (α -SMA)	Dako Deutschland GmbH, Hamburg, DE
	Fibrin	Abcam, Cambridge, UK
	CD61	Abcam, Cambridge, UK
	Myeloperoxidase (MPO)	Abcam, Cambridge, UK
	Citrullinated histone H3 (Cit-H3)	Cell signaling, Danvers, MA
FACS	Anti-mouse P-selectin	Biolegend, USA
	Anti-mouse CD11b	BD, USA
	Anti-mouse Ly6C	BD, USA
	Anti-mouse Ly6G	BD, USA
Neutrophil depletion	Anti-mouse Ly6G	BioXCell, USA
	Isotype control IgG2a	Invivo Gen, DE

Table 8: Interventions and drugs:

Name	Manufacturer
Recombinant human DNase I	Merck, Darmstadt, DE
Necrostatin-1s (Nec-1s)	BioVision, USA
Cl-amidine	Merck, Darmstadt, DE
MCC950	Invivo Gen, DE
Calcein/PI	Invitrogen, DE
Heparin	Ratiopharm, DE
Urokinase	Actilyse Cathflo, Alteplase, Boehringer, DE
Clopidogrel hydrogensulfate	Merck, Darmstadt, DE

3.2 Experimental procedures

3.2.1 Animals

C57BL/6J, wild type (WT) mice, obtained from Charles River (Sulzfeld, Germany), the same background *Mkl*^{-/-} mice were kindly provided by James. M. Murphy and Warren Alexander, Parkville, Australia. Mice were housed in polypropylene cages under SPF standard conditions with the temperature of $22 \pm 2^\circ\text{C}$ with 12 h light and dark cycle, unlimited access to water and standard chow diet (Sniff, Soest, Germany) duration of the study. Cages, bedding, nestle, food, and water were sterilized by autoclaving before use. All the aspects of animal handling and experiments were approved by the Regierung von Oberbayern.

3.2.2 Animal models

Cholesterol crystal embolism induced acute kidney injury, acute kidney disease, and acute kidney infarction

To induce CCE, 6-8 weeks WT male or female mice were anesthetized by i.p. injection of medetomidine (0.5 mg/kg), midazolam (5 mg/kg), and fentanyl (0.05 mg/kg) under maintenance of normal body temperature by employing pre-operative heat supply in a heating chamber (147). After a median laparotomy aorta and left renal artery were carefully exposed. I used a 33-Gauge needle for cannulation of the left kidney artery from across the aorta and to inject various amounts of CC stock solution or normal saline as specified. The successful injection was visually verified by the decolorization of the kidney (Fig. 4A). Upon removal of the needle bleeding control involved light local pressure and cyanoacrylate polymer closure. The right kidney artery remained untouched. I used standard absorbable sutures to close the abdominal wall and skin, subcutaneous injection of atipamezole 2.5 mg/kg, and flumazenil 0.5 mg/kg to antagonize the anesthesia and subcutaneous injections of buprenorphine 1 mg/kg every 8 h for pain control.

To study CCE-induced AKI, different doses of CC (5, 10, 20, 30 mg/kg) were unilaterally injected to WT male mice left kidney via the artery. Mice were sacrificed after CC injection 24 h by cervical dislocation after measuring GFR. AKI was evaluated by GFR, kidney infarct size was quantified by the TTC method (148). The study design is shown in Fig. 5B.

To study CCE-induced AKD, WT male mice were sacrificed at days 1, 3, 7, and 14 at a dose of 10 mg/kg CC (Fig. 5C). AKD was characterized by monitoring kidney function throughout the study period of 4 weeks, associated with tubular injury and loss of brush border of the proximal tubule, interstitial edema, immune cells infiltration especially neutrophils, and macrophages leading to the secretion of inflammatory cytokines and thrombosis obstruction. At the end of each experiment, I measured GFR before sacrificing and tissue harvest. Kidneys were fixed in formalin before embedding in paraffin for histological analysis.

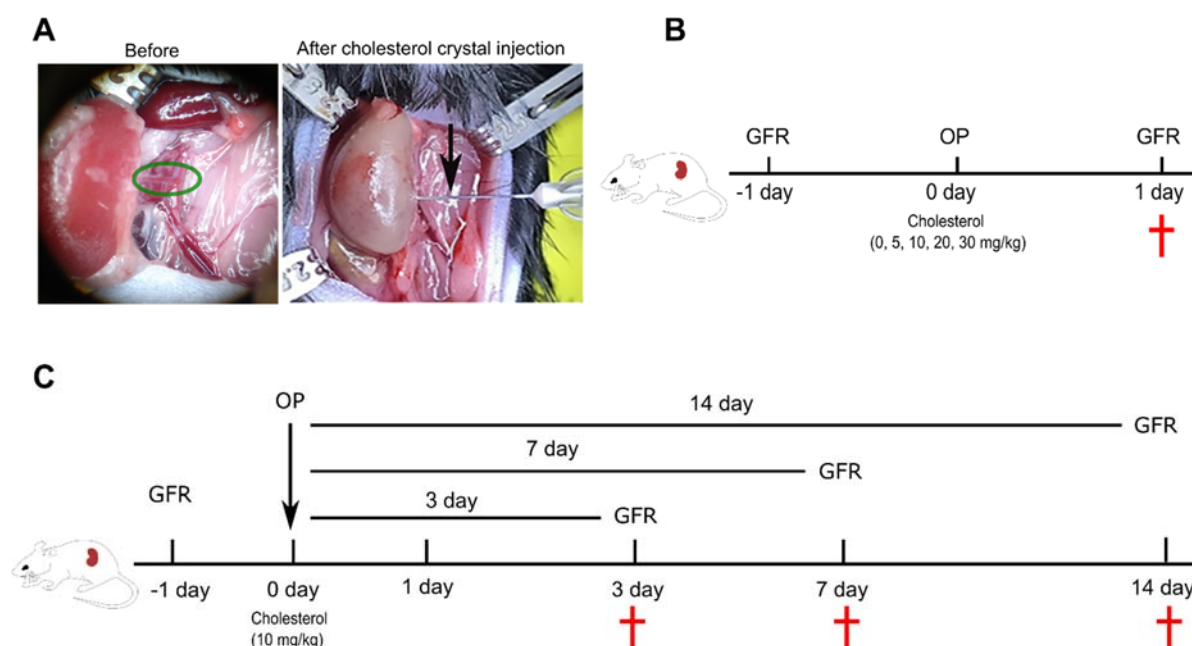


Figure 5. Schematic of study design for CCE-induced AKI and AKD. A: Cholesterol crystal injection into the kidney artery. Left panel: a healthy kidney. Right panel: CC perfused kidney. B: 24 h model design. C: Study design of time-course experiments.

3.2.3 Basic experimental design of the cholesterol crystal embolism-induced acute kidney injury model

Study 1: Establishment of the cholesterol crystal embolism model in murine kidney

The surgery was performed under general anesthesia. CCE was induced in the WT male mice by a single unilateral injection of different doses of CC through the left kidney artery. The Control group received a PBS solution. μ CT was employed to display tissue defects and to show arterial occlusion with associated blood vessel volume change and vasoconstriction induced. All mice were sacrificed 24 h after the CC injection and GFR measurement before sacrifice.

Analysis of kidney infarct size quantification by TTC staining, kidney injury assessment by PAS scoring, immune cells infiltration by Ly6B2+ immunostaining, vascular rarefication, and endothelial cells injury by CD31 sections, and artery thrombosis occlusion by α SMA/fibrin.

Study 2: Cholesterol crystal-induced clot formation in intrarenal arteries

To study the time course of the formation of crystal clots in the intrarenal arteries, WT male mice were injected with 10 mg/kg CC, then sacrificed at 3, 6, and 12 h after CC injection. I quantified the ratio of obstructed arteries using immunostaining for α SMA/fibrin. I set nine parameters (Tab. 9) based on three different size arteries: interlobar, arcuate, and interlobular, counted the number of completely and partially obstructed and empty vessels (Fig. 6). Kidneys' weight and infarct size were measured. Analysis of kidney infarct size by TTC staining, kidney injury scored by PAS staining, immune cell infiltration by Ly6B2+ immunostaining, vascular rarefication and endothelial cells injury by CD31 section, and artery thrombosis occlusion by α SMA/fibrin.

Table 9: Parameters used to quantify obstructed arteries

		Interlobar (number)	Arcuate (number)	Interlobular (number)
Total number		A+B+C	A'+B'+C'	A''+B''+C''
Artery Conditions of obstruction	No	A	A'	A''
	Partially	B	B'	B''
	Completely	C	C'	C''
Ratio of obstructed arteries (%)	No	A / (A+B+C)	A' / (A'+B'+C')	A'' / (A''+B''+C'')
	Partially	B / (A+B+C)	B' / (A'+B'+C')	B'' / (A''+B''+C'')
	Completely	C / (A+B+C)	C' / (A'+B'+C')	C'' / (A''+B''+C'')

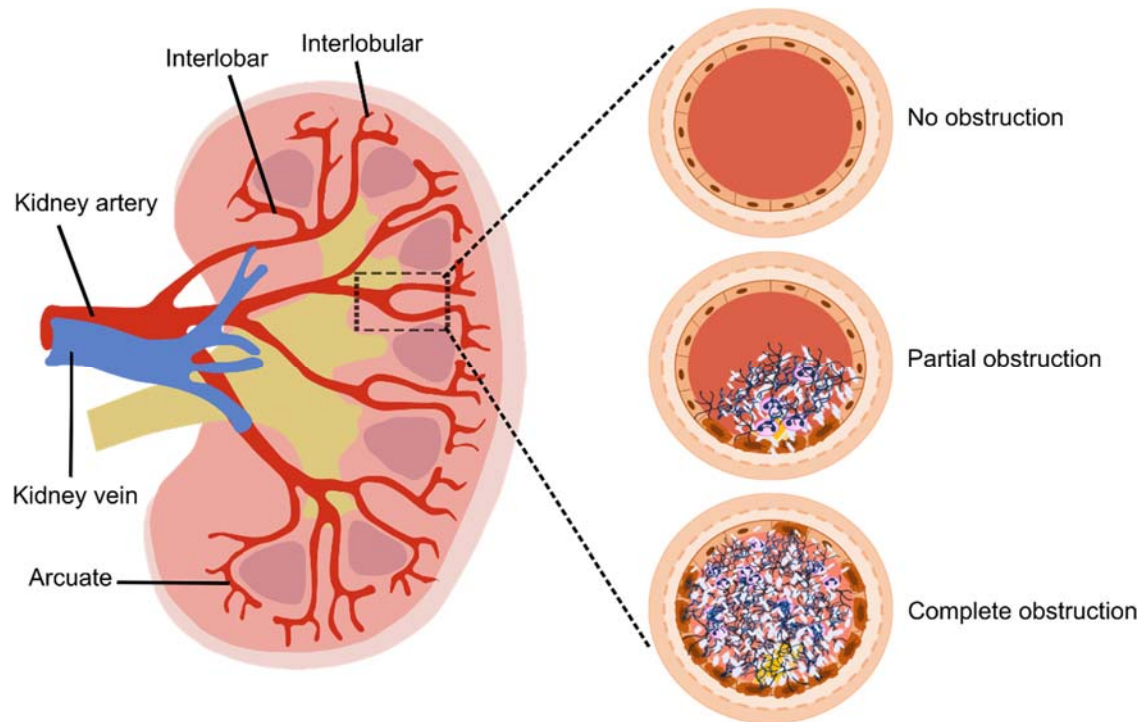


Figure 6: Schematic illustration of kidney vascular tree and obstruction levels. The left panel shows different sizes of kidney arteries and their location inside the kidney. The right panel illustrates three states of arterial obstruction used to quantify vascular obstruction.

Study 3: Role of platelets in cholesterol crystal-induced clot formation

To study the role of platelets in clot formation, I used a platelet antagonist clopidogrel. C57BL/6J male mice received an i.p. injection of 5 mg/kg platelet P2Y₁₂ receptor antagonist 10 min before surgery and immediately received another 5 mg/kg after CC injection, control mice received the same volume of PBS at the same time (Fig. 7A). All mice were sacrificed 24 h after CC injection and GFR was measured before sacrifice. Analysis of kidney infarct size by TTC staining, kidney injury scored by PAS staining, immune cell infiltration by Ly6B2+ immunostaining, vascular rarefaction and endothelial cells injury by CD31 section, and artery thrombosis occlusion by α SMA/fibrin.

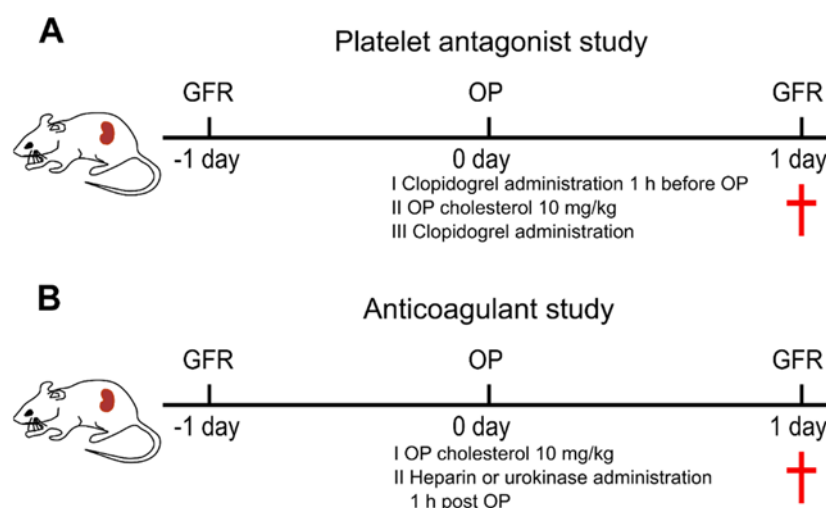


Figure 7: Schematic of study design for platelet contributions in CCE-related obstruction, AKI, and infarction.

Study 4: Role of plasmatic coagulation in cholesterol crystal-induced clot formation

To study the role of plasmatic coagulation in the formation of the clot, groups of C57BL/6J male mice received single i.v. injections of heparin 100 U/mouse or urokinase 24 mg/kg 1 h after CC injection. The control group received the same volume of normal saline (Fig. 7B). All mice were sacrificed 24 h after the CC injection and GFR measurement before sacrifice. Analysis of kidney infarct size by TTC staining, kidney injury scored by PAS staining, immune cell infiltration by Ly6B2+ immunostaining, vascular rarefication and endothelial cells injury by CD31 section, and artery thrombosis occlusion by α SMA/fibrin.

Study 5: Role of neutrophils in cholesterol crystal-induced clot formation, and infarction

To study the role of neutrophils in clot formation and infarction, I used two strategies:

a) Neutrophils depletion: WT male mice neutrophils were depleted by a single i.p. injection of anti-mouse Ly6G at 100 μ g/mouse, control mice received the same dose of irrelevant IgG2a antibody. Peripheral blood samples were collected at different times (6, 24, 72 h) to determine the numbers of neutrophils in the circulation using FACS. According to the FACS result, neutrophils depletion group mice received single i.p. injection of anti-mouse Ly6G 100 μ g/mouse 24 h before CC injection (Fig. 8A).

b) Blocking PAD4-dependent NET formation: To do so, WT male mice received single i.p. injection of PAD4 inhibitor Cl-amidine 20 mg/kg 30 min before CC injection, the control group received the same dose of PBS (Fig. 8B).

All mice were sacrificed 24 h after the CC injection and GFR measurement before sacrifice. Analysis of kidney infarct size by TTC staining, kidney injury scored by PAS staining, immune cell infiltration by Ly6B2+ immunostaining, vascular rarefication and endothelial cells injury by CD31 section, and artery thrombosis occlusion by α SMA/fibrin.

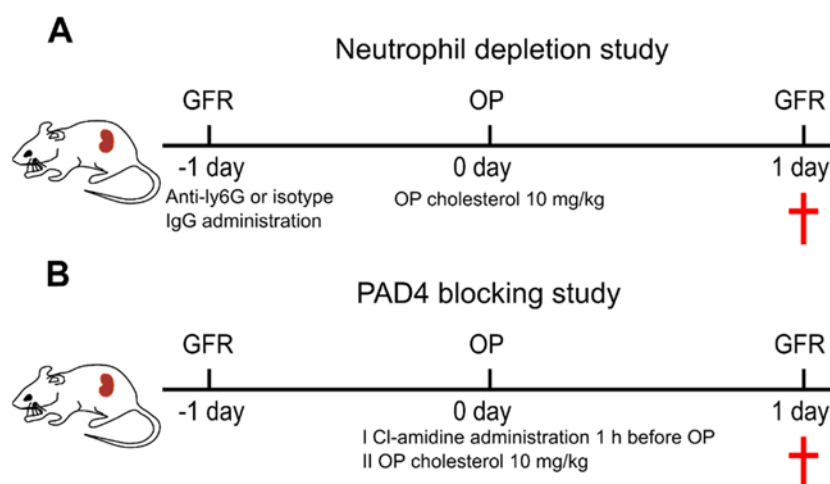


Figure 8. Schematic of study design for neutrophil contributions in CCE-related acute kidney injury and infarction.

Study 6: Role of necroinflammation in CCE-related kidney infarction and acute kidney injury

To study the role of necroinflammation in CCE-related kidney infarction and acute kidney failure, *Mkl*-dependent necroptosis, and NLRP3 inflammasome-dependent sterile inflammation were investigated.

a) Role of NLRP3 inflammasome-dependent sterile inflammation in CCE: WT male mice received single i.p. injection of NLRP3 inhibitor MCC950 20 mg/kg 30 min before CC injection, the control group received the same dose of PBS (Fig. 9B).

b) Role of necroptosis in CCE: On one hand, WT male mice received single i.p. injection of 10 mg/kg Necrostatin-1s (Nec-1s) 30 min before CC injection, the control group received the same dose of PBS (Fig. 9B). On the other hand, I performed the surgery on the same background *Mkl*^{-/-} male mice (Fig. 9A).

All mice were sacrificed 24 h after the CC injection and GFR measurement before sacrifice. Analysis of kidney infarct size by TTC staining, kidney injury scored by PAS staining, immune cell infiltration by Ly6B2+ immunostaining, vascular rarefication and endothelial cells injury by CD31 section, and artery thrombosis occlusion by α SMA/fibrin.

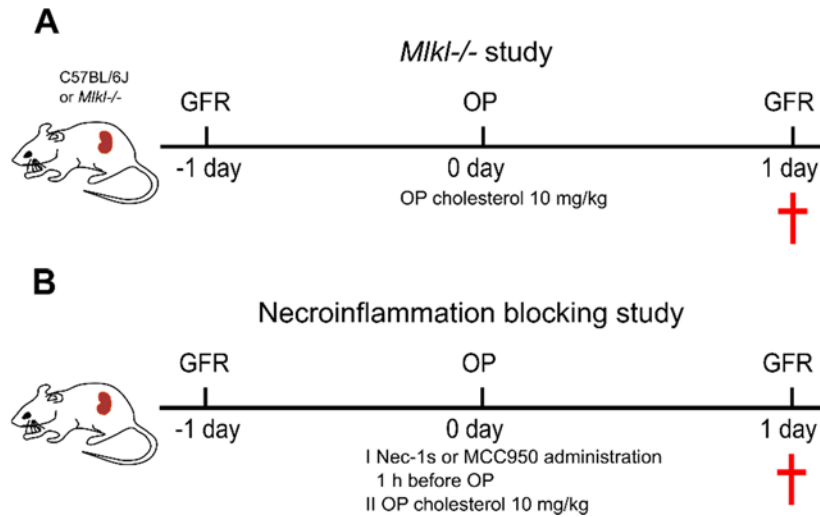


Figure 9. Schematic of study design for necroinflammation in CCE-related acute kidney injury and infarction.

Study 7: Role of extracellular DNA in cholesterol crystal-induced clot formation

To study the role of ecDNA in clot formation, WT male mice received i.p. injections of 50 µg recombinant DNase I before CC injection and 100 µg at 0 h and 12 h after CC injection, control mice received the same volume of normal saline at the same time (Fig. 10A). All mice were sacrificed 24 h after surgery.

To test the window of opportunity to prevent clot formation, mice received single i.p. injection of 250 µg recombinant DNase I at 3, 6, and 12 h after CC injection. All mice were sacrificed 24 h after the CC injection and measurement GFR (Fig. 10B).

Analysis of kidney infarct size by TTC staining, kidney injury scored by PAS staining, immune cell infiltration by Ly6B2⁺ immunostaining, vascular rarefication and endothelial cells injury by CD31 section, and artery thrombosis occlusion by αSMA/fibrin.

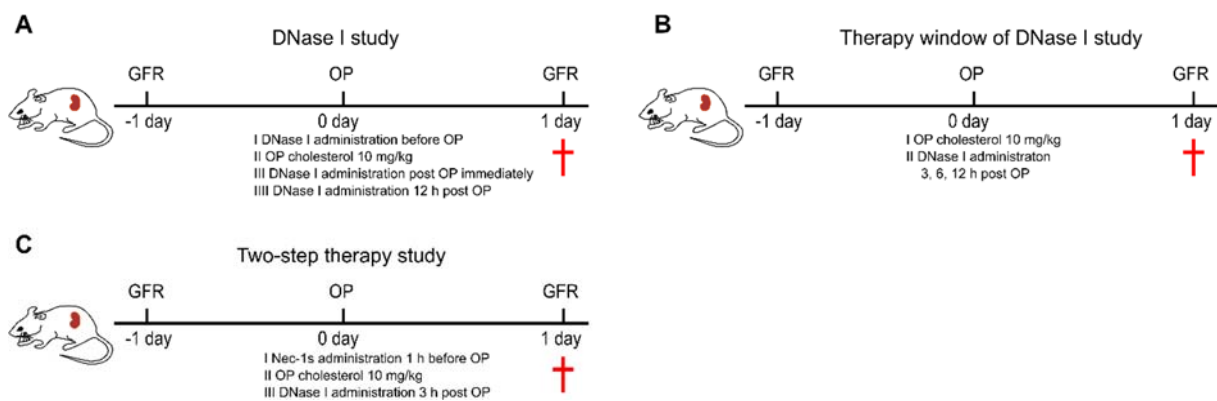


Figure 10. Schematic of study design for extracellular DNA in cholesterol crystal-induced clot formation.

Study 8: A two-step strategy to improve outcomes of cholesterol crystal embolism

According to the results of study 6 and study 7, a two-step strategy was employed. C57BL/6J male mice received i.p. injection of Nec-1s 10 mg/kg 30 min before CC injection and following recombinant DNase I injection of 250 µg 3 h after CC injection (Fig. 10C). All mice were sacrificed 24 h after CC injection and GFR measurement before sacrifice. Analysis of kidney infarct size by TTC staining, kidney injury scored by PAS staining, immune cell infiltration by Ly6B2+ immunostaining, vascular rarefaction and endothelial cells injury by CD31 section, and artery thrombosis occlusion by αSMA/fibrin.

3.3 Preparing of cholesterol crystal stock solution

10 mg cholesterol powder was suspended in a 5 ml sterile PBS, sonicated, and filtered through a 33-Gauge needle right before use.

3.4 Primary and secondary endpoints

Primary endpoint: Glomerular filtration rate (GFR)

All mice were anesthetized with isoflurane to mount a miniaturized imager device onto the shaved neck using a double-sided adhesive patch. The imager device has light-emitting diodes and a photodiode that connects to a battery (149). The background signal of the skin was recorded for 5 min before the i.v. injection of 150 mg/kg FITC-sinistrin. The animal was conscious and unrestrained in a single cage, the signal recording duration is approximate 1.5 h. After removing the imager device, the data were analyzed using MPD Lab software. The GFR (µl/min) was calculated from the decrease of fluorescence intensity over time using a three-compartment model together with body weight, and an empirical conversion factor (150).

Secondary endpoint: infarct size of kidney

After 24 h of CC injection, kidneys were harvested and sectioned transversely into 2 mm slices in a slicer. Each section was incubated with 1 % 2,3,5-triphenyl tetrazolium chloride (TTC) for 15 min at 37°C, then fixed in 4 % formalin for 2 h at RT. The infarct size (percentage of the kidney) was calculated by Image J.

3.5 Immunostainings

For immunohistological studies, I immediately fixed the middle part of each kidney in 4 % formalin for 24 h. Kidneys were processed using tissue processors (Leica) and embedded in paraffin blocks. Kidney paraffin sections were cut to 2 μm followed by de-paraffinization, sections were kept in xylene for 5 min and 3 times. The re-hydration was performed by 3 min x 3 in 100 % ethanol, 3 min twice in 95 % ethanol, and 3 min in 70 % ethanol. In the end, washing the sections with PBS for 5 min and repeat twice. Next, endogenous peroxidase was blocked in H_2O_2 and methanol mixture (20 ml of 30 % H_2O_2 in 180 ml of methanol) for 20 min in dark, then washed in PBS for 5 min twice. Endogenous biotin was blocked with one drop of Avidin for 15 min then Biotin for another 15 min. Sections were washed with PBS for 5 min twice after the incubation. The sections were prepared for further immunostaining.

Different primary antibodies were incubated overnight at 4°C in a wet chamber, after washing with PBS (2x 5 min), sections were incubated with biotinylated secondary antibodies for 30 min at RT followed by a wash with PBS (2x 5 min). Sections were incubated with substrate solution for 30 min at RT in a wet chamber followed by a wash with PBS for 5 min. Rinsing sections in Tris buffer for 5 min before staining with DAB, the following is counterstaining with methyl green. To remove excess stain and xylene, sections were washed with 96 % ethanol, then dried and mounted with VectaMount.

The primary antibodies used in studies were mentioned above in section 3.1. For each immunostaining, a negative control was performed by incubation with the respective isotype antibody instead of the primary antibody.

3.5.1 Neutrophils

The number of infiltrated neutrophils in the whole kidney was counted in the sections stained with the Ly6B2+ antibody. Positive cells were counted by Image J software.

3.5.3 CD31 staining

Kidney sections were stained with CD31 antibody to show the presence of CD31 on the surface of endothelial cells, which was a healthy marker of endothelial cells (CD31 positive area). This staining method shows the endothelial cells' injury.

3.5.4 Citrullinated histone H3 (Cit-H3) and myeloperoxidase (MPO)

Kidney sections were stained for MPO and Cit-H3 antibody to show the presence of NETs within the MPO and Cit-H3 positive area, which was in close association with NET formation. This staining method shows the cytotoxicity associated with NETs in the kidney.

3.5.5 Alpha-smooth muscle actin (α SMA) / fibrin staining

Total artery numbers in one kidney were quantified by α -SMA, thrombosis occlude arteries were quantified by fibrin.

3.6 Periodic acid Schiff (PAS) staining

Tissue processors processed paraffin kidney blocks were cut to 2 μ m for PAS staining. Prepared sections were de-paraffinized in xylene for 5 min and 3 times. The following is re-hydration that was performed by 3 min x 3 in 100 % ethanol, 3 min twice in 95 % ethanol, and 3 min in 70 % ethanol. After washing with distilled water (2 x 5 min), sections were ready for PAS staining.

Kidney sections were first incubated with 2 % Periodic acid for 5 min followed by washing with distilled water for 5 min. Next, incubated with Schiff reagent for 20 min at RT. After washing with tap water for 7 min, counterstaining was performed with Hematoxylin solution for another 2 min. Then washed with tap water for 5 min. Finally, stained kidney sections were dipped in 90 % ethanol, then dried and mounted with coverslips.

3.6.1 Kidney injury evaluation by Periodic acid Schiff staining

Mouse kidney injury was evaluated based on tubular injury and interstitial injury. This semi-quantitative scoring system includes five different parameters: tubular necrosis, tubular dilation, cast formation, loss of brush border, and interstitial edema. Each parameter has ten thresholds, as described in tab. 10. Kidney sections were evaluated using a light microscope Leica DII. Quantification is expressed as mean \pm SD in percentage.

Table 10: Score for evaluation of kidney injury

Parameters	Estimated damage	Score	Estimated percentage
a: Tubular necrosis	None	0	0
b: Tubular dilation	Very mild	1	0 - 10
c: Tubular cast		2	10 - 20
d: Loss of brush border	Mild	3	20 - 30
e: Interstitial edema		4	30 - 40
	Severe	5	40 - 50
		6	50 - 60
	Significant	7	60 - 70
		8	70 - 80
	Very severe	9	80 - 90
		10	90 - 100

3.7 Feulgen staining and TUNEL staining

Feulgen staining was used to detect nuclear or free DNA, the staining process followed the instruction of the kit. Slides were evaluated with a light microscope Leitz I and subsequently photographed.

TdT-mediated dUTP-biotin nick end labeling (TUNEL) detection kit aimed to identified dead cells in the kidney. Slides were evaluated with a light microscope Leitz I and subsequently photographed. TUNEL positive cells were assessed using the Image J software.

3.8 Immunohistochemistry in human tissue

The human kidney and spleen biopsies were obtained from a patient with CCE and supplied by the Institute of Pathology, RWTH Aachen, and processed anonymously. The study was approved by the local review boards of Aachen in line with the Declaration of Helsinki. Human biopsies were fixed in 4 % formalin and followed with embedded in paraffin. PAS and Feulgen stains were performed on kidney and spleen samples.

3.9 Micro-computed tomography (μ CT) imaging

To perform the μ CT, dead mice were perfused with a contrast agent Microfil, a lead-containing silicone rubber radiopaque agent, via a perfusion pump (150 ml/h; catheter diameter: 1.0 cm; catheter length: 75 cm), as described previously in more detail (151). Microfil solidifies

approximately 20 min after application within the vascular, then kidneys were harvested 20 min after Microfil perfused and fixed in formalin. Then scanned using a high-resolution SkyScan 1272 μ CT system that enables the high-resolution 3D image of the microarchitecture of kidney blood vessels. After 3D volume rendering of the reconstructed μ CT data sets and threshold-based segmentation of blood vessels, vessel volume and diameter as well as embolism volume were analyzed, using Imalytics Preclinical software (Version 2.1.7.2) (152). Imaging was performed in collaboration with Twan Lammers, *et al.* RWTH Aachen.

3.10 Flow cytometry

Ex vivo isolated neutrophil and platelet from human and mouse flow cytometric analysis was performed on a BD FACS Calibur flow cytometer. A variety of antibodies were used to determine neutrophils, and platelet activation, as shown in table 7.

3.11 *In vitro* studies

3.11.1 Human neutrophil isolation

All healthy blood donors provided written informed consent forms approved by the local ethical committee for human neutrophil isolation. Whole blood was collected into heparin tubes and put at 4°C to allow RBCs to settle down. After 30 min, separating the upper clear yellowish layer to get leucocyte. The remaining RBCs were lysed using hypotonic lysis (ddH₂O) for 2 min, and the same volume 0.15 M KCl was added to stop the reaction. The gradient centrifugation based on Biocoll was used to enrich neutrophils. All the procedures were performed on ice to avoid neutrophil activation, no aggressive shaking, or glass material. The pure neutrophils pellet was suspended in 1 ml plain RPMI media to count the cell number using a Neubauer chamber. Appropriate cells were seeded into 96-well plate or 8-well chamber that was used for different experiments then incubated cells at 37°C for 30 min to rest.

3.11.2 Formation of the neutrophil extracellular trap (NET) and cell death

To check the cytotoxic effect of CC on neutrophils, neutrophils were pretreated with 0.5 U/ μ l DNase I or PBS for 10 min. To induce NETs, various stimuli were used CC (5 mg/ml), 0.1 % Triton X-100 at 37 °C for 2 h. 8-well chamber was used for confocal live-cell imaging to visualize ecDNA release by Sytox Green Nucleic Acid Dye. In 96-well plate, the stimulated neutrophil

supernatants were collected for cell death detection or ecDNA quantification by LDH and Pico Green dsDNA Assay kit, separately.

3.11.3 Human and mouse endothelial cell culture

Mouse glomerular endothelial cells (GEnCs) were cultured in a flask in complete DMEM media containing 10 % fetal calf serum (FCS) and 1 % penicillin-streptomycin (PS). When cell confluence reached 80-90 %, they were detached by trypsin for 2-3 min and complete DMEM media was added to neutral the trypsin reaction. After centrifugation, the cell pellet was re-suspended in 1 ml complete DMEM to count the number using a Neubauer chamber. The required number of cells was used for different experiments.

HUVEC (human microvascular endothelial cells) were routinely propagated in complete endothelial growth media containing 10 % supplement mix and 1 % PS.

3.11.4 Endothelial cell death detection and extracellular DNA quantification

GEnCs were stimulated with different doses of CC (1, 5, 9 mg/ml). Cells were pre-treated with 0.5 U/ μ l DNase I, 20 μ M Nec-1s, 100 μ M Cl-amidine, 10 μ M MCC950 or PBS stimulation whenever required. Then, GEnCs were stimulated with 5 mg/ml CC at 37°C for 24 h. In 96-well plates, cell death and DNA release were quantified by the LDH assay and Pico Green dsDNA Assay Kit. Meanwhile, DNA release was also visualized by Sytox Green Nucleic Acid Dye under confocal microscopy. HUVEC were stimulated with 5 mg/ml CC for 24h, cell death of HUVEC was stained by Calcein/PI and visualized by confocal microscopy, DNA release from HUVEC was quantified by Pico Green dsDNA Assay Kit.

The supernatants of neutrophils, GEnC, and HMVEC were harvested after stimulation to detect cell death and DNA release.

Cell death detection: The supernatant was transferred to a new 96 well plate, the following is incubated with substrates of the LDH cytotoxicity detection kit. During this assay, LDH activity is determined by a coupled enzymatic reaction between LDH and substrate dye. The absorbance of the dye was read at 492nm, which directly correlates, to the amount of LDH present in the supernatant.

DNA release: The supernatant was centrifuged at 1500 rpm for 5 min to remove floating free nuclei. DNA release was determined by Pico Green dsDNA assay kit, and fluorescence intensity

was read after 5 min incubation, the excitation and emission wavelengths are 485 and 535 nm. For 3D cultures, HUVEC were seeded in a two-lane OrganoPlate with 400 μm \times 220 μm (w \times h) channels. 4 mg/ml Collagen I was used to creating the extracellular matrix and seeded 5×10^4 cells per chip, as previously described (153). The OrganoPlate was incubated at 37 °C with 5 % CO₂ on an interval rocker that set between a + 7 °C and -7 °C inclination every 8 min to allow bi-directional flow. For live/dead cell imaging, cells were stained with Calcein-AM (2 $\mu\text{g}/\text{ml}$) and Propidium Iodide (PI) (1 $\mu\text{g}/\text{ml}$) for 20 min. Images were taken using Leica SP5 AOBs confocal microscope equipped with a Chameleon Ultra-II two-photon laser. To generate 3D images, I used the image processing software Leica Application Suite X.

3.11.5 Confocal imaging

To visualize CC stimulated ecDNA release from neutrophils, endothelial cells, and NETs formation, 0.1 μM Sytox Green dye was added before confocal detection. Sytox Green is an impermeable DNA dye. Thus, cell death, the release of ecDNA, and NETs formation can be detected by confocal microscopy with LSM 510 microscope and LSM software.

3.11.6 Human platelet studies

Blood obtained from healthy volunteers that had provided a written informed consent approved by the local ethics commission (Ethikkommission der Medizinischen Fakultät der LMU). Blood was centrifuged at 800 rpm for 6 min at RT. Supernatant and buffy coat were transferred into a new tube to obtain platelet-rich plasma (PRP). To prepare washed platelets, PRP was centrifuged at 2,800 rpm for 5 min at RT and the pellet was resuspended in 1 ml Ca²⁺-free Tyrode's buffer containing apyrase (0.02 U/ml) and prostaglandin EI (PGEI, 0.5 μM). After 10 min incubation at 37 °C, the sample was centrifuged at 2,800 rpm for 5 min. After a second washing step, the platelet pellet was resuspended in the appropriate volume of Tyrode's buffer containing only apyrase (0.02 U/ml) and left to incubate for at least 30 min at 37 °C before analysis. Mitochondrial DNA release from washed platelets was visualized by MitoTracker Deep Red (100 nM) incubated for 45 min at 37 °C before Sytox Green Nucleic Acid Dye was added and DNA observed using confocal microscopy with an LSM 510 microscope and LSM software (Carl Zeiss AG).

3.12 Statistical analysis

All figures and statistical analyses were performed using Prism 7.0 software (GraphPad Software, San Diego, CA). Before every statistical analysis, data were checked for normal distribution (Shapiro-Wilk test), homoskedacity (Levene's test), and outliers (Grubb's test). Normally distributed and homoskedastic data sets were tested for significant differences via ANOVA and posthoc Bonferroni's correction was used for multiple comparisons. Heteroskedastic data were corrected following Games-Howell's posthoc test. Not normally distributed data sets were compared using Kruskal-Wallis and Nemenyi testing. Data are expressed as mean \pm SD.

4. Results

4.1 A new mouse model of cholesterol crystal-embolism

4.1.1 Cholesterol crystal injection-induced acute kidney injury and kidney infarction

To establish a CCE model, different doses of CC (5, 10, 20, 30 mg/kg) were injected into the left kidney artery of WT mice. Control mice received the same volume of PBS. Kidney artery injection can avoid discomfort from skin ulcerations, pancreatitis, peritonitis, or uremia. When kidneys were successfully perfused they changed color from dark red to pink (Fig. 5A). At 24 h, CC-perfused kidneys showed visible swelling (Fig. 10A), and the weight of CC kidneys increased in a dose-dependent manner (Fig. 10A'). To assess how CC injection affects kidney function, I measured GFR in mice without surgery and upon surgery 24 h. The result has shown that injecting different amounts of CC resulted in a dose-dependent decline of GFR at 24 h, i.e. AKI (Fig. 10C). Kidney infarct size was quantified using the TTC method (Fig. 10B). Interestingly, CC injection-induced high variability infarct size of different groups (Fig. 10B'). Therefore, CC injection-induced kidney infarction, and acute organ failure at 24 h.

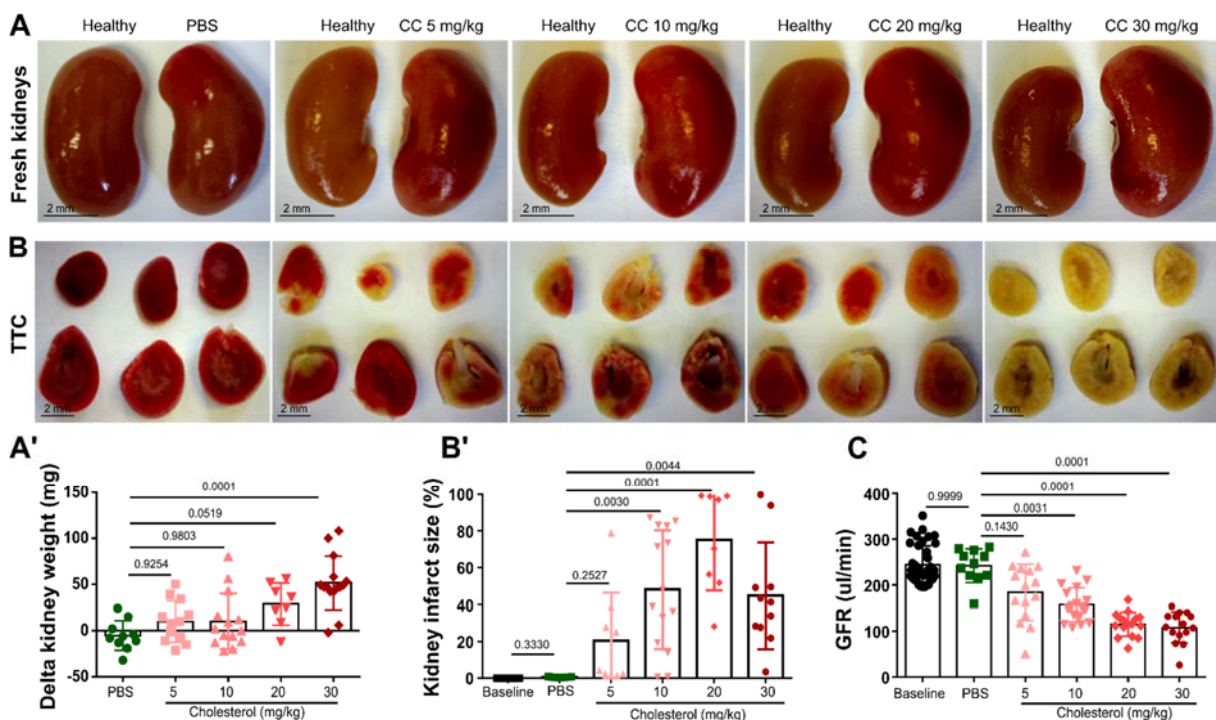


Figure 10. CC injection-induced acute kidney failure and kidney infarction at 24 h. A: Representative images of fresh kidneys in different groups. A': Delta kidney weight = CCE kidney – contralateral kidney. B: TTC-stained kidney slices of different groups. B': CCE-induced infarct size in different groups. C: CC injection-induced GFR loss in different groups. All quantitative data are means \pm SD.

To better characterize the structure of renal arteries, we performed arterial contrast μ CT and 3D reconstructions of the vascular tree. The 3D- μ CT showed CC injection caused rarefaction of peripheral arteries and partial and complete arterial occlusions (Fig. 11A). Statistical analysis found a significant change in the volume and diameter of the blood vessel (Fig. 11B-C). Therefore, CC injection-induced diffuse arterial thrombosis, as a manifestation of CCE.

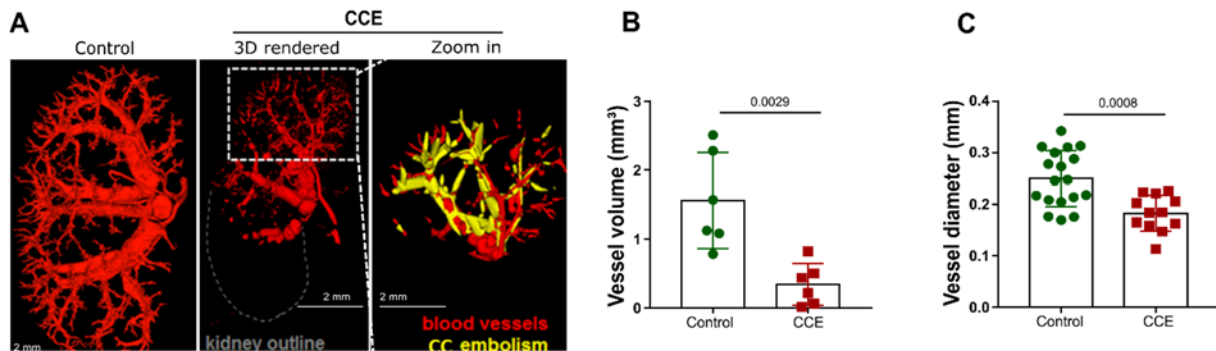


Figure 11. CCE-induced arterial thrombosis formation at 24 h. A: 3D μ CT displays peripheral vascular rarefaction in the CCE kidney. B: Blood vessel volume change in CCE kidney. C: CCE induced vasoconstriction in the CCE kidney. All quantitative data are means \pm SD.

Traditionally, arterial thrombosis is defined as blood clots formed within an artery, or the capillary system, which largely comprises of platelets, therefore it is also referred to as “white clots” (155). Exposure of the subendothelial matrix and activation of endothelial cells are the two most important events following the vessel injury (156). In terms of the most clinically substantial acute arterial thrombosis, thrombosis happened to the coronary arteries, the brain arteries, and peripheral arteries typically lead to AMI, cerebral ischemia, and stroke or peripheral arterial occlusive disease respectively (155). CCE is known as one of the arterial thrombosis. Taken together, CC injection-induced acute kidney failure and kidney infarction by forming arterial thrombosis that obstructing the kidney artery at 24 h.

4.1.2 Crystal clots-induced kidney injury, inflammation and vascular injury at 24 h

PAS staining was performed to verify CC injection-induced kidney injury. CCE kidney shows marked tubular cell necrosis, dilation, brush border loss, lumen cast presence, interstitial edema at 24 h (Fig. 12A-A’). PAS score shows injury in CCE kidneys follow the CC doses (Fig. 12C). PAS and thrombin stained sections visualized CC and artery thrombosis inside a kidney artery under polarized light (Fig. 12D-E’).

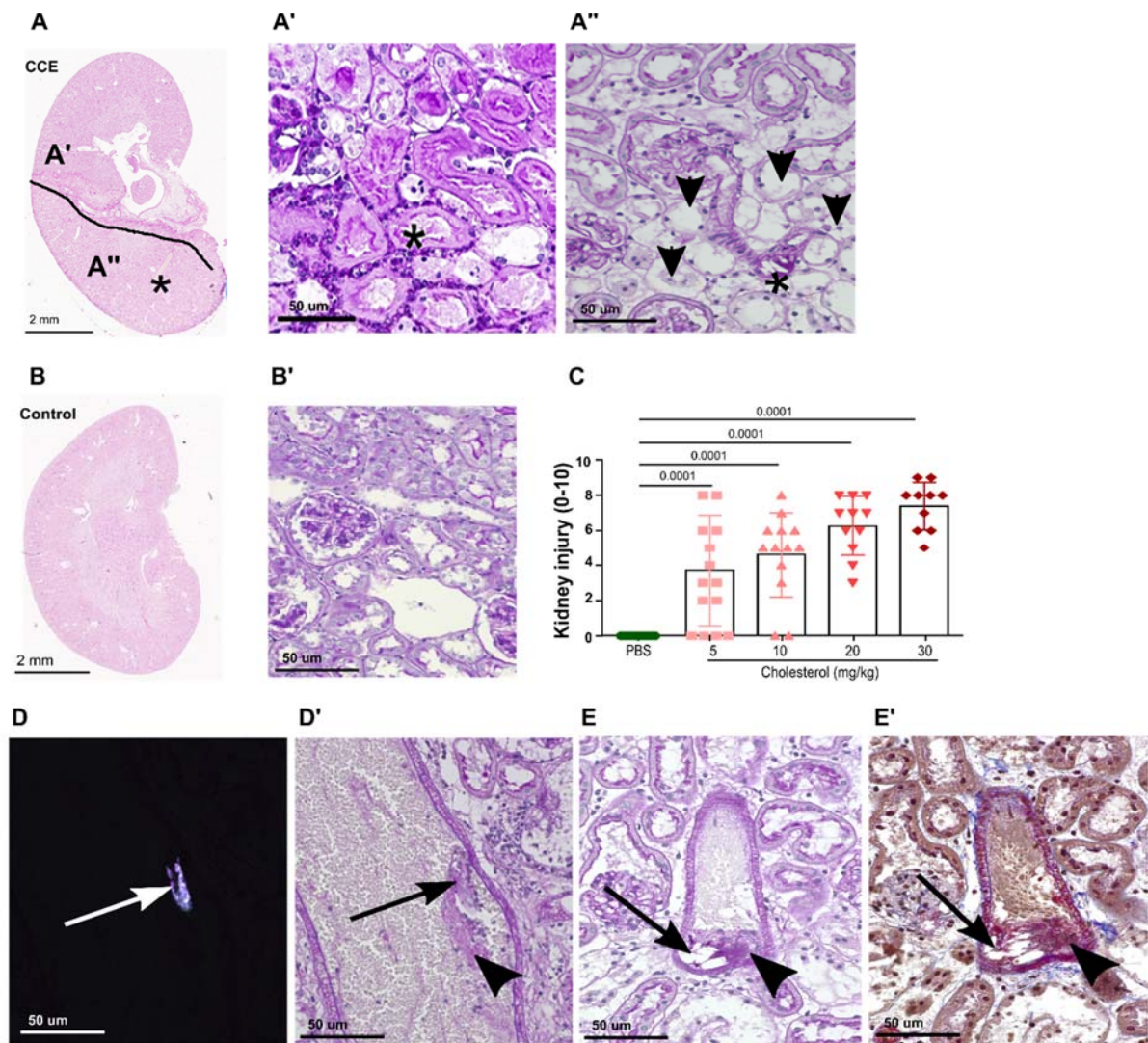


Figure 12. Crystal clots-induced kidney injury at 24 h. A: Representative image of PAS-stained CCE kidney sections. A': Infarct (*) demarcation (tubular damage, bleeding, neutrophils). A'': Diffuse (tubular) ischemic damage and arterial crystal (*). B-B': PAS-stained healthy kidney. C: CC injection-induced kidney injury score. D-E': CC and related thrombosis inside the kidney artery in PAS-stained CCE kidney. E': CC cleft and thrombosis in thrombin-stained CCE kidney. All quantitative data are means \pm SD.

TUNEL staining also showed massive dead cells presenting inside CC perfused kidney (Fig. 13A). Inflammation is the response of the immune system to an injurious trigger. Therefore, the inflammatory component in the CC-perfused kidney was evaluated. Immunostaining for the neutrophil marker Ly6B2+ revealed an increased infiltration of neutrophils into the tubulointerstitial space of CC-perfused kidneys compared to control kidneys (Fig. 13B). Immunostaining for the endothelial cell marker CD31 indicated vascular injury and obstruction in CC-perfused kidneys (Fig. 13C).

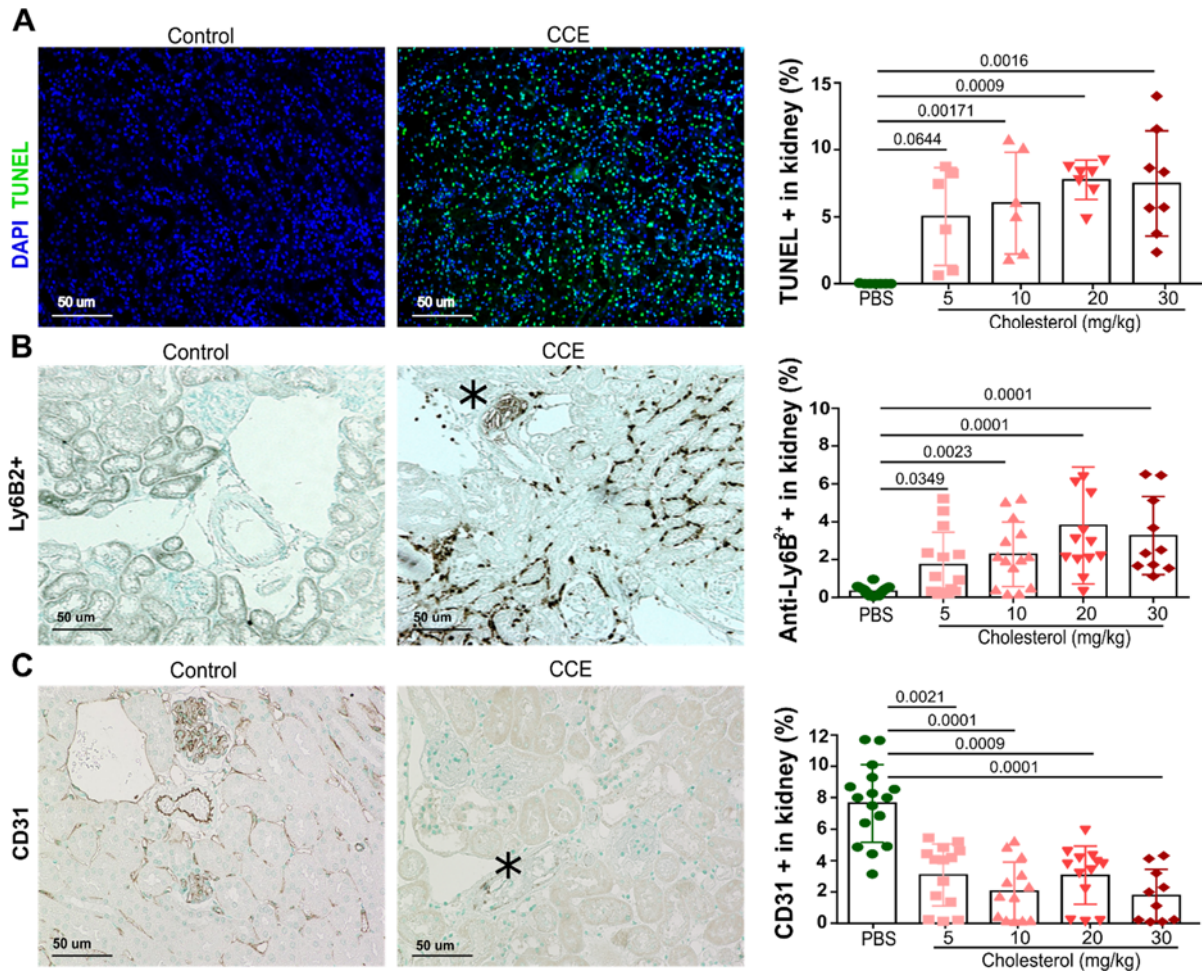


Figure 13. Crystal clots-induced kidney inflammation, and vascular injury at 24 h. A: Representative images of TUNEL-stained sections, and TUNEL + dead cells in CCE and control kidneys. B: CC injection-induced neutrophils infiltration. C: CC injection-induced vascular injury. All quantitative data are means \pm SD.

To identify the number of arteries obstructed with CC, we performed α SMA and fibrin co-immunostaining. I distinguished interlobar, arcuate, and interlobular kidney arteries by size and location, and those arteries were graded into either completely, partially or non-obstructed (Fig. 14A). Results showed that all those arteries showed partial and complete obstructions at 24 h, and the ratio of obstructed arteries was CC dose-dependent (Fig. 14B-D'). The 10 mg/kg of CC was selected for further studies to detect diseases, improvement, or aggravation. Taken together, CC injection-induced kidney injury, inflammation, and vascular injury by forming fibrin positive crystal clots inside arteries at 24 h.

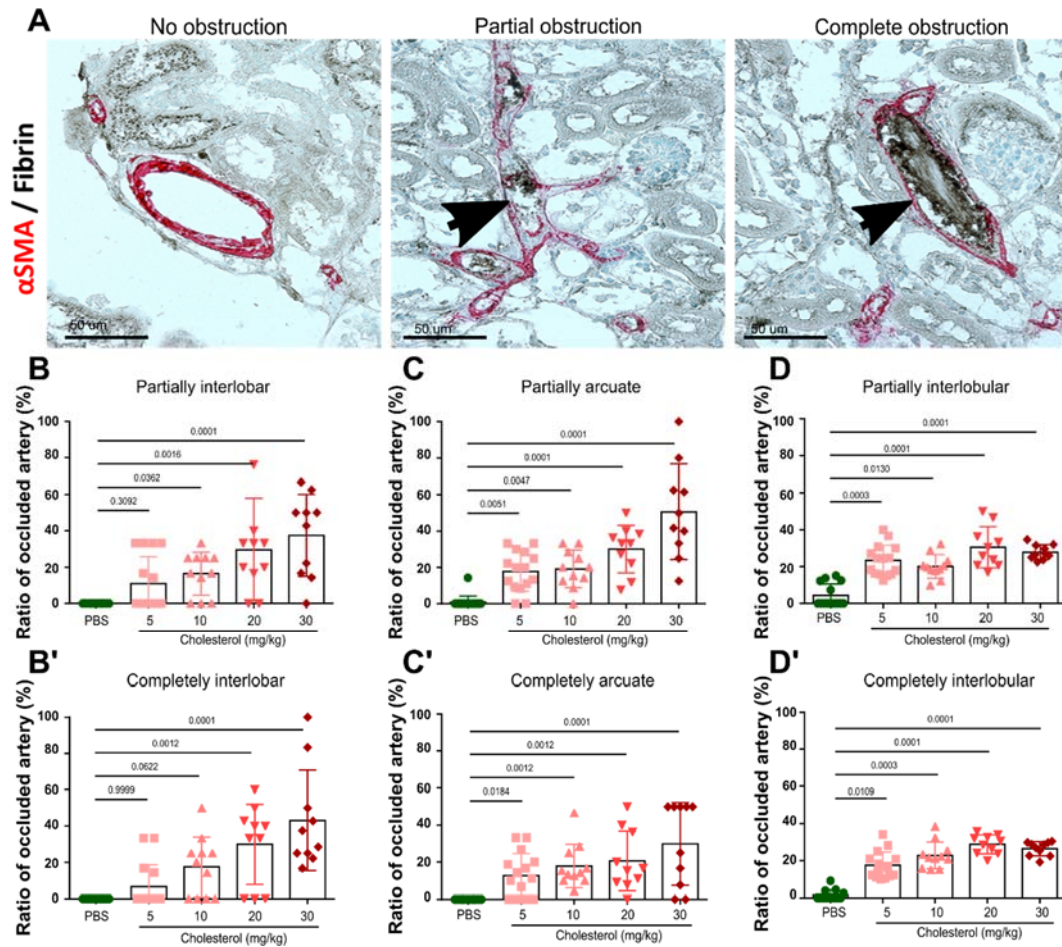


Figure 14: Quantification of CC-induced occlusion of intrarenal arteries of different sizes. A: Immunostaining for α SMA and fibrin displays partial or complete arterial occlusions. Arrows point to CC-thrombosis. B-D: Partially obstructed interlobar, arcuate, and interlobular arteries in different groups. B'-D': Completely obstructed arteries in different groups.

4.1.3 Crystal clots obstruct intrarenal arteries at 24 h

PAS section shows an intrarenal artery completely occluded by CC and some surrounding foreign-body granuloma-like matrix, indicating that crystal clots occurred some time ago (Fig. 15A). To better characterize the matrix surrounding CC that leads to vascular obstruction further immunostainings were performed, for example for Ly6B2+, MPO, and Cit-H3 and found neutrophils and NETs present (Fig. 15D-F). This indicates that neutrophils and NETs are involved in crystal clot formation. As fibrin was also present in crystal clots, and by staining for CD61 a marker of platelets we confirmed that beyond fibrin also platelets were involved in clots formation (Fig. 15B-C). The essential cause of arterial thrombosis in this model is CC that accumulates in the artery wall initiating the development of thrombosis. In the blood,

platelets act as guards of vascular integrity and can be immediately activated and aggregated at the vascular injury sites to form a primary haemostatic plug (157). When an atheromatous plaque ruptures or CC in the arterial wall, platelets are immediately mobilized through the interaction with collagen and vWF via specific surface receptors (158). Following platelets recruitment to the arterial wall, activated platelets release their granule contents, which in turn promoting platelet recruitment, adhesion, aggregation, and activation that forms a cascade cycle leading to the rapid development of the thrombus. Of note, CC was a minor component of the vascular occlusions, while vascular obstruction was rather more related to CC-triggered arterial thrombosis which ultimately obstructed many intrarenal arteries.

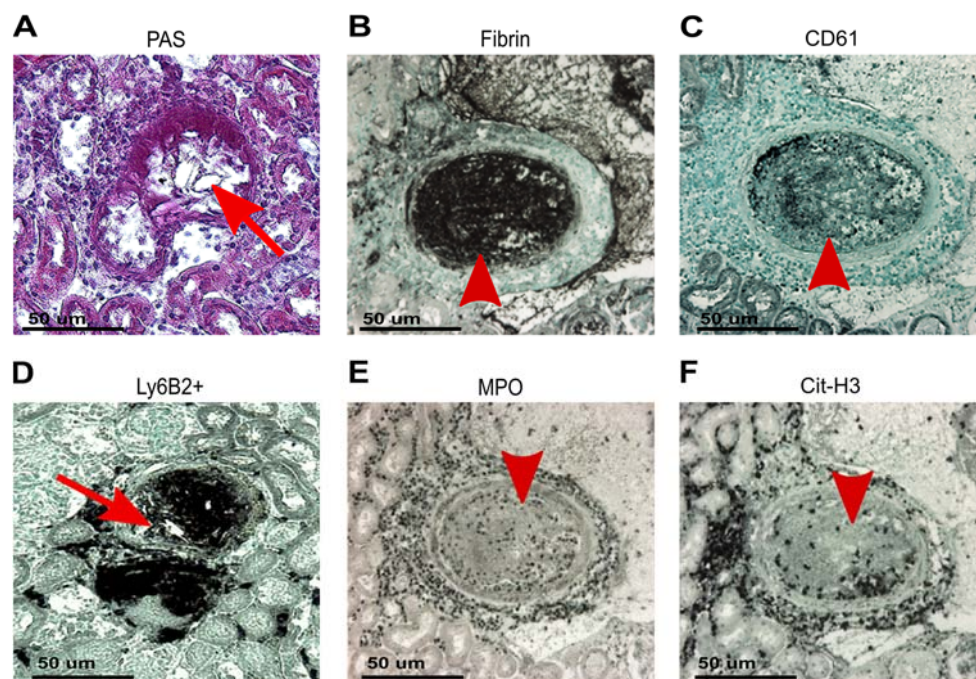


Figure 15. Components of intraarterial crystal clots. A: PAS-stained section showed that intravascular crystals are surrounded by a biological mass. Immunostaining of crystal clots with prominent positivity CC for fibrinogen (B), platelets (C), and neutrophils (D). E-F: NET formation illustrated by extracellular positivity of cit-H3 and MPO.

4.1.4 Time-dependent intravascular crystal clot formation

To verify the process of clot formation triggered by CC inside renal arteries, C57BL/6J WT mice were sacrificed at 3, 6, 12 h after CC injection. Although kidneys displayed swelling 3 h after CC injection compared to PBS control kidneys (Fig. 16A-A'), no infarction inside kidneys was detectable (Fig. 16B-B'). PAS staining did not show injury at 3 h (Fig. 17A). Immunostaining for Ly6B2+ revealed few neutrophils in the interstitial space (Fig. 17B). The α SMA/fibrin staining

showed very few obstructed arteries at 3 h (Fig. 17C-C'). At 6 h, kidneys displayed swelling and neutrophil infiltration (Fig. 16A, 17B), similar to the 3 h result. PAS staining showed tubular injury in CCE kidney (Fig. 16C), and more partial obstructed arteries (Fig. 17C-C'). At 12 h, CC-perfused kidneys showed significantly increased infarct size (Fig. 16B), neutrophil infiltration (Fig. 17B), and obstructed interlobar, arcuate, and interlobular arteries, especially the complete obstructed arteries number increased (Fig. 17C-C'). PAS score revealed massive tubular necrosis (Fig. 17A). At the cellular level, arterial thrombosis largely consists of activated platelets as their distinct ability to adhere to the injured vascular wall and aggregate to additionally activated platelets under rapid blood flow (159), therefore, platelets and blood coagulation play a critical role in promoting arterial thrombus growth.

Taken together, CC-induced intraarterial clot formation was time-dependent. CC triggered arterial thrombosis obstructing renal vessels, not CC itself. The vascular obstruction induced ischemia-related AKI and kidney infarction was also time-dependent.

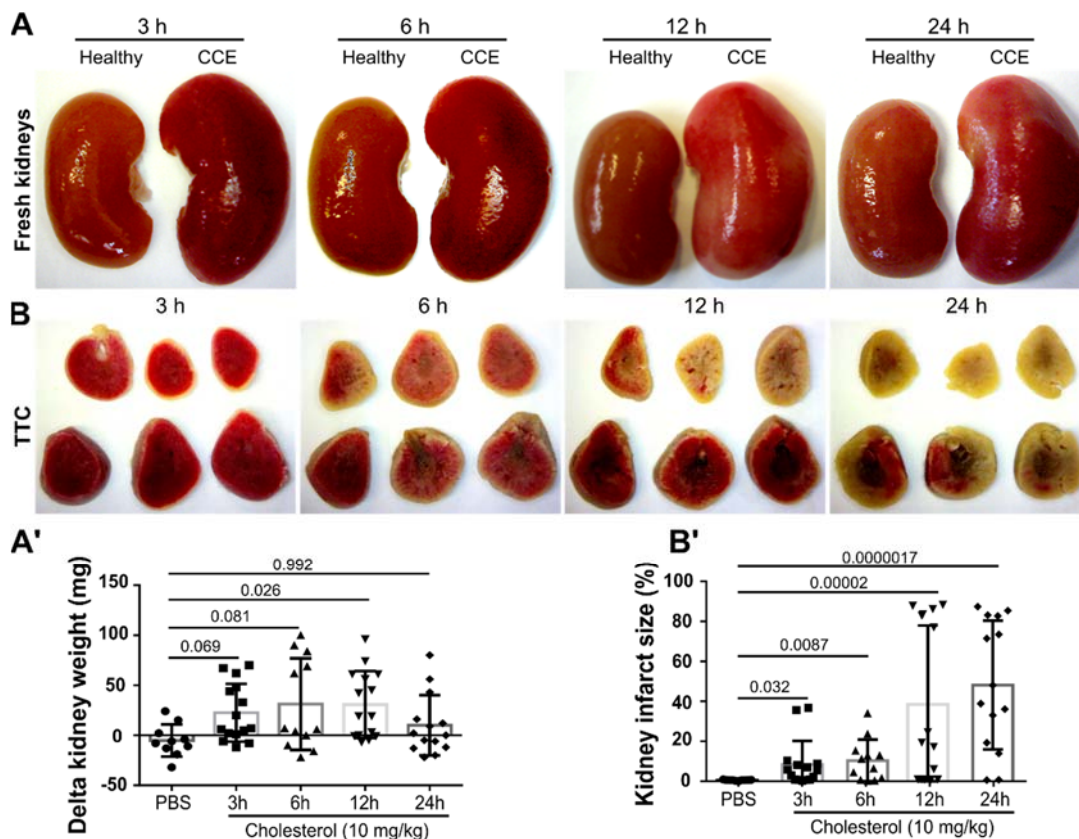


Figure 16. Time-dependent infarction in CCE kidney. A: Representative images of fresh kidney and delta kidney weight. B: TTC-stained CCE kidney, and quantified infarct size (B').

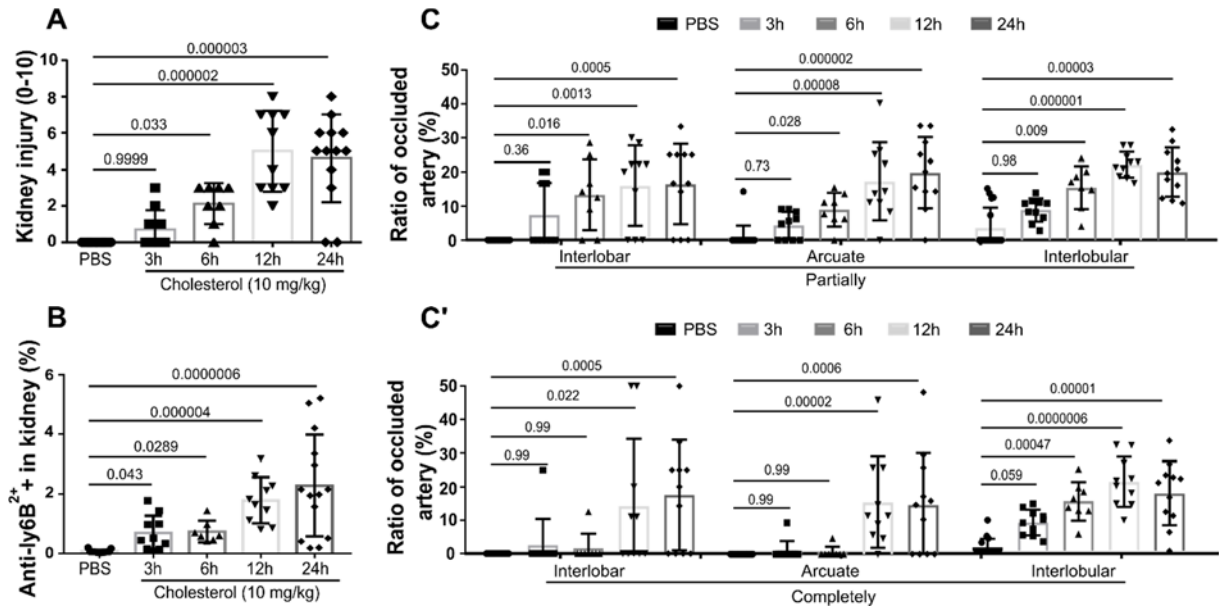


Figure 17. Time-dependent inflammation, injury, and intrarenal clot formation in CCE kidney. A: CCE-related kidney injury was time-dependent. B: CCE-related inflammation was time-dependent. C-C': Time-dependent intrarenal arterial occlusion. All quantitative data are means \pm SD.

4.1.5 The influence of gender on cholesterol crystal embolism

To test for the role of gender on CC injection-related AKI, and infarction, 10 mg/kg CC were injected to male and female C57BL/6J mice. Female mice showed similar results in kidney swelling (Fig. 18A), kidney infarction (Fig. 18B), and GFR loss (Fig. 18C). Accordingly, microscopic analysis revealed CC injection-induced severe kidney injury (Fig. 18D), a mass of neutrophil infiltration (Fig. 18E), vascular injury (Fig. 18F), and arterial thrombosis formation to the same extent (Fig. 18G-G'). In conclusion, gender did not affect CCE-related outcomes at 24 h. Therefore, C57BL/6J male mice were selected for further studies.

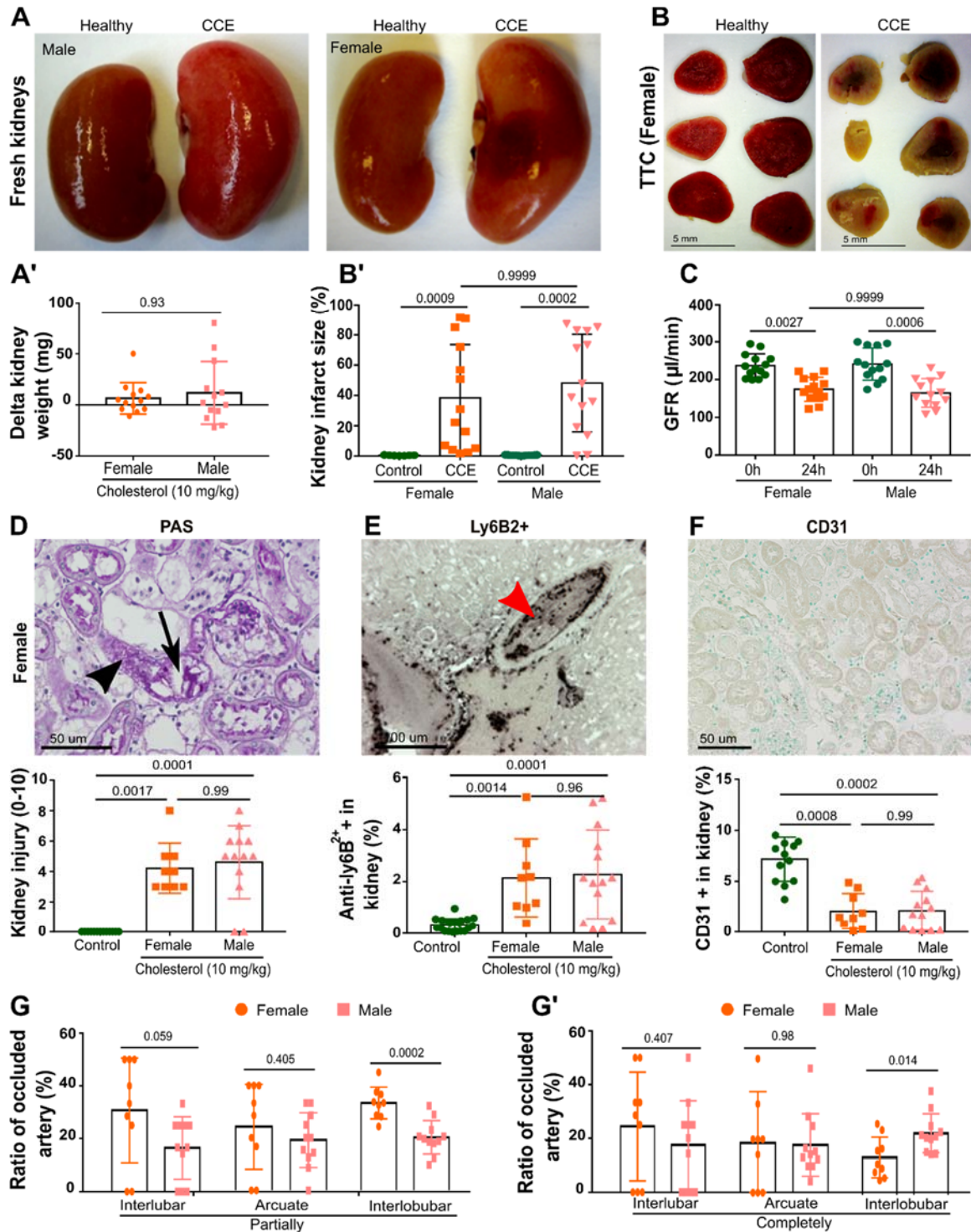


Figure 18. The effect of gender on CC injection-related AKI, infarction, and intrarenal arterial occlusion at 24 h. A: Fresh kidneys in male and female mice upon kidney CCE. A': Delta kidney weight. B-B': TTC-stained kidney slices and quantified infarct size. C: CC injection-induced GFR loss in male and female mice. D: Representative image of PAS-stained CCE kidney of the female. The arrow shows CC cleft and related thrombosis inside the renal artery in females. Male and female CCE kidneys show similar injury at 24 h. E: Neutrophils infiltration in male and female CCE kidneys. F: CC injection-induced vascular rarefication in male and female mice. G-G': Intrarenal arterial occlusion in male and female CCE kidneys. All quantitative data are means \pm SD.

4.1.6 Cholesterol crystal embolism-induced acute kidney disease

Time-course analysis showed that after 14 days GFR recovered back to baseline (Fig. 19A) and infarct size declined (Fig. 19B). From the PAS stained CCE kidney sections, at 3 days, the CCE shows obvious tubular cell death in all compartments, the arrow pointing the thrombi in a kidney vessel, the interstitial can see immune cell infiltration and edema (Fig. 19C, F, G). In this time, the contralateral kidney is normal and healthy (Fig. 19C, F, G). After 7 days, the CCE kidney displayed tubular necrosis, tubular casts and tubular atrophy, strong inflammation, in particular the massive infiltration of neutrophils, as well as interstitial fibrosis (Fig. 19D, F, G). While the contralateral kidney also showed tubular stress of mild dilation and loss few of brush borders (Fig. 19D, F, G). At 14 days, CCE kidney had strong monocytic inflammation, interstitial fibrosis, and tubular atrophy, tubular casts. The contralateral kidney showed tubular stress, focal interstitial inflammation, focal interstitial fibrosis, and tubular atrophy. Thus, this CCE model induced AKD within 2 weeks, associated with tubular injury, interstitial edema, immune cell infiltration especially neutrophils and macrophages leading to the secretion of inflammatory cytokines and thrombosis obstruction.

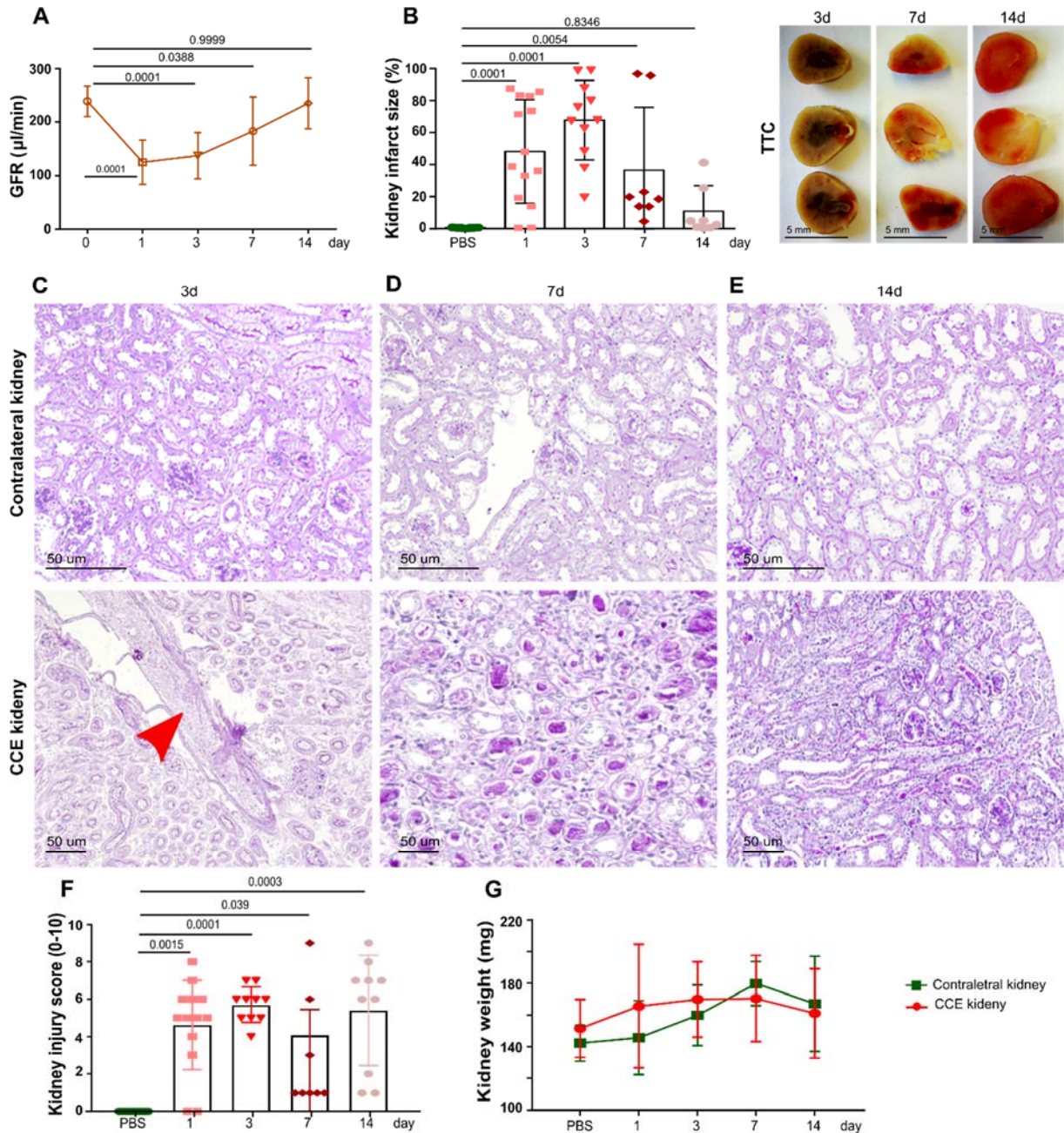


Figure 19. CCE-induced acute kidney disease within 2 weeks. A: GFR change after CCE induction within 14 days. At 14 d, GFR returns to the baseline. B: CCE-induced kidney infarction at days 3, 7, and 14. C-E: Representative images of PAS-stained CCE and contralateral kidney sections at day 3, 7, and 14. F: Kidney injury score after CCE induction 3, 7, and 14 days. G: Kidney weights of contralateral and CCE. From 14 d, the contralateral kidney compensates for the function loss by hypertrophy.

4.2 Role of plasmatic coagulation in crystal clot formation

Besides the platelets-dependent hemostasis, fibrinolysis is another important hemostatic pathway and it is rapidly activated after the clot has been fixed by the coagulation cascade (160). Fibrinolysis can degrade the fibrin polymers to eliminate blood clots and thereby

promotes physiological wound healing and hemostasis. Plasminogen is known as the central component of the fibrinolytic pathway, which can transform into the serine proteinase plasmin by two main types of plasminogen activators (PA), tissue PA (tPA) and urokinase PA (uPA). In the circulating, the plasmin digests fibrin and various extracellular matrix proteins and thereby regulates hemostasis and thrombus development (161). The PA inhibitors and plasmin inhibitors produced under steady conditions are tightly involved in the fibrinolytic process (162). Therefore, a fine and complex dynamic equilibrium between consecutive fibrin generation and fibrinolysis determine the constituents and sizes of arterial thrombus. Using anticoagulants to reduce thrombin generation or fibrinolytic to lyse the fibrin component of thrombi both influence managing arterial thrombosis.

The finding from fibrinogen staining confirmed that fibrin was present in crystal clots inside CC perfused kidney. Therefore, the new model should be suitable to mimic the *in vivo* conditions of CCE and to study the positive effects of anticoagulants on the CCE outcomes. Hence, this study selected anticoagulant heparin and the fibrinolytic agent urokinase to test their effects on CC-induced CCE-related AKI and kidney infarction at 24 h.

To do so, mice received heparin or urokinase treatment 1 h after CC injection, control group mice received NaCl. At 24 h, both heparin- and urokinase- treatment significantly reduced the CC perfused kidneys swelling compared to the NaCl control (Fig. 20A). Moreover, heparin- and urokinase- treated kidneys showed a significant reduction in infarct size (Fig. 20B). Furthermore, both treatments significantly reduced the numbers of arterial occlusions in interlobar, arcuate, and interlobular, albeit the crystal component persisted (Fig. 21A). Both treatments also completely protected mice from GFR loss (Fig. 21B).

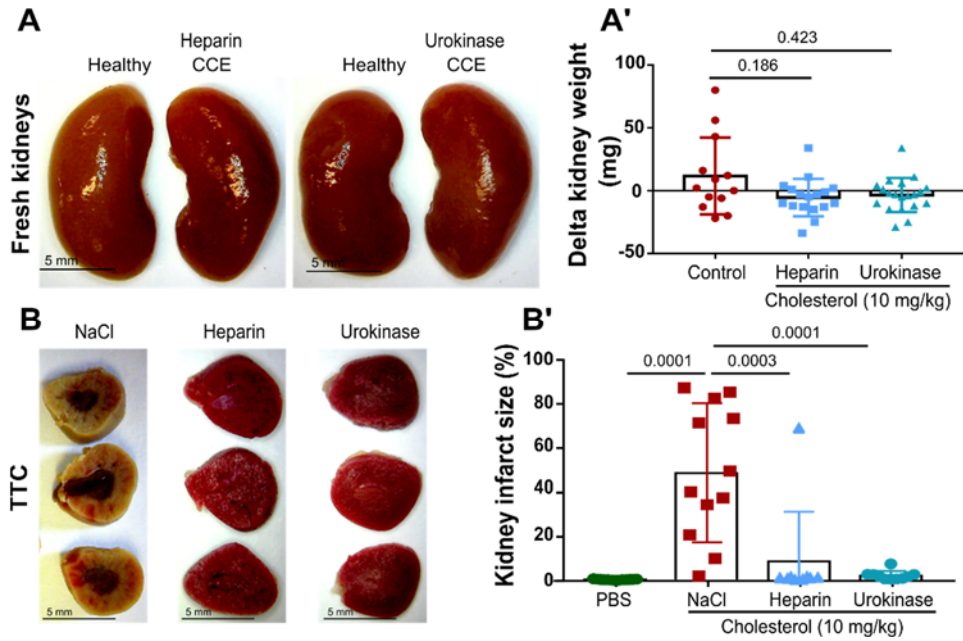


Figure 20. Anticoagulants prevent kidney infarction at 24 h. A: Fresh kidneys in the heparin and urokinase group. A': Delta kidney weight in control, heparin- and urokinase-treated groups. B-B': TTC-stained kidneys and quantified infarct size. All quantitative data are means \pm SD.

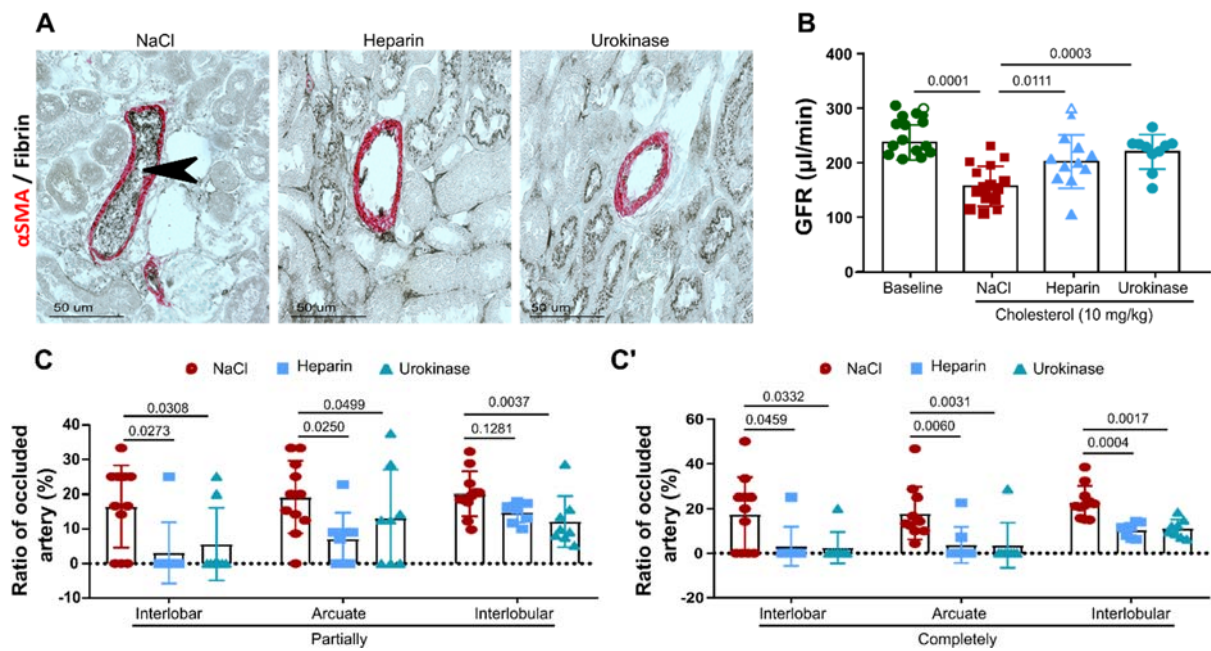


Figure 21. Anticoagulants protect from AKI and arterial occlusions at 24 h. A: Representative α SMA/fibrin-stained section in heparin and urokinase treatment groups. C-C': Occlusion of renal arteries of various sizes were identified and quantified. B: CC injection-induced GFR loss in heparin and urokinase treatment groups. All quantitative data are means \pm SD.

As expected, PAS staining revealed that heparin and urokinase both significantly reduced tubular necrosis, dilation, brush border loss, lumen casts, and interstitial edema (Fig. 22A). As

well as both treatments abolished TUNEL+ dead cells (Fig. 22B). Moreover, the numbers of infiltrating neutrophils and the loss of CD31+ blood vessels were dramatically reduced by heparin and urokinase treatments compared to NaCl controls (Fig. 22C-D). Taken together, not the CC *per se* but rather crystal-induced clots caused arterial obstruction, tissue infarction, and organ failure.

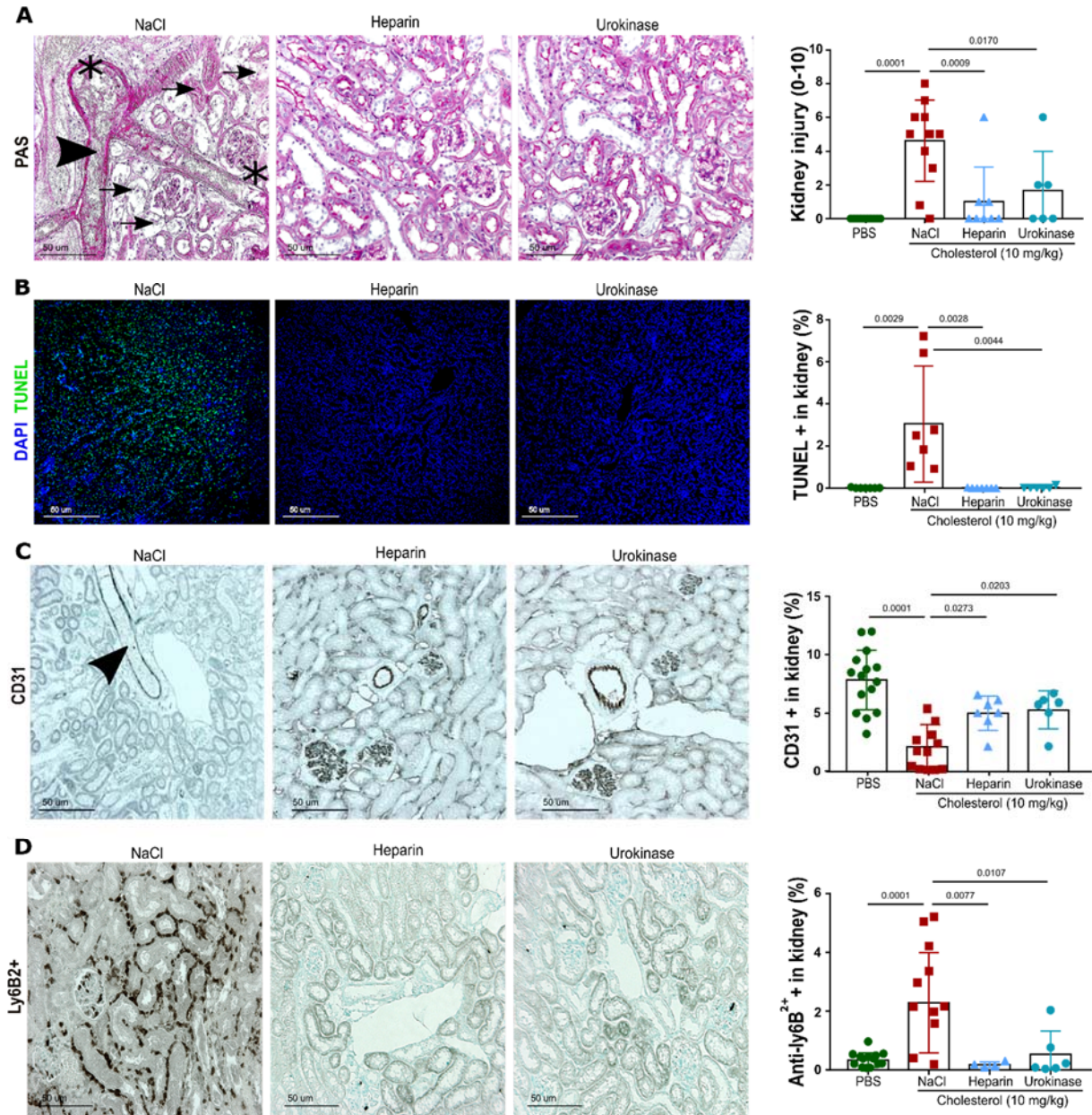


Figure 22. Anticoagulants protect from cell death and inflammation at 24 h. A: Representative PAS-stained section and kidney injury scores. B: Representative TUNEL-stained section and TUNEL + dead cells in CCE kidneys. C-D: Representative CD31- and Ly6B2+-stained sections, and quantified vascular injury, and neutrophils infiltration. All quantitative data are means \pm SD.

4.3 Role of platelets in crystal clot formation

CC was only a minor component of vascular occlusions and vascular obstruction was rather related to the surrounded materials with the presence of platelets as indicated by CD61+ staining (Fig. 14C) the typical component of arterial thrombi (160). Platelet degranulation can modulate coagulation and fibrin clot formation due to the release of granular resident fibrinogen, ATP, and other factors. To address the role of platelets in the formation of crystal clots and CCE-related AKI and infarction, a set of experiments were performed *in vivo* and *in vitro*. Many pharmacological antiplatelet therapies have been developed to treat arterial thrombosis e.g. by targeting the P2Y12 receptor (163). Clopidogrel as one typical antiplatelet molecule was selected for my study.

4.3.1 Clopidogrel completely inhibited cholesterol-mediated pathological processes in the kidney by preventing crystal clots formation

To do so, mice received the purinergic platelet P2Y12 receptor antagonist clopidogrel. At 24 h, clopidogrel significantly reduced kidney swelling (Fig. 23A). As expected, clopidogrel also showed complete protection from GFR loss (Fig. 23B), and kidney infarction (Fig. 23C).

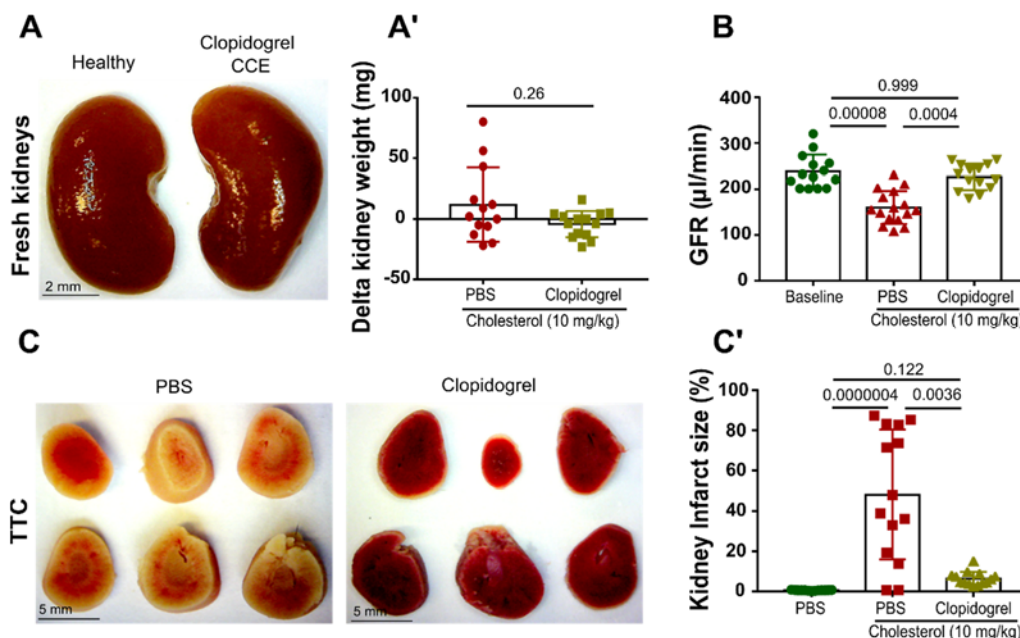


Figure 23. Clopidogrel protects from acute infarction and AKI at 24 h. A: Representative kidney images of healthy and clopidogrel-treated mice with CCE. A': Delta kidney weight. B: Clopidogrel completely protected mice from GFR loss. C-C': TTC-stained kidney and quantified infarct size. All quantitative data are means \pm SD.

Histological analysis of α SMA/fibrin stains found that clopidogrel significantly decreased the number of occluded arteries compared to the control group, especially it completely abolished the completely obstructed interlobar arteries (Fig. 23A-B'). Furthermore, microscopic analysis revealed that clopidogrel significantly reduced tubular necrosis, dilation, lumen casts, interstitial edema, as well as vascular injury and neutrophil infiltration (Fig. 24C-E). Taken together, CC injection-mediated pathological processes in the kidney were completely inhibited by clopidogrel. CC occlude arteries by forming crystal clots consisting of platelets, which were central for CCE-related arterial occlusion, organ failure, and tissue infarction.

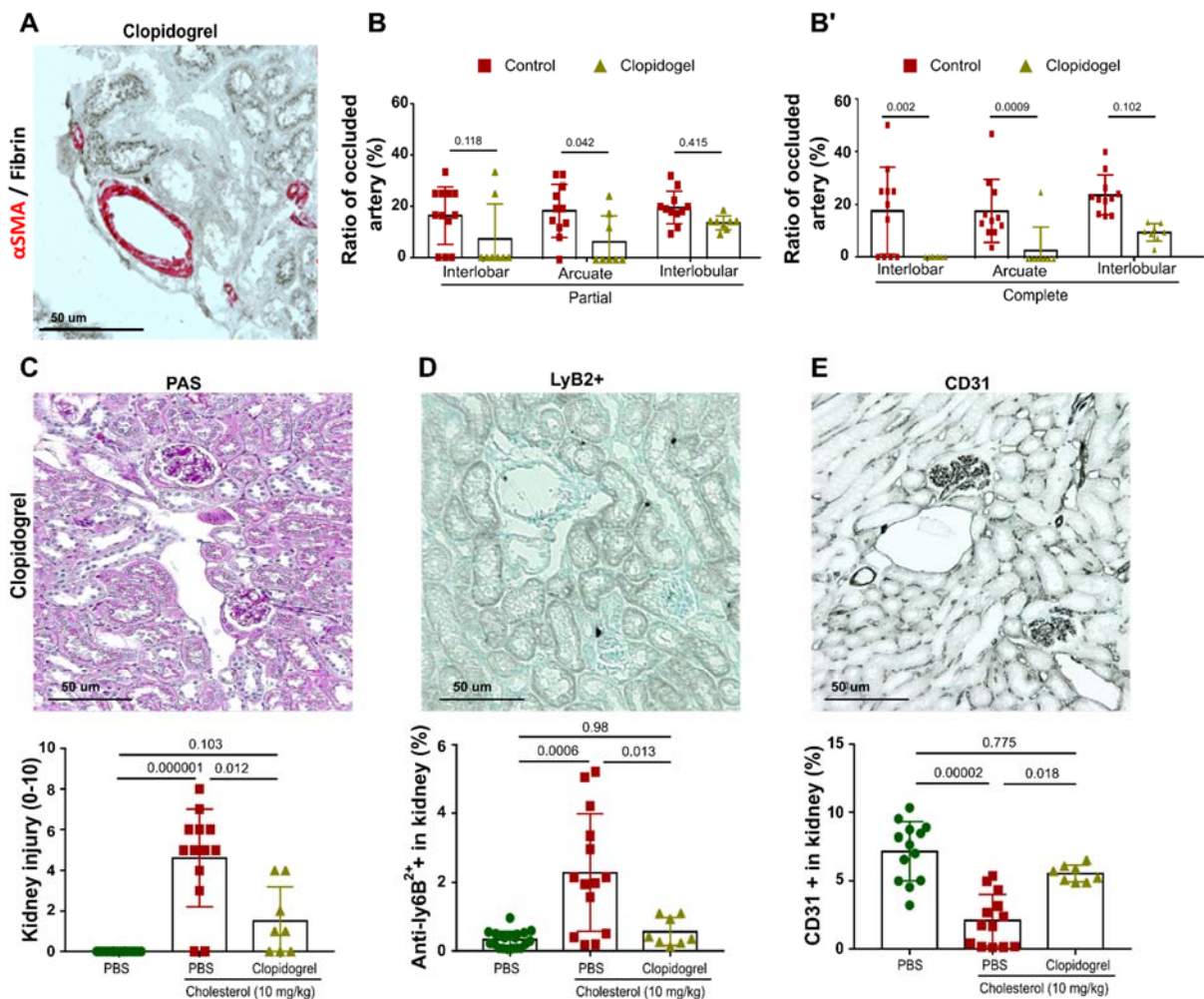


Figure 24. Clopidogrel prevents CC-induced AKI, inflammation, and arterial clot formation at 24 h. A: Representative α SMA/fibrin-stained section of the clopidogrel treatment group. B-B': Occlusion of renal arteries of various sizes were identified and quantified. C-E: Representative image of PAS-, Ly6B2⁺- and CD31-stained CCE kidney of the clopidogrel treatment group. Clopidogrel significantly reduced kidney injury, neutrophil infiltration, and vascular rarefaction. All quantitative data are means \pm SD.

4.4 Role of neutrophils in crystal clots formation

Crystal clot surrounding material stained also positive for Ly6B2+ neutrophils, although weakly positive for histological markers of NETs including ecDNA, citrullinated histone H3, and cytoplasmic proteins such as elastase or granular proteins such as MPO(164). It has been previously reported that neutrophils contribute to arterial thrombosis by releasing NETs, a process can be initiated by activated platelets (165).

To further test the potential contribution of neutrophils to crystal clot formation, mouse neutrophils were depleted with anti-Ly6G antibody before CC injection. Flow cytometry was employed to confirm blood neutrophils were depleted (Fig. 27A). According to flow cytometry results, mice received the anti-Ly6G antibody 24 h before CC injection. At 24 h, neutrophil depleted mice had completely extinguished the periinfarct neutrophil infiltrates (Fig. 27B), and significantly decreased kidney infarct size compared to the IgG control group (Fig. 27C).

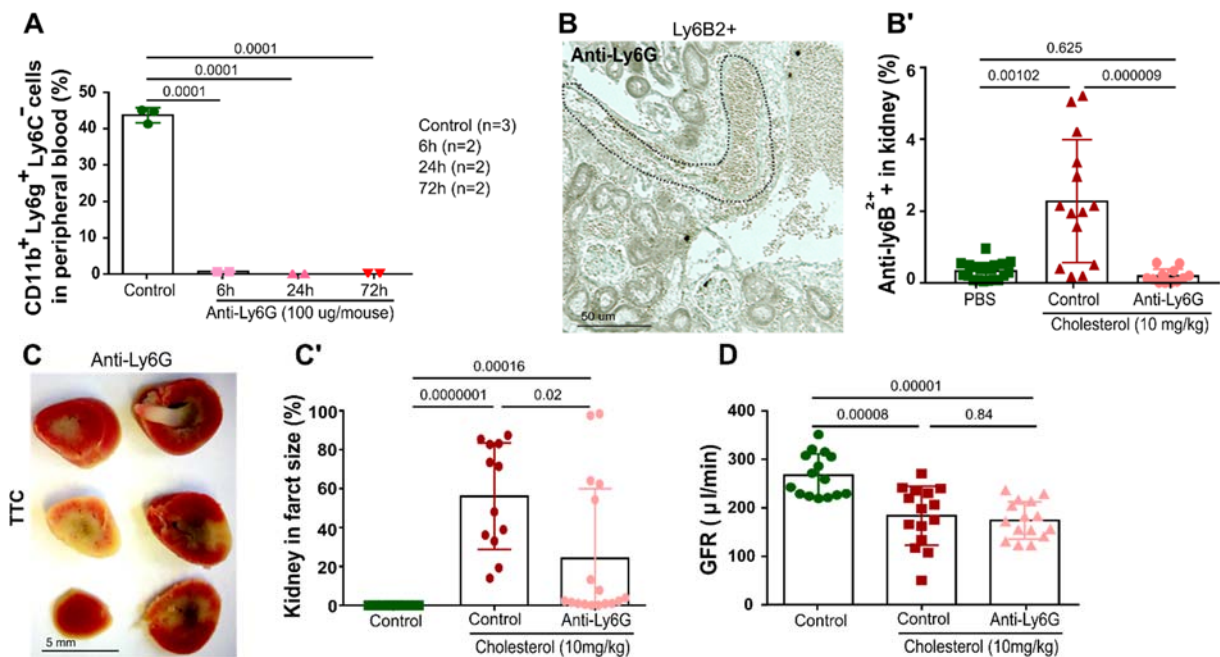


Figure 27. Neutrophil depletion protects from acute kidney infarction but not AKI at 24 h. A: FACS analysis of neutrophils in blood after anti-Ly6G administration 6, 24, and 72 h. B: Representative image of Ly6B2+-stained CCE kidneys in the anti-Ly6G-treated group. B': Anti-Ly6G treatment significantly reduced neutrophil infiltration into the CCE kidney compared to the control IgG group. C: TTC-stained kidney slices in the anti-Ly6G group. C': Anti-Ly6G treatment significantly reduced acute kidney infarction. D: Neutrophil depletion does not affect CCE-induced GFR loss. All quantitative data are means \pm SD.

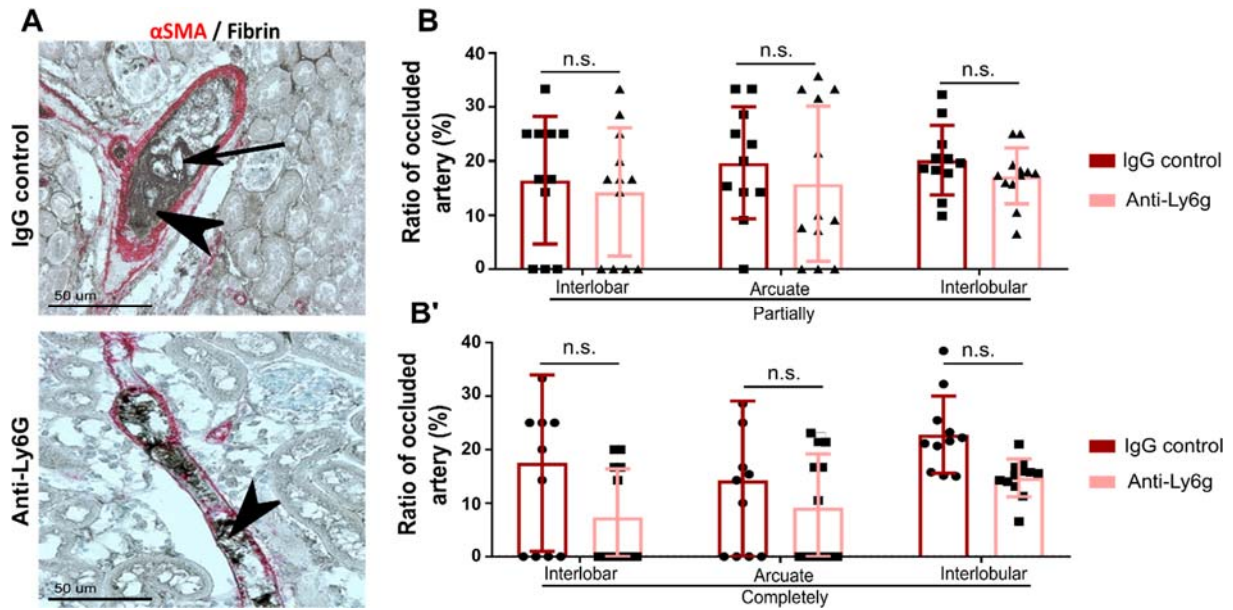


Figure 28. Role of neutrophils in CCE-induced CC clot inside kidney arteries. A: Representative images of α SMA/fibrin-stained CCE kidneys in control and anti-Ly6G treatment groups. B-B': Ratio of occluded artery numbers of various sizes. All quantitative data are means \pm SD.

In contrast, this had no significant effect on GFR loss (Fig. 27D), or arterial obstructions (Fig. 28A-B'). PAS and immunostainings revealed anti-Ly6G treatment has no significant effects on overall kidney injury or vascular injury of CCE kidney (Fig. 29A-C). To find reasons for the inconsistent result, more immunostainings were performed, and found mononuclear cells present in crystal clots, partially replacing the missing neutrophils in the crystal clots (Fig. 29D). Additionally, Feulgen's staining found that ecDNA was still present in crystal clots of the neutrophil depleted kidneys (Fig. 29E), and neutrophil depletion had no significant effect on the artery occlusions with ecDNA (Fig.29F).

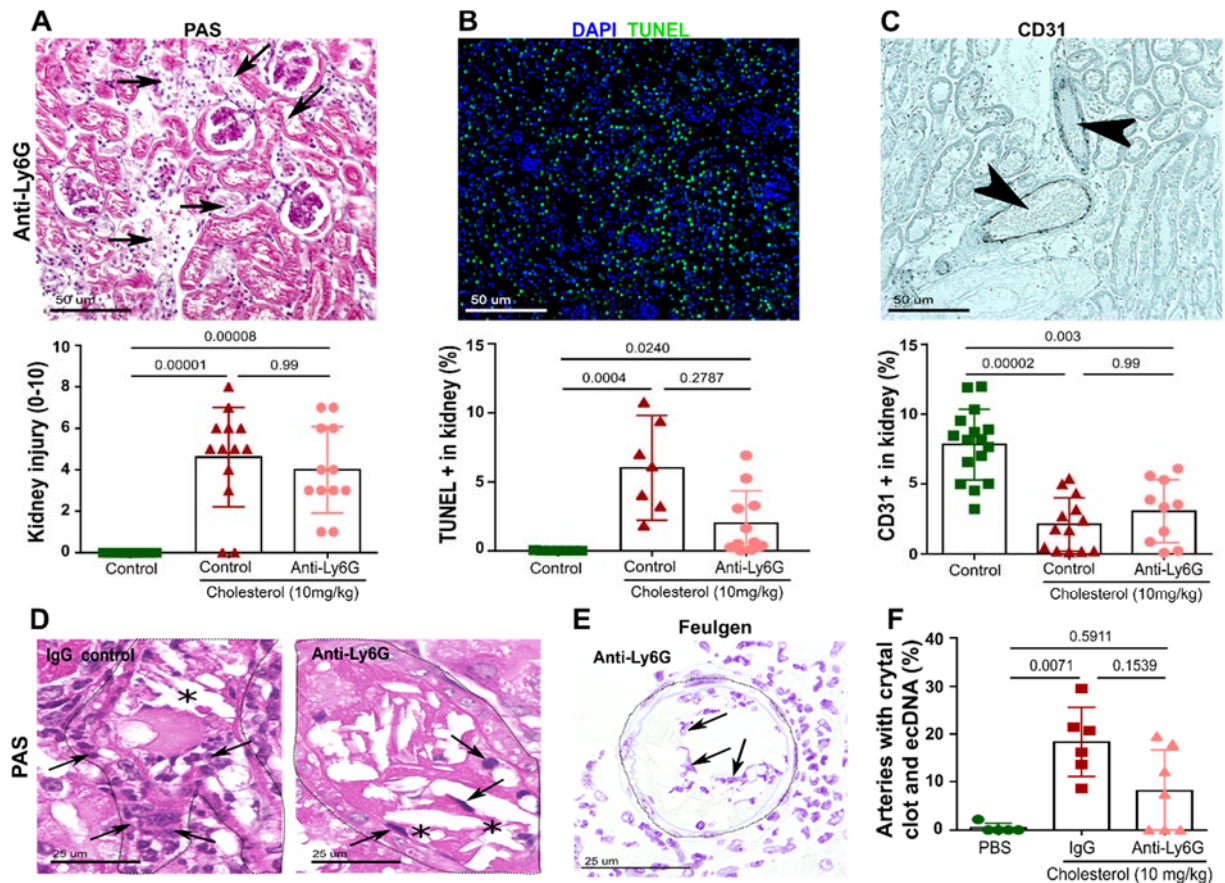


Figure 29. Role of neutrophils in CCE-induced tubular injury and vascular injury at 24 h. A: Representative images of PAS-stained CCE kidneys in the anti-Ly6G treatment group and kidney injury score. B: Representative images of TUNEL-stained CCE kidney in the anti-Ly6G treatment group and TUNEL + dead. C: Representative images of CD31-stained CCE kidney in the anti-Ly6G treatment group and vascular injury. D: PAS-stained CCE kidneys in the IgG or anti-Ly6G-treated group. Left panel (IgG) shows obstructed artery with clots + neutrophils (shown as arrows), right panel (anti-Ly6G) shows obstructed artery with clots + few mononuclear cells (shown as arrows). * shown cholesterol clefts. E: Feulgen staining shows ecDNA presence in crystal clots of anti-Ly6G-treated kidneys. Arrows indicate ecDNA. F: Quantification of clots inside the artery with ecDNA in healthy, IgG control, and anti-Ly6G treatment kidneys. All quantitative data are means \pm SD.

Neutrophils release NETs via different intracellular pathways the decondensation of nuclear chromatin is the first step that can through peptidyl arginine deiminase type IV (PAD4)-catalyzed histone citrullination or neutrophil elastase-mediated histone cleavage, the following is chromatin extrusion after the nuclear envelope rupture. Therefore, as another approach, Cl-amidine was used to block PAD4-dependent NETs formation *in vivo*. Accordingly, Cl-amidine treatment showed similar results as neutrophil depletion, this had no significant effects on kidney swelling, kidney infarct, or GFR loss (Fig. 30A-C'). More immunostainings also found Cl-amidine treated CCE kidneys show similar injury, neutrophil infiltration, or vascular

injury with control CCE kidneys (Fig. 31A-C), as well as no effects on vascular occlusion (Fig. 31D-E'). Taken together, perilesional neutrophils largely contribute to CCE-induced perifocal infarction but few to crystal clot formation and hence to CCE-related kidney failure.

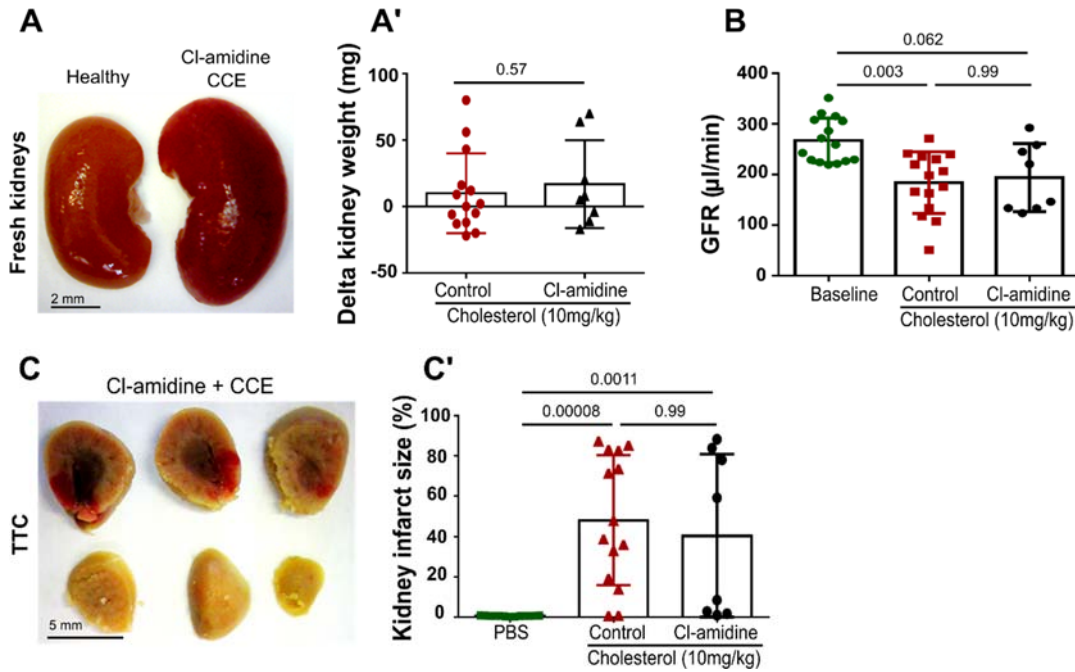


Figure 30. Role of NETs in CCE-induced kidney infarction and AKI at 24 h. A: Fresh kidneys of healthy and Cl-amidine-treated groups. A': Delta kidney weight. B: GFR loss in control and Cl-amidine-treated groups. C-C': The TTC method quantified kidney infarct size. All quantitative data are means \pm SD.

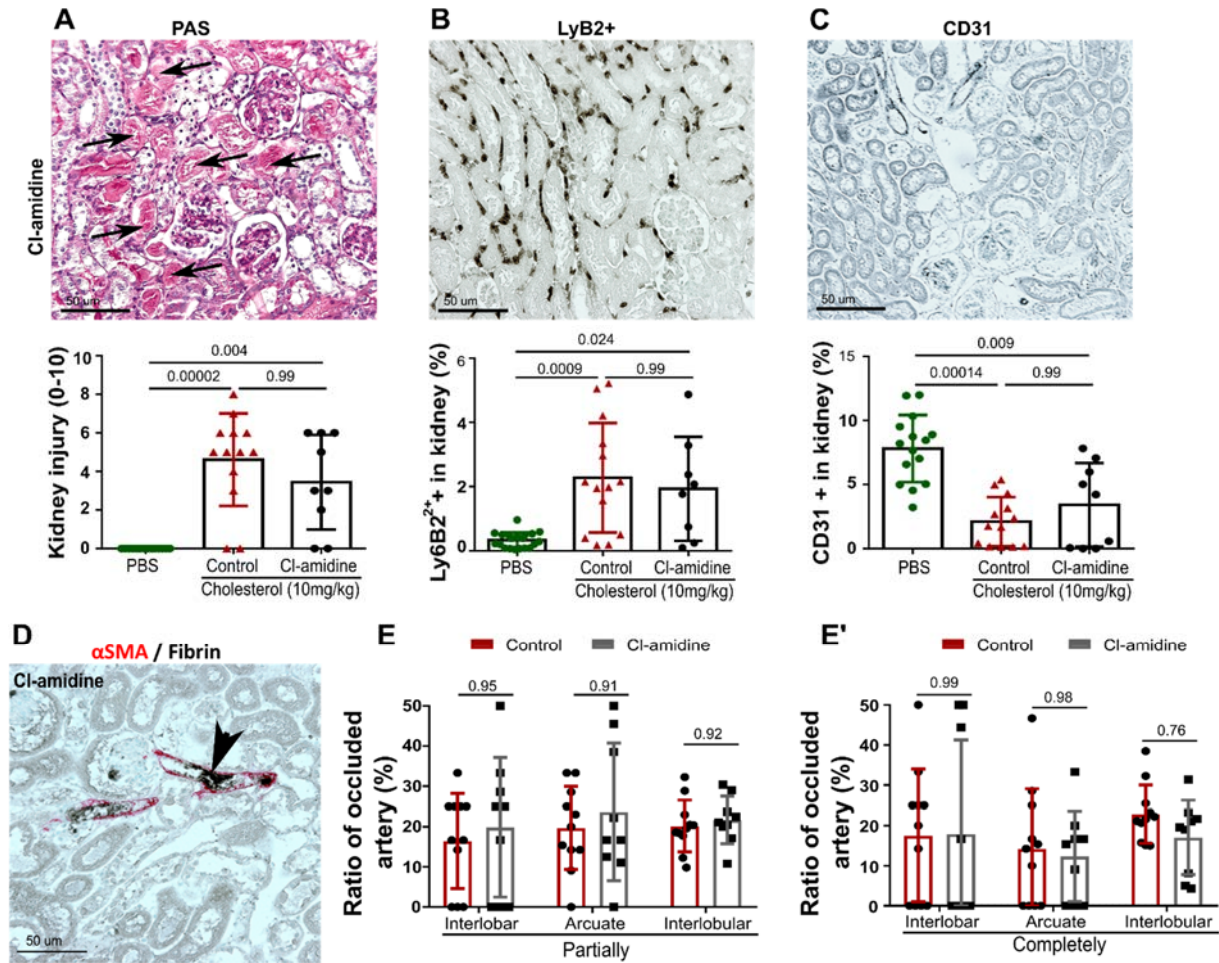


Figure 31. Role of NETs in CCE-induced injury, inflammation, and arteries obstruction at 24 h. A: Representative image of PAS-stained CCE kidneys of the Cl-amidine group and kidney injury score. B: Representative images of Ly6B2⁺-stained CCE kidney of the Cl-amidine group and neutrophil infiltration into CCE kidneys. C: Representative images of CD31-stained CCE kidneys and vascular injury analysis. D: Representative images of α SMA/fibrin-stained CCE kidneys of the Cl-amidine group. E-E': Ratio of occluded artery numbers of various sizes. All quantitative data are means \pm SD.

4.5 Role of necroinflammation in CCE-induced kidney injury

It has been previously reported that mixed lineage kinase domain-like (MLKL)-dependent necroptosis and NOD-like receptor pyrin domain-containing protein 3 (NLRP3) inflammasome-dependent sterile inflammation contribute to tubule necrosis and loss of kidney function upon transient artery clamping and kidney ischemia (166).

4.5.1 Necroptosis inhibition improved CCE-related kidney infarction but not AKI

To address the role of *Mkl*-dependent necroptosis in CCE-related AKI, kidney infarction, and vascular occlusion, surgery was performed on WT and *Mkl*^{-/-} male mice. Indeed, at 24 h, *Mkl*^{-/-} mice kidneys showed less swelling, and significantly reduced infarct size (Fig. 32A-B'). Additionally, PAS and immunostainings also found significantly less kidney injury, perilesional neutrophil counts, and vascular injury in *Mkl*^{-/-} kidneys (Fig. 33A-C).

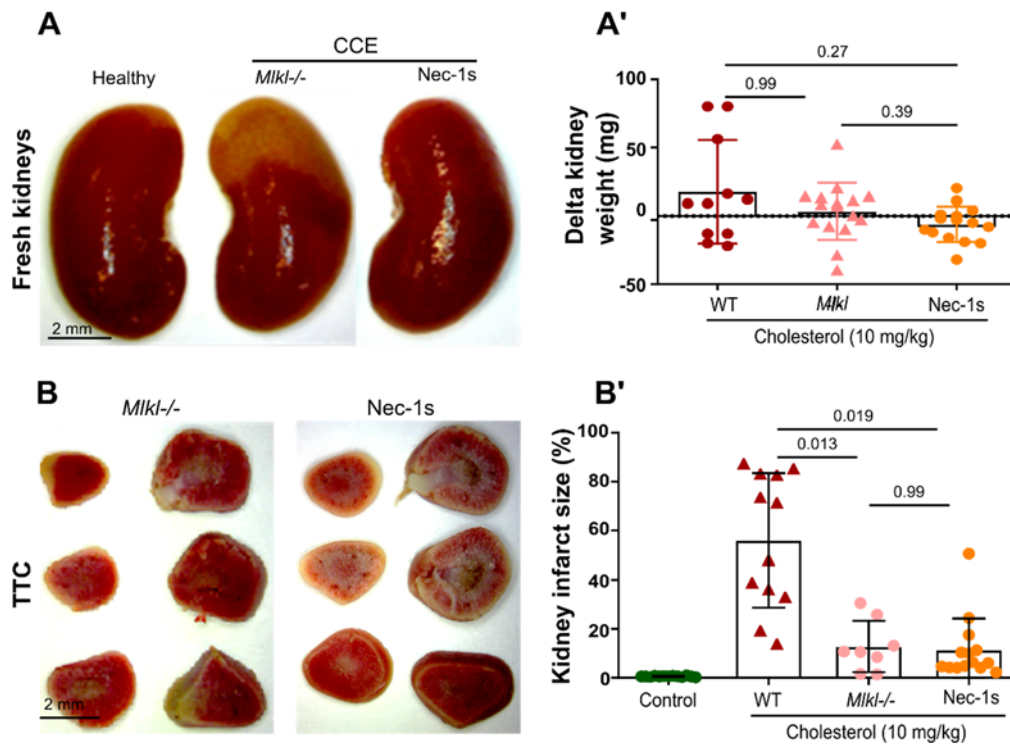


Figure 32. Role of necroptosis in CCE-related kidney infarction at 24 h. A: Fresh kidneys of healthy, *Mkl*^{-/-}, and Nec-1s-treated groups. A': Delta kidney weight. B-B': TTC method quantified kidney infarct size in control, WT, *Mkl*^{-/-}, and Nec-1s-treated groups. All quantitative data are means \pm SD.

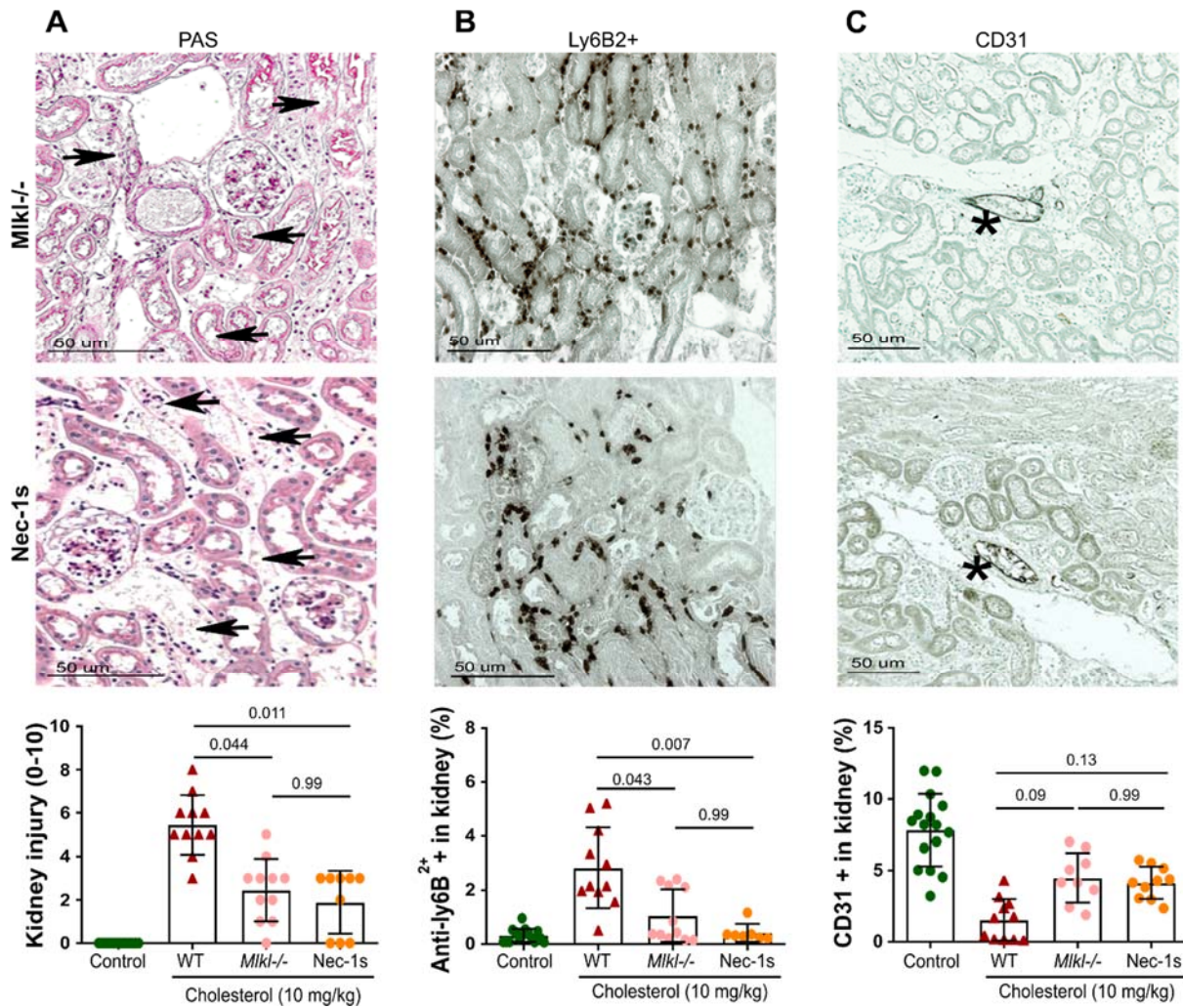


Figure 33. Role of necroptosis in CCE-induced injury and inflammation at 24 h. A: Representative image of PAS-stained CCE kidneys in *Mkl1*^{-/-} and *Nec-1s* administration groups, and kidney injury score. B: Representative images of Ly6B2⁺-stained CCE kidneys of *Mkl1*^{-/-} and *Nec-1s* administration groups, and neutrophil infiltration into CCE kidney. C: Representative images of CD31-stained CCE kidneys and vascular injury analysis. All quantitative data are means \pm SD.

However, the lack of *Mkl1* did not affect kidney excretory function loss (Fig. 34A). Consistently, *Mkl1* deficiency had no significant effect on arterial thrombosis occlusions (Fig. 34B-C'). Accordingly, C57BL/6J mice pretreated with the necroptosis inhibitor *Nec-1s* significantly reduced infarct size, kidney injury, and neutrophil infiltration at 24 h compared to controls (Fig. 32A-B', Fig. 33A-C). However, *Nec-1s* treatment did not affect CCE-related loss of GFR or arterial occlusions (Fig. 34A-C').

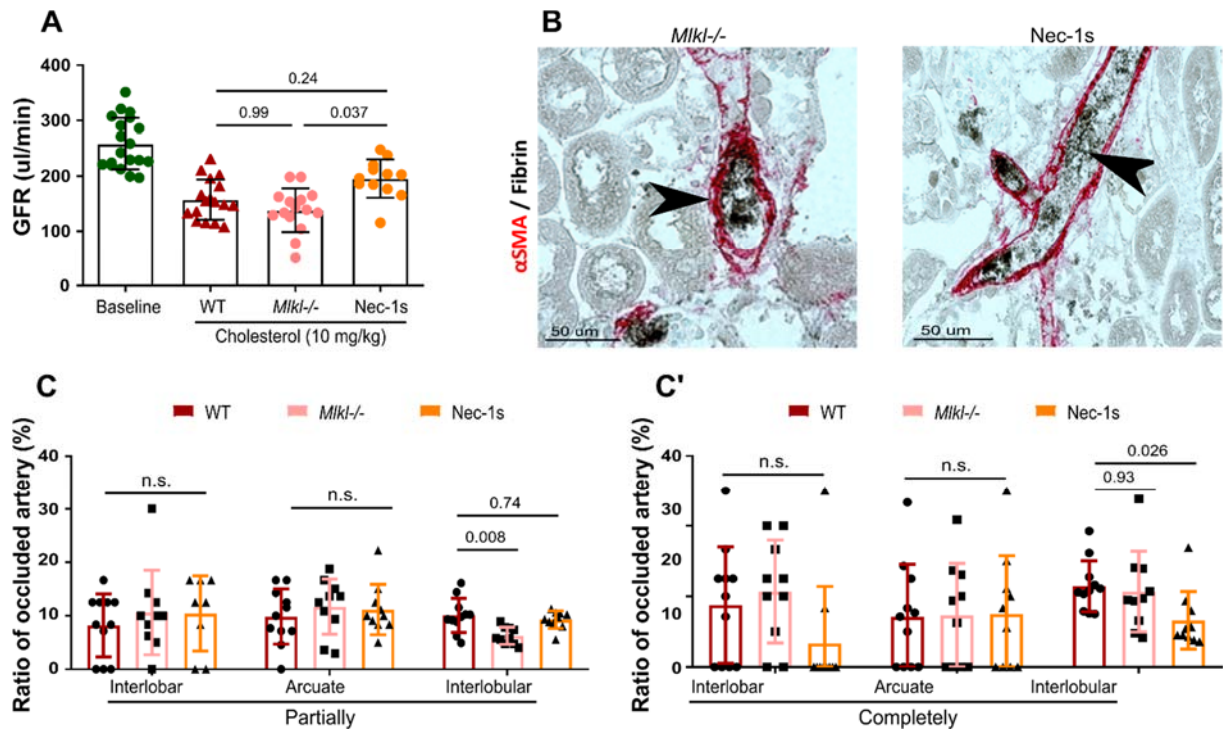


Figure 34. Role of necroptosis in CC-induced arterial occlusions at 24 h. A: GFR loss in WT, *Mkl*^{-/-}, and *Nec-1s* group. D: Representative images of α SMA/fibrin-stained CCE kidneys of the *Mkl*^{-/-} and *Nec-1s* groups. C-C': Ratio of occluded artery numbers of various sizes. All quantitative data are means \pm SD.

4.5.2 Inflammasome inhibition protected from cholesterol crystal embolism-related kidney infarction but not acute kidney injury

To address the role of NLRP3 in CCE-related AKI, kidney infarction, and vascular occlusions, C57BL/6J male mice pretreated with the NLRP3 inhibitor MCC950 showed significantly reduced infarct size, kidney injury, and neutrophil infiltration at 24 h (Fig. 35A-E). However, MCC950 treatment did not affect CCE-related loss of GFR or arterial occlusions (Fig. 36A-C'). Thus, interfering with necroptosis or inflammation had no impact on arterial occlusions at 24 h. Taken together, as nephron perfusion is ultimately required for kidney function, inhibiting necrosis without targeting arterial occlusions does not prevent kidney failure.

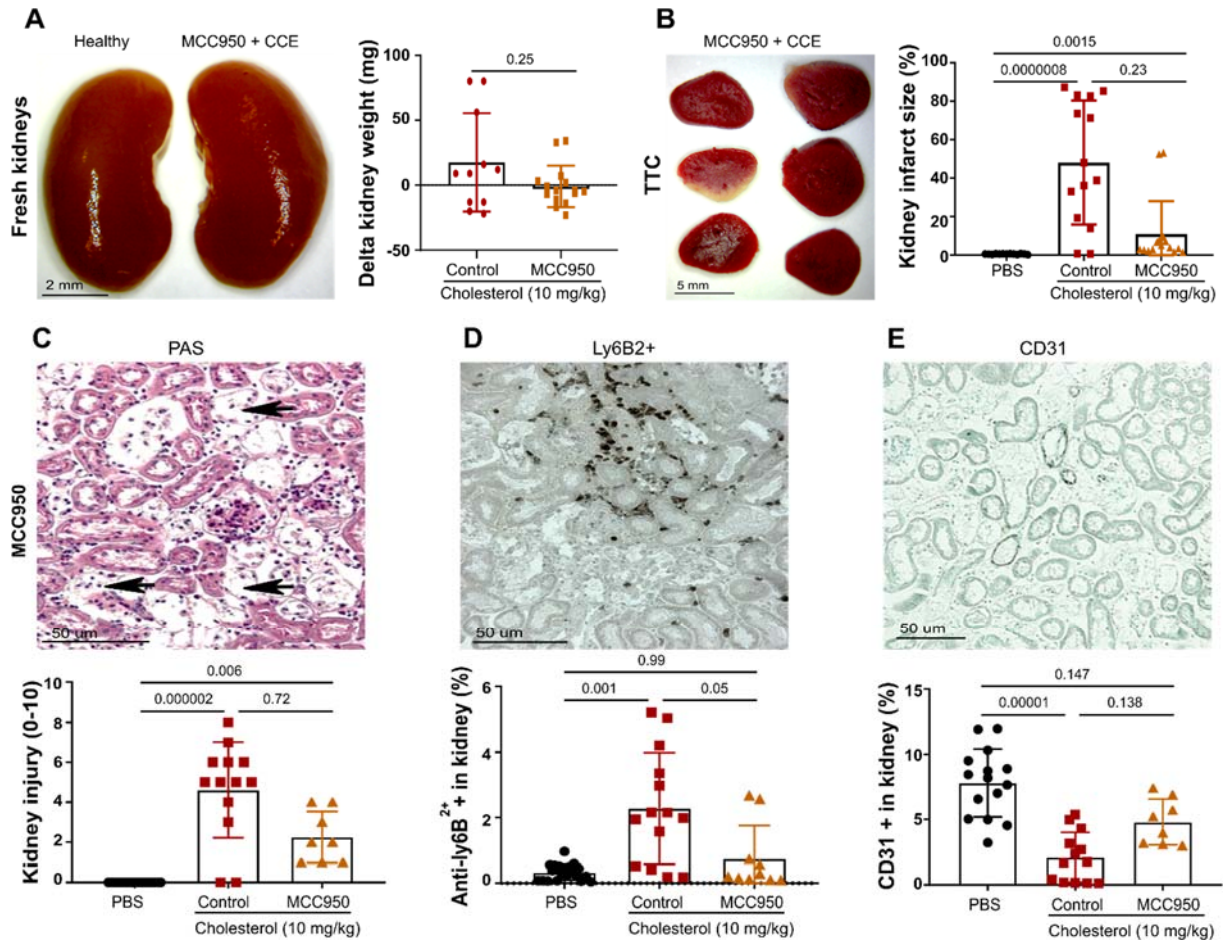


Figure 35. Role of the inflammasome in CCE-related infarction, injury, and inflammation at 24 h. A: Fresh kidneys of healthy, and MCC950-treated groups. A': Delta kidney weight. B: TTC method quantified kidney infarct size in control, and MCC950-treated groups. C: Representative image of PAS-stained CCE kidneys in MCC950 administration groups, and kidney injury score. D: Representative images of Ly6B2+-stained CCE kidneys in MCC950 administration groups, and neutrophil infiltration into CCE kidneys. E: Representative images of CD31-stained CCE kidney and vascular injury analysis. All quantitative data are means \pm SD.

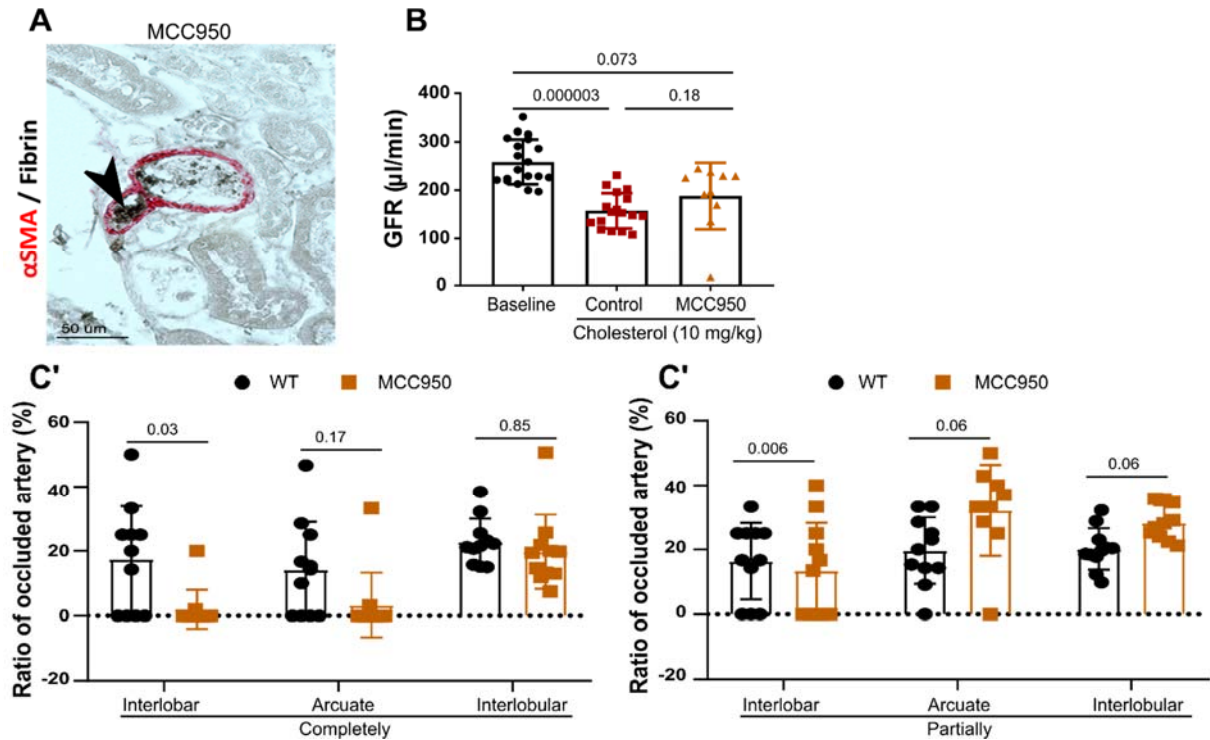


Figure 36. Role of the inflammasome in CCE-related GFR loss and arterial clot at 24 h. A: Representative images of α SMA/fibrin-stained CCE kidneys of the MCC950 groups. B: GFR loss in control and MCC950 groups. C-C': Ratio of occluded artery numbers of various sizes. All quantitative data are means \pm SD.

4.6 Role of extracellular DNA in crystal clots formation

Previous studies showed that ecDNA can be an important component of vascular thrombosis (167). DAPI staining was suggestive for the presence of ecDNA in crystal clots in CC-perfused kidneys (Fig. 37). To investigate the functional contribution of ecDNA for arterial occlusions induced by CC, kidney infarct, and organ failure, a set of experiments were performed on *in vivo* and *in vitro*.

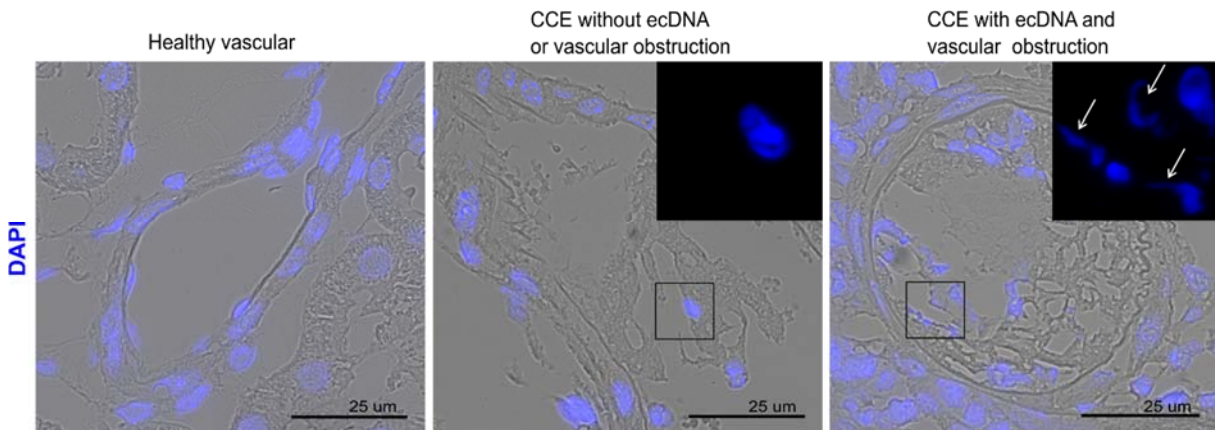


Figure 37. Extracellular DNA presence in CC clots. Representative DAPI stained sections in CCE kidneys showing crystal clots without and with ecDNA (arrows).

4.7.1 Recombinant DNase I inhibited CC injection-mediated pathological processes in the kidney by preventing crystal clot formation

To do so, C57BL/6J male mice received treatment with recombinant DNase I. At 24 h DNase I treatment had abrogated intraarterial ecDNA together with a reduction in the number of arterial occlusions and the fibrin and cellular components of crystal clots, while the crystal component persisted (Fig. 38A, C-C'). This effect was also confirmed by 3D μ CT imaging. As shown in Fig. 38B, DNase I treatment significantly reduced vascular rarefaction and arterial occlusions (Fig. 38D), and kidneys displayed intact vascular tree.

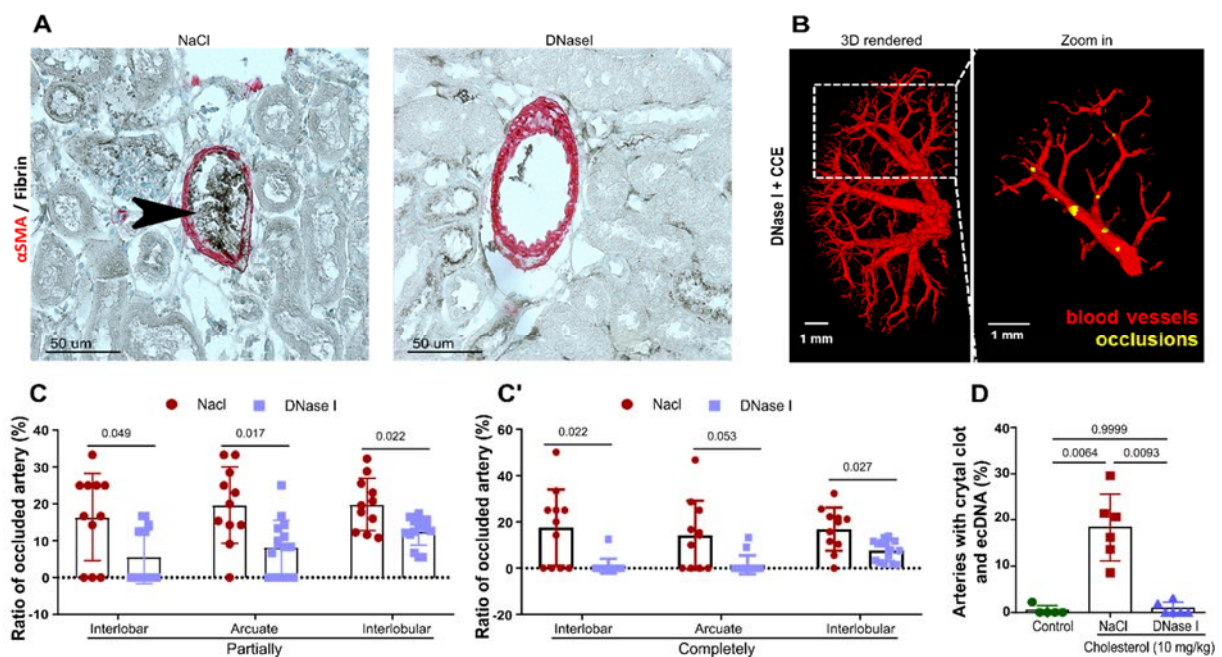


Figure 38. Neutralization of ecDNA prevents crystal clot formation and arterial occlusions at 24 h. A: Representative images of α SMA/fibrin-stained CCE kidneys of the control and DNase I groups. B: 3D μ CT of CCE kidneys confirmed the attenuation of vascular occlusions by a higher density of microvascular perfusion. The right panel shows the foremost artery branch outlined by the dashed rectangle in the left panel. C-C': Ratio of occluded artery numbers of various sizes. All quantitative data are means \pm SD.

As expected, preventing arterial occlusions of DNase I was associated with complete protection from GFR loss (Fig. 39A), a significant reduction in kidney infarct size (Fig. 39B) as well as kidney injury and cell death as indicated by PAS section and less TUNEL+ cells (Fig. 39C-D). Immunostaining revealed DNase I treatment significantly decreased neutrophil infiltrates and vascular rarefaction (Fig. 39E-F). Taken together, the observed ecDNA accumulation is a non-redundant critical component of CCE-related arterial thrombosis obstruction, tissue

infarction, and organ failure.

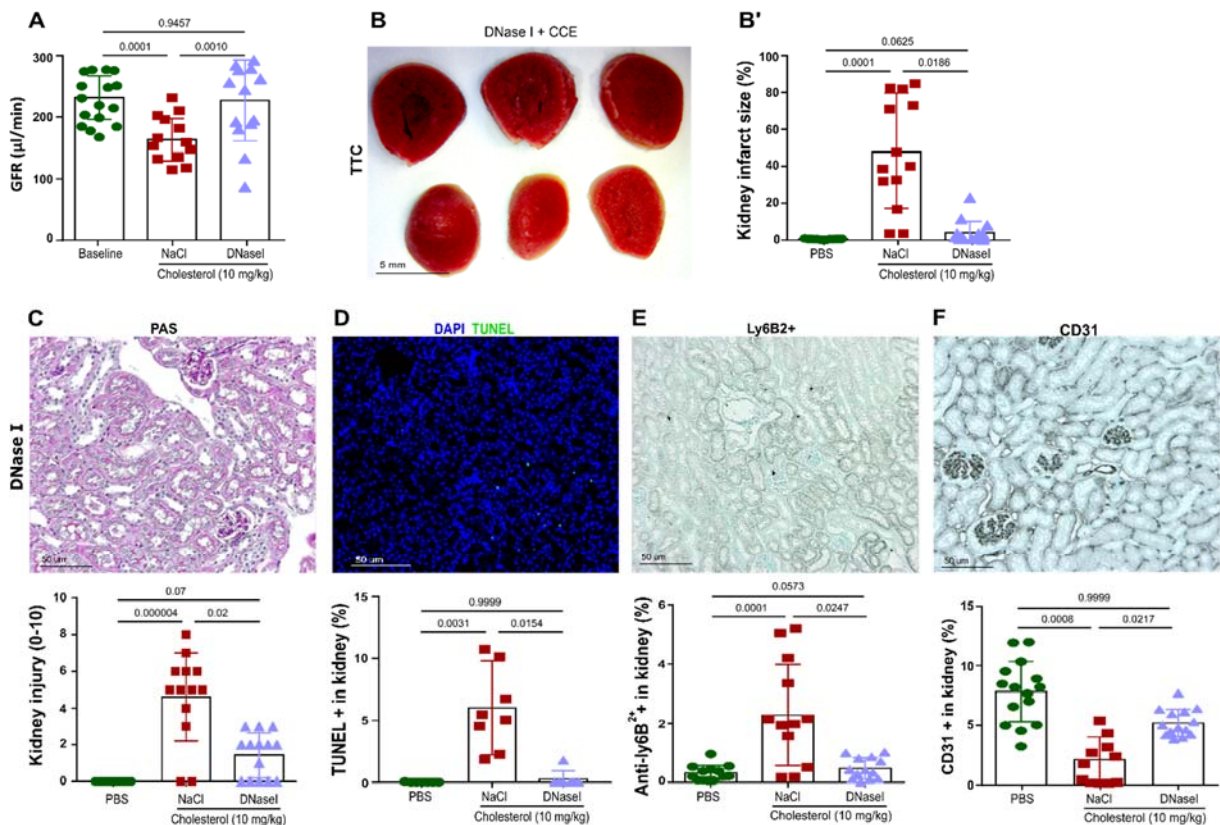


Figure 39. Neutralization of ecDNA prevents CCE-related tissue infarction and organ failure at 24 h. A: DNase I administration significantly reduced CCE-related GFR loss. B-B': TTC method analysis of kidney infarct size. C: Representative image of PAS-stained CCE kidneys of the DNase I group, and kidney injury score. D: Representative images of TUNEL-stained CCE kidneys of the DNase I groups, and TUNEL + dead cells in CCE kidneys. E: Representative images of Ly6B2⁺-stained CCE kidneys of the DNase I groups, and neutrophil infiltration into CCE kidneys. F: Representative images of CD31-stained CCE kidneys and vascular injury analysis. All quantitative data are means \pm SD.

4.7.2 *In vitro* studies to identify the origin of extracellular DNA

To investigate the source of ecDNA, a series of *in vitro* studies were performed on endothelial cells and neutrophils of humans and mice.

4.7.2.1 CC directly induce DNA release from endothelial cells

Mouse endothelial cell studies: To explore whether CC can induce the release of DNA from the endothelial cell, GEnCs were cultured in 96-well plates at a cell density of 1×10^4 to 1.5×10^4 cells/well in the presence of different concentrations of CC (1, 5 or 9 mg/ml) and without any treatment. After 24 h of stimulation with CC, the Pico Green assay showed that exposure to

increasing doses of CC directly induced DNA release from renal endothelial cells (Fig. 40A'), and confocal microscopy confirmed that endothelial cells undergo necrosis (Fig. 40A). In contrast, pre-treated GENCs with Nec-1s, MCC950, or Cl-amidine 30 min before CC exposure did not affect DNA release corroborated by Pico green assay or confocal microscope (Fig. 40B-B'). LDH assays demonstrated that CC directly induced massive cell death (Fig. 41A-C).

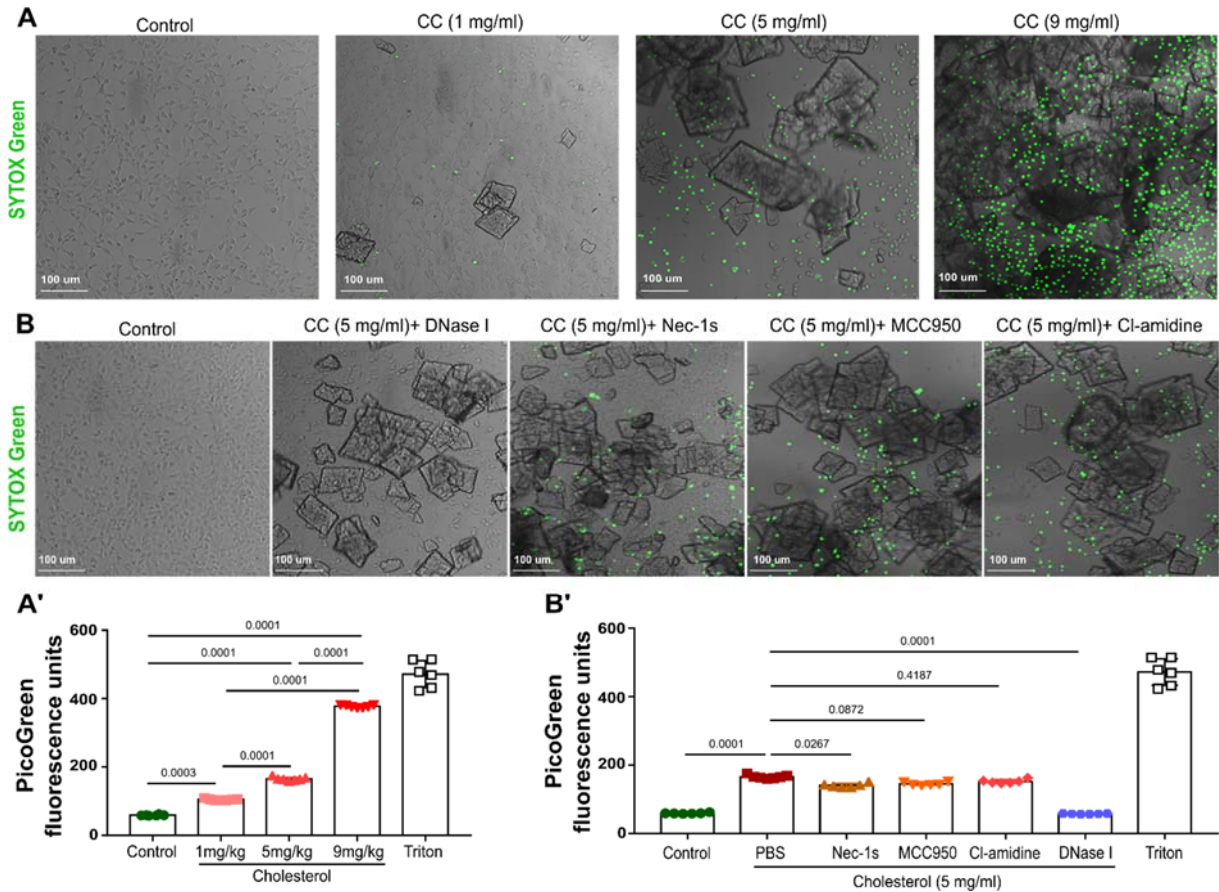


Figure 40. CC-induced ecDNA release from mouse endothelial cells. A: Representative confocal images of GENC stimulated with different doses of CC. Sytox Green dye to show ecDNA release. A': PicoGreen method analysis of ecDNA release upon stimulation with CC. B: Representative confocal images of GENC stimulated with CC and various inhibitors. Sytox Green dye to show ecDNA release. A': PicoGreen method analysis of ecDNA release upon stimulation with CC and various inhibitors. All quantitative data are means \pm SD.

Human endothelial cell studies: HUVEC were 3D cultured in an Organo plate, after 24 h stimulation with CC cells were stained with Calcein/PI for live/dead cell confocal imaging. Confocal imaging proved that CC directly induced HUVEC to release DNA and undergo necrosis (Fig. 41D). Pico green assay also confirmed HUVEC released free DNA into the supernatant after CC stimulation (Fig. 41F). Taken together, CC can directly induce endothelial cells necrosis and release free DNA, which contributed to CC-induced arteries occlusion.

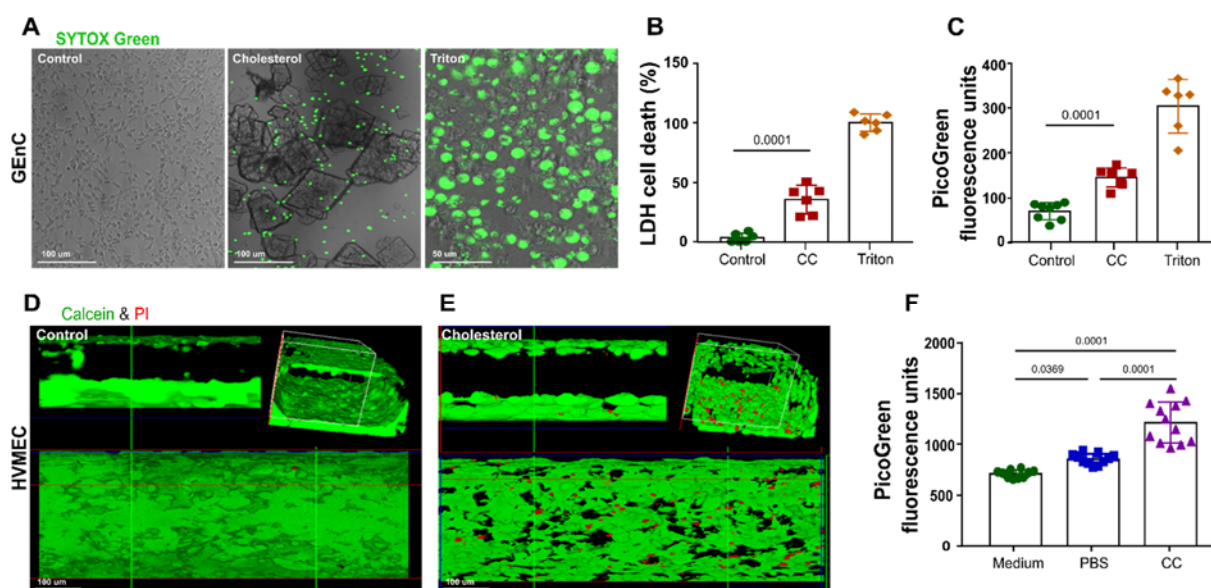


Figure 41. CC-induced ecDNA release from human endothelial cells. A: Representative confocal images of GENC stimulated with CC. Sytox Green dye to show ecDNA release. B: LDH method analysis of CC-induced GENC cell death. C: PicoGreen method analysis of ecDNA release upon stimulation with CC and triton. D: Representative confocal image of healthy HUVEC. E: Representative confocal image of HUVEC stimulated with CC. Calcein and PI to show ecDNA release. F: PicoGreen method analysis of ecDNA release upon stimulation with CC. All quantitative data are means \pm SD.

4.7.2.2 CC-induced DNA release from human neutrophils and platelets

CC exert direct cytotoxic effects leading to necrotic cell death during injury. Since neutrophils are the first responder cells to reach the site of injury and infection, therefore, to verify the cytotoxic effect of CC on neutrophils, human neutrophils were exposed to CC or supernatant of CC-activated platelets 2 h at 37 °C. Confocal images revealed CC-induced neutrophil necrosis and NET-like chromatin release confirmed by Sytox green staining (Fig. 42A). Pico green and LDH assays also demonstrated neutrophil cell death and the release of free-DNA into the supernatant (Fig. 42B-C). Interestingly, supernatants from CC-treated platelets induced NETosis, and free-DNA was detected in the cell culture supernatant of human neutrophils (Fig. 42A, C). Therefore, CC induce human neutrophils necrosis, and DNA release could be a contributing factor in CC-induced arterial obstruction.

Exposure of human platelets to CC also induced the release of minor amounts of ecDNA from their mitochondria (Fig. 42D). Thus, *in vitro* studies support that CC- and platelet-dependent DNA release from neutrophils and endothelial cells could be a contributing factor in CC-induced arterial obstruction.

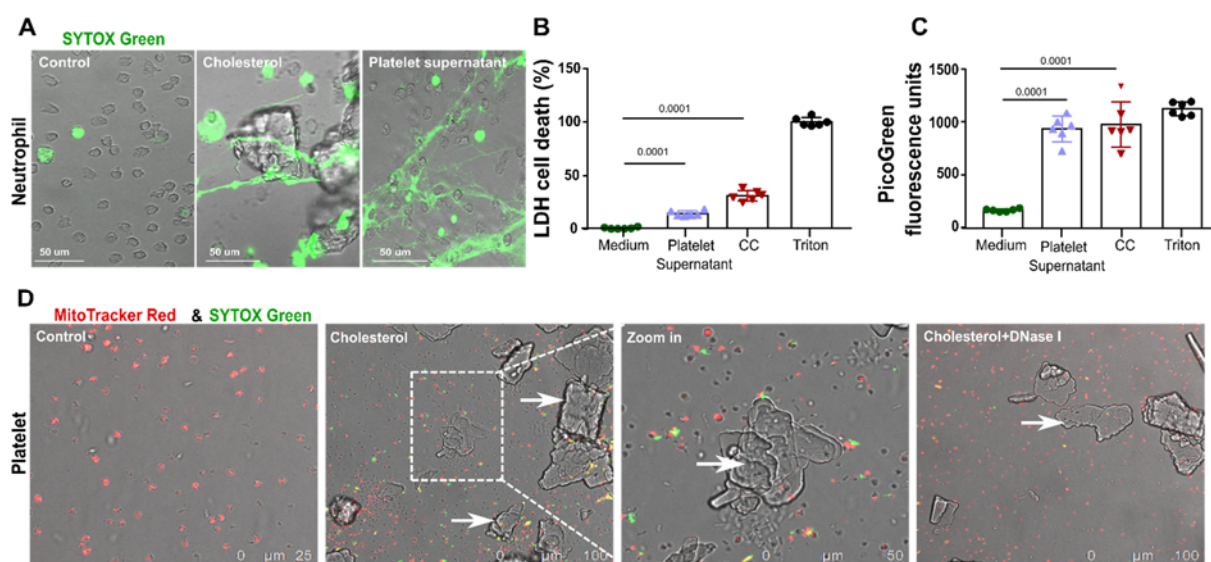


Figure 42. CC-induced DNA release from human neutrophils and platelets. A: Representative confocal images of human neutrophils stimulated with CC and CC-stimulated platelet supernatant. Sytox Green dye to show ecDNA release. B: LDH assay analysis of neutrophil cell death. C: PicoGreen method analysis of ecDNA release from neutrophils. D: Representative confocal image of human platelet upon CC stimulation. MitoTracker Red and Sytox Green to show ecDNA release from platelets mitochondrial. All quantitative data are means \pm SD.

4.8 A two-step strategy to prevent cholesterol crystal embolism-related outcomes

4.8.1 The window of opportunity to improve cholesterol crystal embolism-related outcomes by DNase I

As heart or aorta surgeries preclude the use of anticoagulants or fibrinolytic agents, we considered recombinant DNase I as a possible candidate therapy to attenuate CC clot formation by inhibiting fibrin formation, ecDNA accumulation, and ATP signaling (168).

To do so, I tested the therapeutic window-of-opportunity of recombinant DNase I for its protective effect in CCE. C57BL/6J male mice were administered recombinant DNase I 3, 6, and 12 h after CC injection, and all mice were sacrificed at 24h. DNase I treatment given 3 h after CC embolism showed trends towards improved outcomes albeit not in a consistent manner. Interestingly, 3 h DNase I treatment shows a tendency in kidney swelling, infarct size, TUNEL+ dead cells, and neutrophil infiltration in CCE kidneys (Fig. 43A-D). Consistently, kidney injury score, GFR loss, and artery thrombosis formation results are similar (Fig. 44A-C'). Unfortunately, DNase I treatment started 6 or 12 h after CC injection did not affect any of those endpoints (Fig. 43A-D). None of the delayed DNase I treatments significantly protected from arterial occlusions (Fig. 44A-C'). Therefore, only DNase I treatment 3 h after CC injection

might be considered but would need additional interventions to improve CCE-related kidney failure.

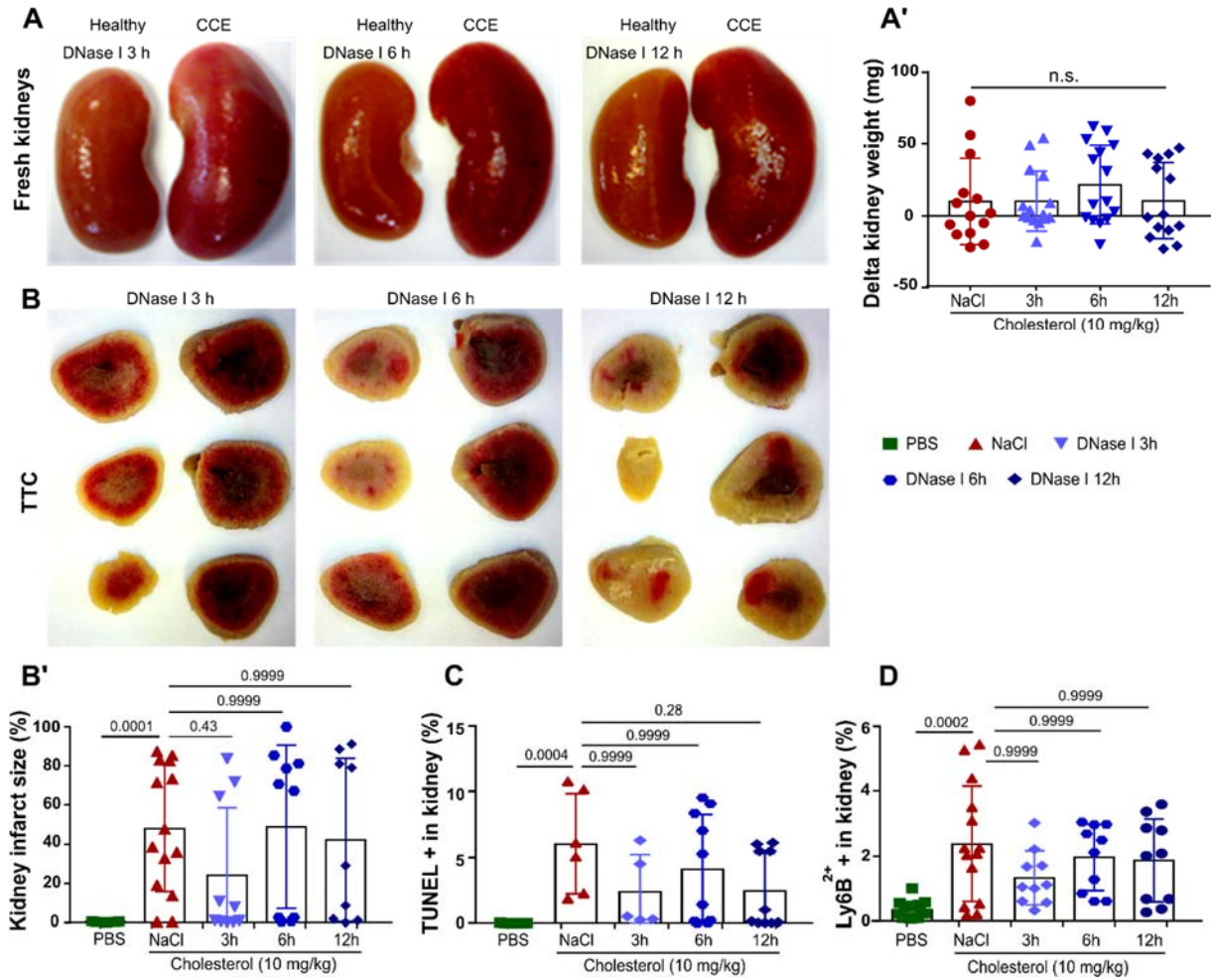


Figure 43. Window-of-opportunity of DNase I treatment at 3 h partially prevents CCE-related tissue infarction and inflammation at 24 h. A: Fresh kidneys of DNase I treatment at 3, 6, and 12 h post-CC-injection. A': Delta kidney weight. B-B': TTC method analysis of infarct size in kidneys upon DNase I administration at different time points. 3 h post-CC-injection partially reduced CCE-related infarction. C: 3 h post-CC-injection partially reduced TUNEL + dead cells in CCE kidneys. D: 3 h post-CC-injection partially reduced neutrophil infiltration in CCE kidneys. All quantitative data are means \pm SD.

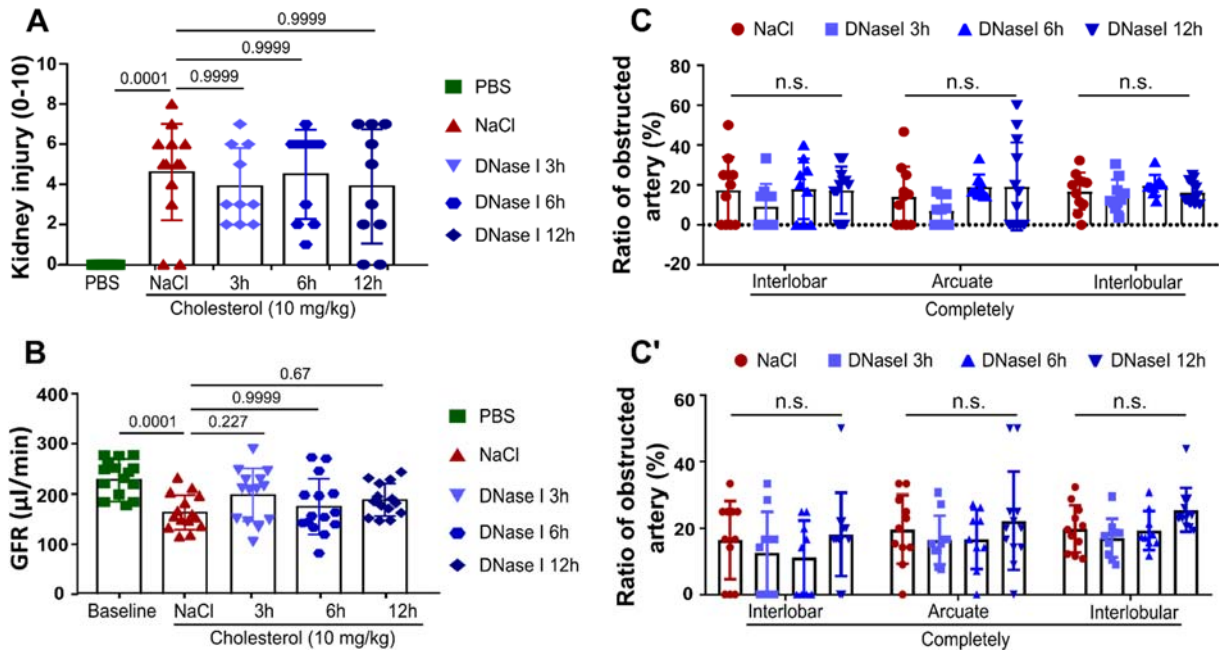


Figure 44. Delayed administration of DNase I did not affect CCE-related injury, AKI, or arterial occlusions at 24 h. A: DNase I administration at different time points did not affect CCE-related kidney injury. B: GFR loss at different time points upon treatment of DNase I. C-C': Ratio of obstructed artery number in various sizes. All quantitative data are means \pm SD.

4.8.2 Nec-1s combined with DNase I treatment prevents cholesterol crystal embolism-related outcomes

Because inhibiting necroptosis significantly improved CCE-related kidney infarction, it might be considered as a combination partner with DNase I treatment that when given 3 h after CC injection significantly reduced kidney infarct size. Therefore, I tested a regimen combining a pre-emptive single dose of the necroptosis inhibitor Nec-1s combined with recombinant DNase I given 3 h after intraarterial CC injection to further optimize outcomes in the setting of a cardiovascular procedure-related CC embolism.

At 24 h, this dual strategy resulted in significant protection from GFR loss, kidney swelling, and infarct size in almost all CCE kidneys (Fig. 45A-C'). As expected, this dual therapy also significantly reduced vascular occlusions by crystal clots (Fig. 46A-B'). PAS scoring showed significantly less injury in treatment group mice compared to the control treatment group (Fig. 47A). CD31 and Ly6B2+ staining analysis revealed a significant reduction in neutrophil infiltration and vascular injury in the treatment group compared to controls (Fig. 47B-C). Taken together, this combined approach could be feasible as prophylaxis given to all patients at risk,

while DNase I would be only given to those with signs of CC embolism into the kidney, e.g. an early decline of urinary output.

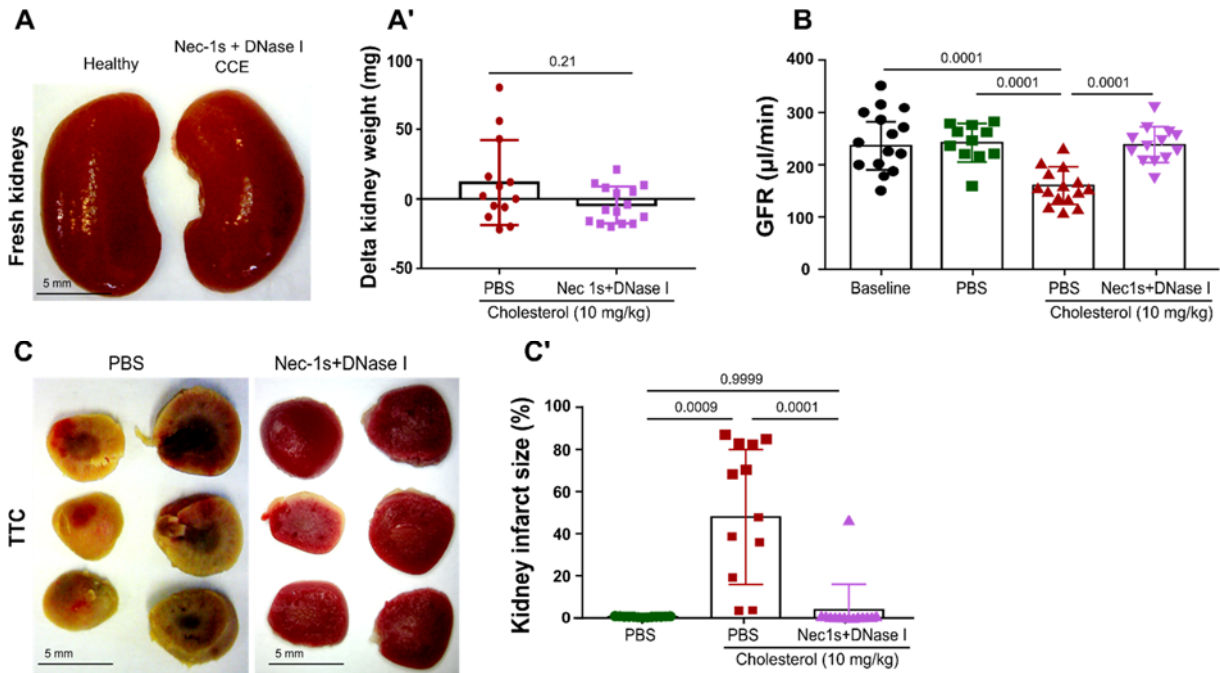


Figure 45. A dual therapy of Nec-1s+DNase I prevents CCE-related tissue infarction and AKI at 24 h. A: Fresh kidneys of DNase I combined with Nec-1s treatment. A': Delta kidney weight. B: Nec-1s+DNase I completely prevented GFR loss. C-C': TTC method analysis of infarct size in the kidney. Nec-1s+DNase I therapy markedly reduced CCE-related infarction. All quantitative data are means \pm SD.

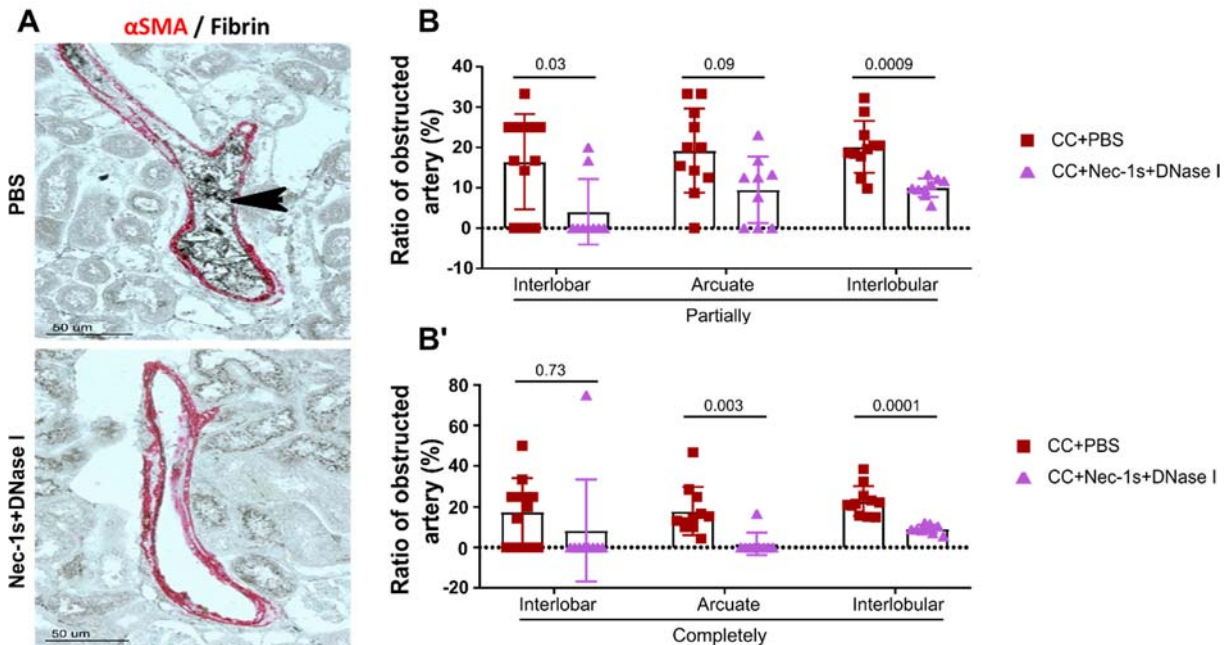


Figure 46. A dual therapy of Nec-1s+DNase I prevents CCE-related arterial occlusion at 24 h. A: Representative images of α SMA/fibrin-stained CCE kidney in Nec-1s+ DNase I and control treatment groups. B-B': Ratio of occluded artery numbers of various sizes. All quantitative data are means \pm SD.

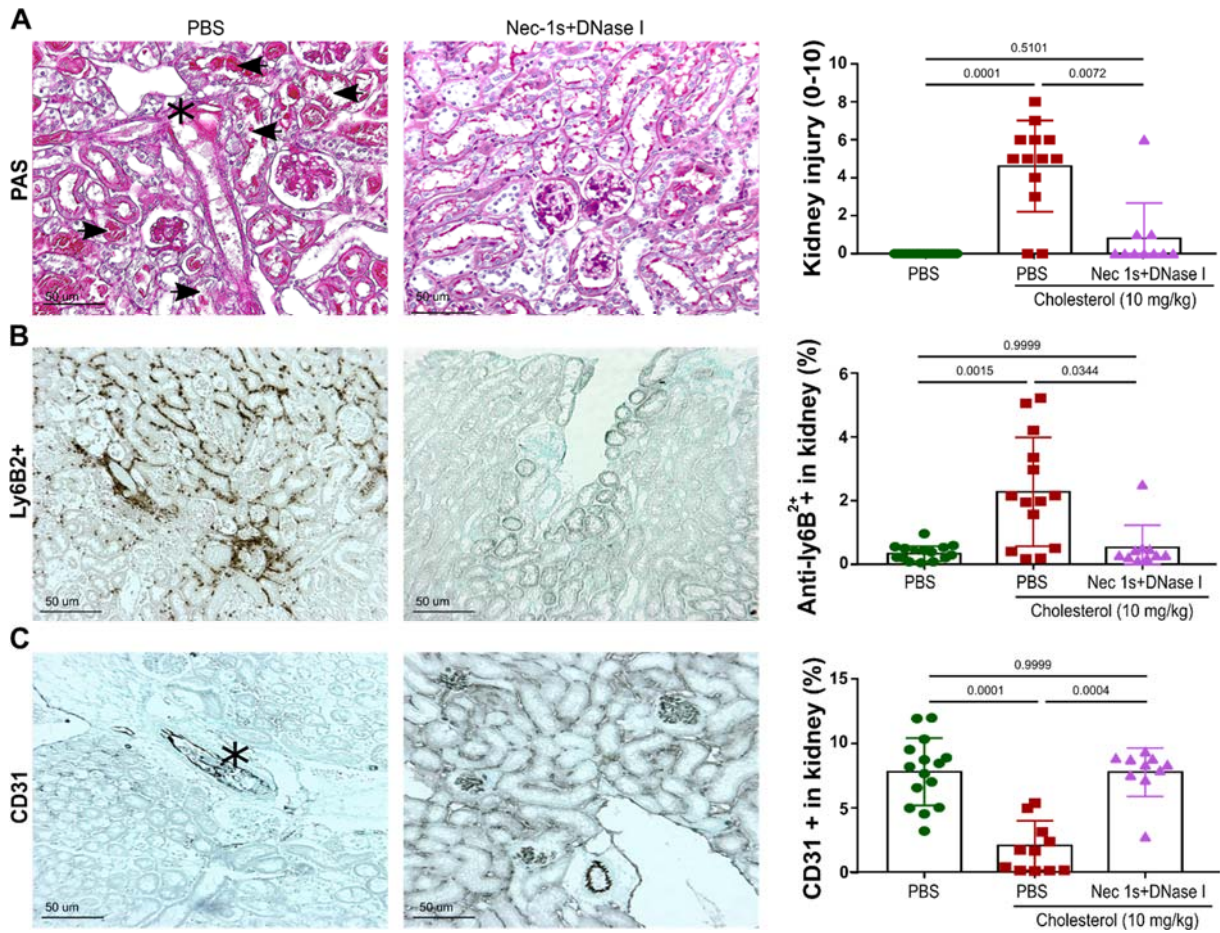


Figure 47. A dual therapy of Nec-1s+DNase I prevents CCE-related injury and inflammation at 24 h. A: Representative image of PAS-stained CCE kidneys in dual therapy and control groups, and kidney injury score. B: Representative images of Ly6B2⁺-stained CCE kidneys in dual therapy and control groups. C: Representative images of CD31-stained CCE kidney and vascular injury analysis. All quantitative data are means ± SD.

5 Discussion

We had hypothesized that developing a reproducible model of CCE would help to dissect the pathophysiology underlying CCE-driven arterial occlusion, tissue infarction, and organ failure. Indeed, the novel model was successfully built by directly injecting CC into one kidney of mice through the kidney artery. In the acute phase, intra-arterial injection of CC leads to multiple microvascular occlusions followed by ischemic territorial infarctions that are similar to all local aspects of human atheroembolic kidney disease. Using this model discovered previously unknown pathomechanisms of vascular occlusion, particularly the early phases that had been not feasible in human pathology. Moreover, this model in mice also allowed for the first time to employ gene-deficient mice as an experimental tool to unravel the molecular pathomechanisms of arterial thrombosis diseases. Indeed, our novel mouse model not only mimics all local aspects of human atheroembolic kidney disease but our data also provide a new pathophysiological concept for CCE, and identify novel molecular targets for prophylaxis and therapy.

In this CCE model, injecting different doses of CC resulted in a dose-dependent GFR loss and kidney infarct with much higher variability. 3D- μ CT of the kidney revealed that CC injection caused peripheral arteries rarefaction and diffuse arterial occlusions, indicating CCE. Immunostaining told us, CC injection formed fibrin positive crystal clots inside arteries, while CC only a minor component of vascular occlusions, and vascular obstruction was rather more related to CC-triggered clot. This process of clot formation was time-dependent. Meanwhile, I also compared whether gender impairs the outcomes of CCE, there was no significant difference between male and female mice in AKI, infarction, or thrombosis obstruction. According to the clinical data, the majority of CCE episodes occur in males (7), which should largely relate to the higher prevalence of cardiovascular risk factors and diffuse atherosclerosis in males. However, our data suggest that gender does not affect the CCE episode and its consequences itself. Thus, we would conclude that only targeting the upstream mechanisms of atherosclerosis such as cardiovascular risk factors could impact the documented gender bias in CCE.

Functionally, in our model, the GFR normalized within 14 days, which is different from human atheroembolic kidney disease. This is most likely related to the unilateral injury model applied here, which involves compensatory hypertrophy of the contralateral kidney, which usually

does not occur the same way in human settings where usually both kidneys are affected. In addition, the *ex vivo* CC preparation used for this model may differ in size and composition from the lipid material dislocating from atheroma in human diseases. Furthermore, in humans, CCE preferentially occurs in elderly patients with diffuse microvascular abnormalities due to long-standing comorbidities such as diabetes mellitus, hypertension, hyperlipidemia, or obesity (6). In contrast, this CCE model was performed using young, healthy, inbred rodents housed under pathogen-free conditions. Altogether, there are many variable factors of this CCE model, for example, the location and size of crystal clots, location of the infarct core, blood pressure, and etiology. Moreover, strictly speaking, CCE-related kidney injury is not only kidney disease but the manifestation of underlying atherosclerosis.

Given those limitations and differences to human CCE, this CCE model nevertheless could provide a new pathophysiological concept for CCE, and identify novel molecular targets for prophylaxis and therapy. Comparing to previous attempts (159,169), this model allowed functional studies in genetically modified mice. Specifically, abrogating necroptosis, a form of regulated necrosis well-known to mediate post-ischemic kidney necrosis, as well as inflammasome-dependent sterile inflammation, i.e. necroinflammation (170). It has been previously reported that *Mkl*-dependent necroptosis and NLRP3 inflammasome-dependent sterile inflammation contribute to tubular necrosis and loss of kidney function upon transient artery clamping (74,171–173). Indeed, at 24 h, *Mkl*^{-/-} prevented CCE-induced kidney infarction and *Mkl*^{-/-} kidneys also showed significantly less swelling. However, lack of *Mkl* had no effect on perilesional neutrophil counts, kidney excretory function, or occluded artery numbers. Consistent results were observed when mice were pretreated with the necroptosis inhibitor Nec-1s. I obtained similar results with an NLRP3 inhibitor that significantly reduced infarct size, kidney injury but not GFR loss, although several studies documented that a critical role for NLRP3 in acute IRI. This mismatch of results between tissue viability and function was already obvious from the different variabilities of CCE-induced GFR loss versus infarct size. This is because, in contrast to other organs, kidney function directly depends on the perfusion of arteries afferent to the glomerular filters, while infarction depends on numerous other factors such as collateral perfusion of tubules, inflammation, and complex stress responses contributing to kidney cell death. Indeed, this finding confirms our choice for GFR as the primary endpoint and infarct size as only a secondary endpoint in the clinically-relevant AKI

context.

In 1973 Warren and Vales reported experiments using injection with human atheromatous plaque material into rabbit kidneys and brains and found thrombotic material around the embolus (174). Our studies extend these observations by showing that not the CC emboli alone account for vascular occlusions, infarction, and kidney failure, but CC triggered the formation of clots inside kidney arteries leading to ischemic tissue injury. This finding is important as it renders the forming arterial clot as a putative target for therapeutic intervention to improve outcomes.

Current recommendations for the management of patients with CCE or arterial clots rely on retrospective reports of a single case or small single-center patient series; no randomized controlled interventional trials have thus far performed (30,41). Partially contradictory outcomes have been reported for the use of steroids or anticoagulants, probably because beyond the peripheral lesions, outcomes also depend on the stability of aortic plaques, intraplaque hemorrhages, and the risk for repetitive episodes (4,21,175). Especially for this model, CC triggered arterial clots consist of fibrin, platelet, neutrophil, monocyte, and ecDNA. The experimental results clearly showed that fibrin mesh-targeting therapies can interfere with the formation of CC clots, i.e. anticoagulant heparin and the fibrinolytic agent urokinase, which largely prevented tissue necrosis and organ failure. This further confirmed that not the CC *per se* but rather crystal-induced clots account for arterial obstruction, tissue infarction, and organ failure.

Given the countless platelets present in other forms of arterial thrombosis, many antiplatelet agents have been developed and are used in this context, e.g. in acute coronary syndrome (2,159). For example, the platelet P2Y₁₂ receptor antagonist clopidogrel completely protected GFR loss and kidney infarction by inhibiting crystal clot formation. This suggested that platelet-derived ATP release and purinergic receptor P2Y₁₂ signaling are directly involved in the formation of crystal clots in the CC-injected kidney.

In line with these *in vivo* results, further *in vitro* studies support that CC enhances platelet activation, ATP secretion, and fibrinogen release from platelet granules which further promotes fibrin activation during crystal thrombosis formation. Those findings are consistent with the previous concept that the collagen matrix together with CC locally promotes platelet adhesion and thrombus growth during CCE. Regarding the future antithrombotic therapies,

thrombin and its interaction with platelets might be considered in CCE. Also, a combination of antiplatelet drugs and safe and effective anticoagulant agents might be beneficial. Thrombin receptor antagonists (PAR1 antagonists) are considered to reduce bleeding complications as they not only reduce platelet thrombin activation without affecting thrombin-related fibrin generation (176). Notably, it seems that PAR1 antagonists are efficacious and safe without enhancing the risk for major hemorrhages when combined with aspirin or clopidogrel according to phase 2 clinical trials (176). Anticoagulant therapy with warfarin has the same efficacy as aspirin in reducing coronary thrombotic events, although it increased the risk of bleeding (177). Hence, a comparison of generally inhibiting platelet function or coagulation and deeper insights into the molecular mechanisms of platelet adhesion and coagulation during the different phases of thrombus growth would probably allow us to develop a more rational and safer combination of antiplatelet agents with anticoagulants (Fig. 48).

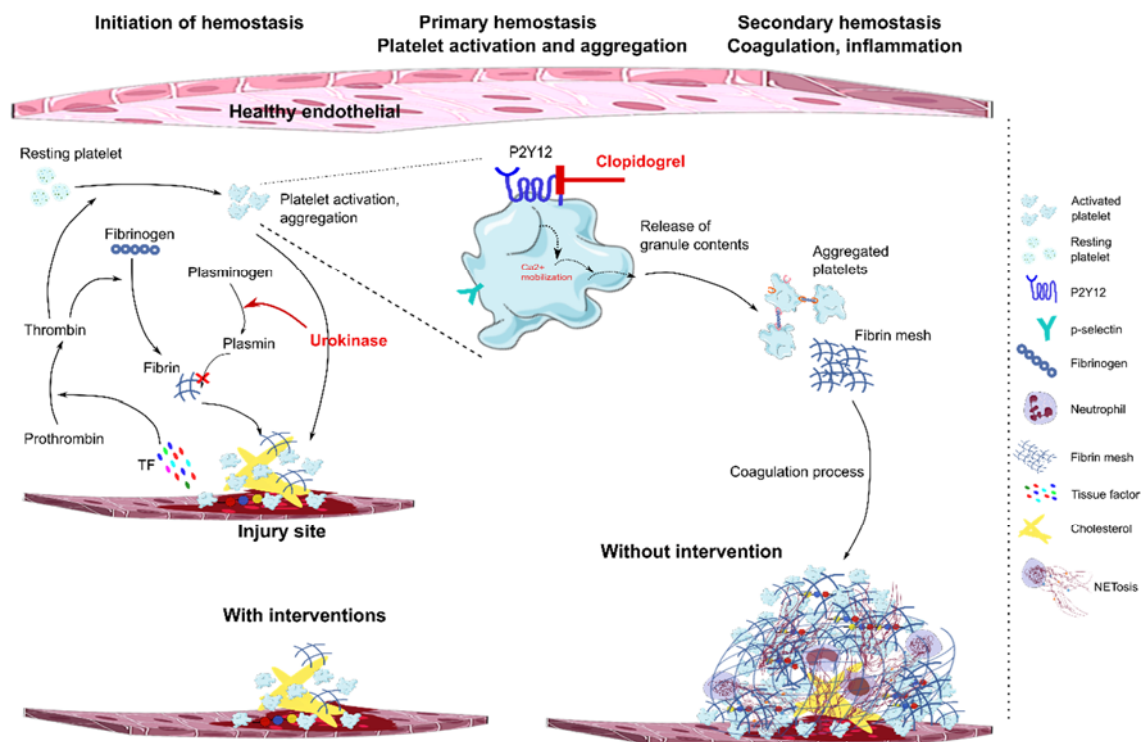


Figure 48. Platelets in thrombosis formation. Damaged endothelial release tissue factor (TF), TF leading to thrombin generation and the following is platelet activation. Following that, the activated platelet releases granule contents (vWF, fibrinogen, ADP, ATP) and exposes $\alpha\text{IIb}\beta\text{3}$ integrin, surfaces marker of GPIb, and p-selectin. Particularly ADP and ATP attracting circulating platelets to the growing thrombus. Activated platelets aggregating together by binding to fibrinogen and vWF causing blood coagulation. Aggregated platelet in turn promoting more platelet activation. All together promote thrombus growth and stabilization. Interventions, such as urokinase can abolish fibrin mesh preventing blood coagulation, clopidogrel can bind to the P2Y12 receptor on the platelet surface to prevent the coagulation process. Thus, urokinase and clopidogrel can prevent cholesterol clot formation, therefore protect from ischemia-related tissue injury and infarction.

Numerous studies suggested also a prothrombotic potential of neutrophils and NET in animal models. Experimental compounds either target neutrophils directly or NET components, for example, citrullinated histones, MPO, NE, and PAD4 (168,178). Blocking PAD4-dependent formation of NETs and targeting neutrophils both were investigated in this model. However, unlike antiplatelet therapy, targeting neutrophils with these compounds had no relevant effect on kidney function, albeit reducing infarct size. Accordingly, PAD4 inhibition showed similar results at 24 h. Most interestingly, mononuclear cells and large amounts of ecDNA could be detected in crystal clots even in kidneys upon neutrophil depletion. Possibly, mononuclear cells partially replaced neutrophils as a source of ecDNA inside the crystal clots. It is of note that macrophages, mast cells and, eosinophils can also release extracellular traps and contribute to arterial thrombosis (179,180). Macrophage extracellular traps can also be a component of arterial thrombosis. Moreover, activated platelets can trigger NETs release and neutrophils actively search for activated platelets to trigger inflammation (158). In particular in AKI, tissue necrosis results in acute inflammation, which in turn leads to more tissue necrosis, i.e. the auto-amplification loop of necroinflammation (110,181). In addition, neutrophils are present in large numbers in the periinfarction area and our neutrophil depletion experiments demonstrate that their presence contributes to overall infarction by causing secondary tissue necrosis, collateral damage of sterile inflammation (Fig. 49).

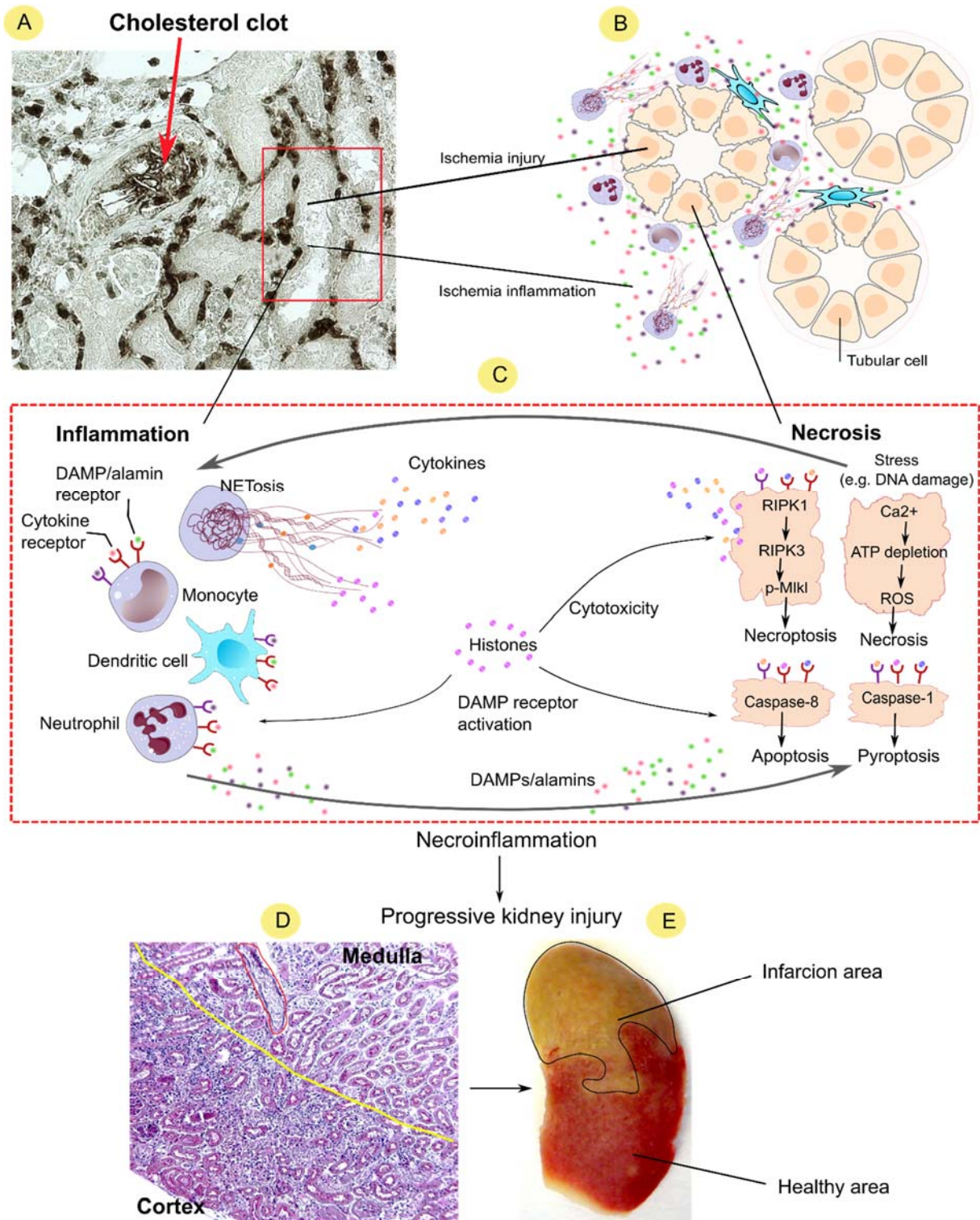


Figure 49. The correlation of necroinflammation and infarction. A: Anti-Ly6B2+-stained section shows cholesterol-induced clot formation inside a kidney artery. Around the obstructed artery locates ischemic tissue injury and inflammation, as shown in B. C: Ischemia triggers primary tubular injury through different pathways, this promotes inflammatory response by attracting immune cells, such as neutrophils, monocytes, macrophages to the inflamed sites, which in turn in further tubule injury. This uncontrolled necroinflammation endorses accelerating kidney injury in AKI. D: Representative PAS sections show injury spread from medulla to cortex area. E: Ultimately, this process leads to kidney infarction (TTC staining of a longitudinal kidney section).

Surprisingly, DNase I can inhibit the effects of ATP released from platelets, and strongly inhibits CC- and collagen-induced platelet aggregation, two functions independent of its DNase activity or NETosis. Whether DNase I directly hydrolyzes ATP and thereby inhibits purinergic signaling in platelets and other cell types remains to be studied.

Extracellular DNA has recently been identified as a critical component of arterial thrombosis, either by employing mice mutant for DNases or by using recombinant DNase I (167,182,183). It is essential to eliminate ecDNA quickly to restrict extravagant thrombus formation and artery occlusion because ecDNA not only acts as a critical constituent of clots but also enhances the stability of the thrombus and increase their resistance to thrombolytic mediators. DAPI and Feulgen's staining both documented ecDNA in large parts of CC clots. Therefore, anti-ecDNA therapy was applied in this model. Indeed, DNase I treatment completely protected from function loss and tissue infarction.

This protective result of DNase I raised another question? What was the source of that ecDNA? *In vitro* experiments were performed because the origin of ecDNA was difficult to ultimately prove *in vivo*. Many studies documented that NETs can release large amounts of ecDNA. I considered the same source also for crystal clots, however, compared to DNase I intervention, interventions of neutrophils or NETs had little effects on vascular obstructions and AKI, probably due to the rather small amount of ecDNA released from neutrophils during clots formation in this model. Importantly, mononuclear cells were also observed in clots, and platelets also released DNA from their mitochondria after activation by CC consistent with a previous report (184). Although the total amount of mitochondrial DNA per platelet is low, the large numbers of platelets involved in blood clotting also render platelets as a potentially significant source of ecDNA *in vivo* (185). Another potential source of ecDNA could be necrotic vascular or parenchymal cells. During thrombosis-induced tissue ischemia, the majority of cells die primarily via ischemic necrosis and this process releases nuclear DNA into the extracellular space. Moreover, CC directly attacks endothelial cells *in vitro* and *ex vivo* (172). In line with this, the data suggest that endothelial cell injury could be the major source of locally accumulated ecDNA within the CC clot. It is important to address that small amounts of CC is not necessarily damage the endothelial cell, therefore CC not directly induces fibrin clot formation and endovascular obstruction (159). Taken together, numerous sources contribute to the pool of ecDNA in CC-induced fibrin clot formation (Fig. 50).

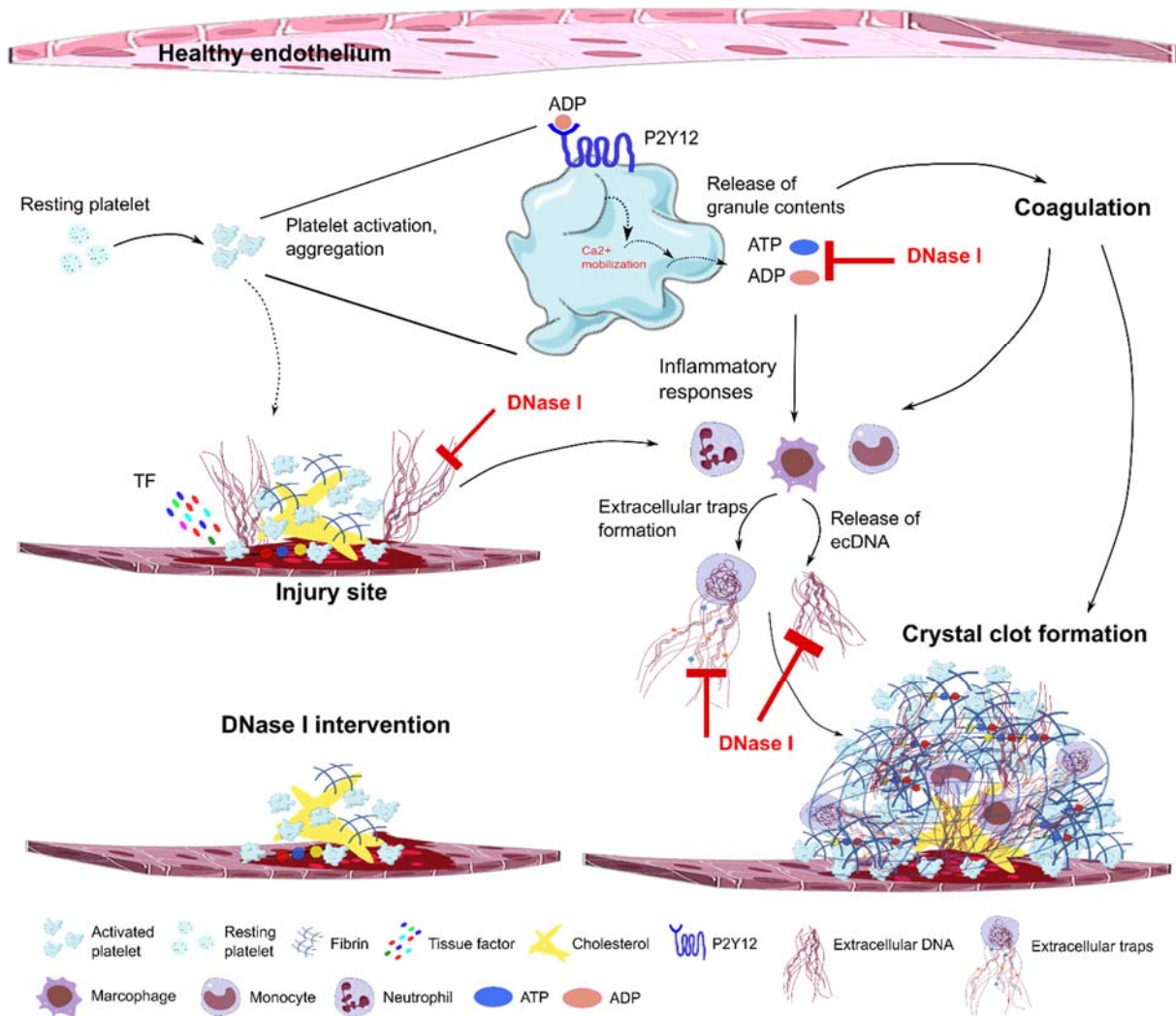


Figure 50. Extracellular DNA plays a critical role during cholesterol clot formation. Damaged endothelial release tissue factor (TF) and ecDNA activate platelets, meanwhile, the role of ecDNA as a DAMP can also trigger an inflammatory response. Activated platelets release granule contents, such as vWF, fibrinogen, ADP, ADP, and expose α IIb β 3 integrin, and surface receptors such as GPIb and p-selectin. In particular, ADP and ATP attract circulating platelets to the growing thrombus. Activated platelets aggregate by binding to fibrinogen and vWF through surface receptors and cause blood coagulation. Aggregated platelets, in turn, promote more platelet activation. Meanwhile, activated platelets and released granule contents can also cause immune cell response leading to more ecDNA release, the formation of extracellular traps, and cytokine release. In particular, neutrophils can bind to activated platelet by p-selectin participating and promoting blood coagulation. All these mechanisms together drive thrombus growth and stabilization. DNase I can degrade ecDNA released from damaged endothelial cells to prevent platelet activation and inflammation. DNase can also hydrolyze ATP and ADP and thereby prevent coagulation and inflammation. DNase I also breaks down extracellular traps by degrading chromatin and DNA. Therefore, DNase I prevents ecDNA mesh as a trap, platelet activation, and aggregation. ADP: adenosine diphosphate, ATP: adenosine triphosphate.

As heart or aorta surgeries preclude the use of anticoagulants or fibrinolytic agents, we considered recombinant DNase I as a possible candidate therapy to attenuate CC clot formation. I identified the therapeutic window-of-opportunity for the intervention with

recombinant DNase I at 3 h. Considering necroptosis inhibition significantly improved kidney infarction in CCE, I preferred it as the combination partner for a DNase I intervention. Indeed, a dual regimen that combines a pre-emptive dose of the necroptosis inhibitor combined with DNase I given 3 h after CC injection completely protected almost all animals. Such a two-step approach could allow giving to all patients at risk necrostatin-1s prophylaxis, while DNase I would be only given to those with signs of CC embolism into the kidney, e.g. an early decline of urinary output.

However, there are some limitations to the present study.

1. This work employed CC alone to induce CCE, which may differ from atherosclerotic plaque materials dislocating in human diseases (186).
2. This study is limited to CCE of the kidney, while spontaneous revascularization can be different in various organs. For example, pulmonary artery CCE or stroke (160).
3. CCE was induced only in young, healthy, inbred mice, while in humans, CCE preferentially occurs in elderly patients with other diseases (23).
4. This model presents with many variable factors, for example, the location and size of crystal clots, location of the infarct core, blood pressure, and etiology.
5. The various interventions were used only at a single dose throughout the studies. It might be possible that higher doses would have been even more protective. We cannot exclude that higher doses of Nec-1s, MCC950, and Cl-amidine might produce a protective effect also on kidney function.
6. Regarding the interventions with anticoagulants and fibrinolytic agents heparin and urokinase, only one time point was studied after CC injection. Whether a later time point of administration of heparin and urokinase would still produce fully protection remains unknown.

In summary, not CC by itself but the fibrin clots forming around CC obstruct peripheral arteries causing tissue infarction and organ failure. Hence, crystal clots represent the primary target for therapeutic interventions. Among the possible molecular targets in thrombosis and hemostasis, especially enhancing fibrinolysis or inhibiting platelet purinergic signaling can reduce arterial occlusions, infarction, and organ failure albeit with a relatively short window-of-opportunity up to 3h. Our results suggest that prophylactic necroptosis inhibition with a combination of DNase I therapy could have a synergistic effect on CC induced clot formation

in mice, and might be a feasible two-step prophylactic/therapeutic approach in human patients with a risk for procedure-related CCE.

Future directions

The circadian rhythm regulates behaviour and physiological actions according to environmental changes, such as the adjustment of sleep-wake cycles, feeding, body temperature, blood pressure, heart rate, hormone secretion, metabolism (including lipid metabolism), and many other biological activities (187,188). In the murine peripheral blood, numbers of leukocyte fluctuate with a peak during the inactive phase (189). Whereas leukocyte numbers show a peak at the beginning of the active phase in tissues, such as bone marrow, skeletal muscle, or the heart, which oscillate inversely with the blood (189).

Acute myocardial infarction (AMI) is best known for its circadian rhythmicity as the onset of the event occurring widely in the morning hours in humans (190). Moreover, neutrophils infiltrate to the heart also following a diurnal rhythm even under steady-state conditions (191). This circadian rhythm-dependent migration of neutrophils into the heart is regulated by CXCR2, the chemokine receptor rhythmic expressed on the neutrophils, and displayed a peak in the evening which is consistent with higher expression of ICAM-1, VCAM-1, and the chemokine ligands in cardiac tissue (192). Consequently, during the active phase, an ischemic event leads to an uncontrollable inflammatory response and worsened cardiac repair, whereas reducing neutrophil numbers efficiently reduces the infarct size and improves cardiac function (193). Clinical evidence also supports the concept that the circadian rhythm critically determines the infarct size in the onset of ischemic events and the mortality in AMI patients with ST-elevation (191). Therefore, it would be also interesting to investigate whether a circadian rhythm is also related to CCE-related kidney infarction, in particular, to unravel the molecular mechanism of neutrophils migration capacity to the kidney during CCE-induced ischemic tubular injury.

6 References

1. Kronzon I, Saric M. Cholesterol embolization syndrome. *Circulation* (2010) **122**:631–641. doi:10.1161/CIRCULATIONAHA.109.886465
2. Branco L. Atheromas of the thoracic aorta: clinical and therapeutic update. *Rev Port Cardiol orgao Of da Soc Port Cardiol = Port J Cardiol an Off J Port Soc Cardiol* (2000) **19**:745–746.
3. Dulíček P, Bártová J, Beránek M, Malý J, Pecka M. The purple toe syndrome in female with factor v Leiden mutation successfully treated with enoxaparin. *Clin Appl Thromb* (2013) **19**:100–102. doi:10.1177/1076029612440033
4. Smith SCJ, Benjamin EJ, Bonow RO, Braun LT, Creager MA, Franklin BA, Gibbons RJ, Grundy SM, Hiratzka LF, Jones DW, et al. AHA/ACCF Secondary Prevention and Risk Reduction Therapy for Patients with Coronary and other Atherosclerotic Vascular Disease: 2011 update: a guideline from the American Heart Association and American College of Cardiology Foundation. *Circulation* (2011) **124**:2458–2473. doi:10.1161/CIR.0b013e318235eb4d
5. Saric M, Kronzon I. Cholesterol embolization syndrome. *Curr Opin Cardiol* (2011) **26**:472–479. doi:10.1097/HCO.0b013e32834b7fdd
6. Kassirer JP. Atheroembolic renal disease. *N Engl J Med* (1969) **280**:812–818. doi:10.1056/NEJM196904102801506
7. Scolari F, Ravani P. Atheroembolic renal disease. *Lancet* (2010) **375**:1650–1660. doi:10.1016/S0140-6736(09)62073-0
8. Arroyo LH, Lee RT. Mechanisms of plaque rupture: mechanical and biologic interactions. *Cardiovasc Res* (1999) **41**:369–375. doi:10.1016/s0008-6363(98)00308-3
9. Flory CM. Arterial Occlusions Produced by Emboli from Eroded Aortic Atheromatous Plaques. *Am J Pathol* (1945) **21**:549–565.
10. Fine MJ, Kapoor W, Falanga V. Cholesterol crystal embolization: a review of 221 cases in the English literature. *Angiology* (1987) **38**:769–784. doi:10.1177/000331978703801007
11. Soufi M, Sattler AM, Maisch B, Schaefer JR. Molecular mechanisms involved in atherosclerosis. *Herz* (2002) **27**:637–648. doi:10.1007/s00059-002-2431-2

12. Kealy WF. Atheroembolism. *J Clin Pathol* (1978) **31**:984–989.
doi:10.1136/jcp.31.10.984
13. Keeley EC, Grines CL. Scraping of aortic debris by coronary guiding catheters: a prospective evaluation of 1,000 cases. *J Am Coll Cardiol* (1998) **32**:1861–1865.
doi:10.1016/s0735-1097(98)00497-5
14. Fukumoto Y, Tsutsui H, Tsuchihashi M, Masumoto A, Takeshita A. The incidence and risk factors of cholesterol embolization syndrome, a complication of cardiac catheterization: a prospective study. *J Am Coll Cardiol* (2003) **42**:211–216.
doi:10.1016/s0735-1097(03)00579-5
15. Blauth CI, Cosgrove DM, Webb BW, Ratliff NB, Boylan M, Piedmonte MR, Lytle BW, Loop FD. Atheroembolism from the ascending aorta. An emerging problem in cardiac surgery. *J Thorac Cardiovasc Surg* (1992) **103**:1102–1104.
16. Ascione R, Ghosh A, Reeves BC, Arnold J, Potts M, Shah A, Angelini GD. Retinal and cerebral microembolization during coronary artery bypass surgery: a randomized, controlled trial. *Circulation* (2005) **112**:3833–3838.
doi:10.1161/CIRCULATIONAHA.105.557462
17. Blankenship JC, Butler M, Garbes A. Prospective assessment of cholesterol embolization in patients with acute myocardial infarction treated with thrombolytic vs conservative therapy. *Chest* (1995) **107**:662–668. doi:10.1378/chest.107.3.662
18. Konstantinou DM, Chatzizisis YS, Farmakis G, Styliadis I, Giannoglou GD. Cholesterol embolization syndrome following thrombolysis during acute myocardial infarction. *Herz* (2012) **37**:231–233. doi:10.1007/s00059-011-3442-7
19. OCTAVIO RIOS C. [Applications of polarized light in the clinical laboratory; research on cholesterol crystals in bile & biliary calculi]. *Rev Sanid Mil Peru* (1956) **29**:71–77.
20. GORE I, MCCOMBS HL, LINDQUIST RL. OBSERVATIONS ON THE FATE OF CHOLESTEROL EMBOLI. *J Atheroscler Res* (1964) **4**:527–535. doi:10.1016/s0368-1319(64)80055-7
21. THURLBECK WM, CASTLEMAN B. Atheromatous emboli to the kidneys after aortic surgery. *N Engl J Med* (1957) **257**:442–447. doi:10.1056/NEJM195709052571002
22. Thadhani RI, Camargo CAJ, Xavier RJ, Fang LS, Bazari H. Atheroembolic renal failure after invasive procedures. Natural history based on 52 histologically proven cases. *Medicine (Baltimore)* (1995) **74**:350–358. doi:10.1097/00005792-199511000-00005

23. Scolari F, Tardanico R, Zani R, Pola A, Viola BF, Movilli E, Maiorca R. Cholesterol crystal embolism: A recognizable cause of renal disease. *Am J kidney Dis Off J Natl Kidney Found* (2000) **36**:1089–1109. doi:10.1053/ajkd.2000.19809
24. Moolenaar W. Cholesterol Crystal Embolization in the Netherlands. *Arch Intern Med* (2011) **156**:653. doi:10.1001/archinte.1996.00440060081009
25. Preston RA, Stemmer CL, Materson BJ, Perez-Stable E, Pardo V. Renal biopsy in patients 65 years of age or older. An analysis of the results of 334 biopsies. *J Am Geriatr Soc* (1990) **38**:669–674. doi:10.1111/j.1532-5415.1990.tb01427.x
26. Kithas PA, Supiano MA. Hypertension and chronic kidney disease in the elderly. *Adv Chronic Kidney Dis* (2010) **17**:341–347. doi:10.1053/j.ackd.2010.04.003
27. Mayo RR, Swartz RD. Redefining the incidence of clinically detectable atheroembolism. *Am J Med* (1996) **100**:524–529. doi:10.1016/s0002-9343(95)00059-3
28. Belenfant X, Meyrier A, Jacquot C. Supportive treatment improves survival in multivisceral cholesterol crystal embolism. *Am J Kidney Dis* (1999) **33**:840–850. doi:10.1016/S0272-6386(99)70415-4
29. Scolari F, Ravani P, Pola A, Guerini S, Zubani R, Movilli E, Savoldi S, Malberti F, Maiorca R. Predictors of renal and patient outcomes in atheroembolic renal disease: a prospective study. *J Am Soc Nephrol* (2003) **14**:1584–1590. doi:10.1097/01.asn.0000069220.60954.f1
30. Meyrier A. Cholesterol crystal embolism: Diagnosis and treatment. *Kidney Int* (2006) **69**:1308–1312. doi:10.1038/sj.ki.5000263
31. Lye WC, Cheah JS, Sinniah R. Renal cholesterol embolic disease. Case report and review of the literature. *Am J Nephrol* (1993) **13**:489–493. doi:10.1159/000168669
32. Hitti WA, Wali RK, Weinman EJ, Drachenberg C, Briglia A. Cholesterol embolization syndrome induced by thrombolytic therapy. *Am J Cardiovasc Drugs* (2008) **8**:27–34. doi:10.2165/00129784-200808010-00004
33. FEDER W, AUERBACH R. “Purple toes”: an uncommon sequela of oral coumarin drug therapy. *Ann Intern Med* (1961) **55**:911–917. doi:10.7326/0003-4819-55-6-911
34. The ultrastructure of the stages of atheroembolic occlusion of renal arteries. *Br J Exp Pathol* (1973) **54**:469–478.

35. Frock J, Bierman M, Hammeke M, Reyes A. Atheroembolic renal disease: experience with 22 patients. *Nebr Med J* (1994) **79**:317–321.
36. Mittal B V, Alexander MP, Rennke HG, Singh AK. Atheroembolic renal disease: a silent masquerader. *Kidney Int* (2008) **73**:126–130. doi:10.1038/sj.ki.5002433
37. Donohue KG, Saap L, Falanga V. Cholesterol crystal embolization: an atherosclerotic disease with frequent and varied cutaneous manifestations. *J Eur Acad Dermatol Venereol* (2003) **17**:504–511. doi:10.1046/j.1468-3083.2003.00710.x
38. Lie JT. Cholesterol atheromatous embolism. The great masquerader revisited. *Pathol Annu* (1992) **27 Pt 2**:17–50.
39. Yücel AE, Kart-Köseoglu H, Demirhan B, Ozdemir FN. Cholesterol crystal embolization mimicking vasculitis: success with corticosteroid and cyclophosphamide therapy in two cases. *Rheumatol Int* (2006) **26**:454–460. doi:10.1007/s00296-005-0012-4
40. Nakayama M, Nagata M, Hirano T, Sugai K, Katafuchi R, Imayama S, Uesugi N, Tsuchihashi T, Kumagai H. Low-dose prednisolone ameliorates acute renal failure caused by cholesterol crystal embolism. *Clin Nephrol* (2006) **66**:232–239. doi:10.5414/cnp66232
41. Scolari F, Ravani P, Gaggi R, Santostefano M, Rollino C, Stabellini N, Colla L, Viola BF, Maiorca P, Venturelli C, et al. The challenge of diagnosing atheroembolic renal disease: clinical features and prognostic factors. *Circulation* (2007) **116**:298–304. doi:10.1161/CIRCULATIONAHA.106.680991
42. Rocha-Singh KJ, Eisenhauer AC, Textor SC, Cooper CJ, Tan WA, Matsumoto AH, Rosenfield K. Atherosclerotic Peripheral Vascular Disease Symposium II: intervention for renal artery disease. *Circulation* (2008) **118**:2873–2878. doi:10.1161/CIRCULATIONAHA.108.191178
43. Hoste EAJ, Schurgers M. Epidemiology of acute kidney injury: how big is the problem? *Crit Care Med* (2008) **36**:S146–51. doi:10.1097/CCM.0b013e318168c590
44. Palevsky PM, Liu KD, Brophy PD, Chawla LS, Parikh CR, Thakar C V, Tolwani AJ, Waikar SS, Weisbord SD. KDOQI US commentary on the 2012 KDIGO clinical practice guideline for acute kidney injury. *Am J kidney Dis Off J Natl Kidney Found* (2013) **61**:649–672. doi:10.1053/j.ajkd.2013.02.349

45. Lameire N, Van Biesen W, Vanholder R. The changing epidemiology of acute renal failure. *Nat Clin Pract Nephrol* (2006) **2**:364–377. doi:10.1038/ncpneph0218
46. Thadhani R, Pascual M, Bonventre J V. Acute renal failure. *N Engl J Med* (1996) **334**:1448–1460. doi:10.1056/NEJM199605303342207
47. Bonventre J V, Yang L. Cellular pathophysiology of ischemic acute kidney injury. *J Clin Invest* (2011) **121**:4210–4221. doi:10.1172/JCI45161
48. Siew ED, Davenport A. The growth of acute kidney injury: a rising tide or just closer attention to detail? *Kidney Int* (2015) **87**:46–61. doi:10.1038/ki.2014.293
49. Lameire NH, Bagga A, Cruz D, De Maeseneer J, Endre Z, Kellum JA, Liu KD, Mehta RL, Pannu N, Van Biesen W, et al. Acute kidney injury: an increasing global concern. *Lancet (London, England)* (2013) **382**:170–179. doi:10.1016/S0140-6736(13)60647-9
50. Zuk A, Bonventre J V. Acute Kidney Injury. *Annu Rev Med* (2016) **67**:293–307. doi:10.1146/annurev-med-050214-013407
51. Susantitaphong P, Cruz DN, Cerda J, Abulfaraj M, Alqahtani F, Koulouridis I, Jaber BL. World incidence of AKI: a meta-analysis. *Clin J Am Soc Nephrol* (2013) **8**:1482–1493. doi:10.2215/CJN.00710113
52. Chawla LS, Bellomo R, Bihorac A, Goldstein SL, Siew ED, Bagshaw SM, Bittleman D, Cruz D, Endre Z, Fitzgerald RL, et al. Acute kidney disease and renal recovery: consensus report of the Acute Disease Quality Initiative (ADQI) 16 Workgroup. *Nat Rev Nephrol* (2017) **13**:241–257. doi:10.1038/nrneph.2017.2
53. Piéroni L, Bargnoux A-S, Cristol J-P, Cavalier E, Delanaye P. Did Creatinine Standardization Give Benefits to the Evaluation of Glomerular Filtration Rate? *EJIFCC* (2017) **28**:251–257.
54. Ronco C, Bellomo R, Kellum J. Understanding renal functional reserve. *Intensive Care Med* (2017) **43**:917–920. doi:10.1007/s00134-017-4691-6
55. Ronco C, Rizo-Topete L, Serrano-Soto M, Kashani K. Pro: Prevention of acute kidney injury: time for teamwork and new biomarkers. *Nephrol Dial Transplant Off Publ Eur Dial Transpl Assoc - Eur Ren Assoc* (2017) **32**:408–413. doi:10.1093/ndt/gfx016
56. Vandenberghe W, Gevaert S, Kellum JA, Bagshaw SM, Peperstraete H, Herck I, Decruyenaere J, Hoste EAJ. Acute Kidney Injury in Cardiorenal Syndrome Type 1

- Patients: A Systematic Review and Meta-Analysis. *Cardiorenal Med* (2016) **6**:116–128. doi:10.1159/000442300
57. Kellum JA, Chawla LS, Keener C, Singbartl K, Palevsky PM, Pike FL, Yealy DM, Huang DT, Angus DC. The Effects of Alternative Resuscitation Strategies on Acute Kidney Injury in Patients with Septic Shock. *Am J Respir Crit Care Med* (2016) **193**:281–287. doi:10.1164/rccm.201505-0995OC
58. Hobson CE, Yavas S, Segal MS, Schold JD, Tribble CG, Layon AJ, Bihorac A. Acute kidney injury is associated with increased long-term mortality after cardiothoracic surgery. *Circulation* (2009) **119**:2444–2453. doi:10.1161/CIRCULATIONAHA.108.800011
59. Verma SK, Molitoris BA. Renal endothelial injury and microvascular dysfunction in acute kidney injury. *Semin Nephrol* (2015) **35**:96–107. doi:10.1016/j.semnephrol.2015.01.010
60. Bonventre J V, Weinberg JM. Recent advances in the pathophysiology of ischemic acute renal failure. *J Am Soc Nephrol* (2003) **14**:2199–2210. doi:10.1097/01.asn.0000079785.13922.f6
61. Han SJ, Lee HT. Mechanisms and therapeutic targets of ischemic acute kidney injury. *Kidney Res Clin Pract* (2019) **38**:427–440. doi:10.23876/j.krcp.19.062
62. Prowle J, Bagshaw SM, Bellomo R. Renal blood flow, fractional excretion of sodium and acute kidney injury: time for a new paradigm? *Curr Opin Crit Care* (2012) **18**:585–592. doi:10.1097/MCC.0b013e328358d480
63. Ergin B, Kapucu A, Demirci-Tansel C, Ince C. The renal microcirculation in sepsis. *Nephrol Dial Transplant Off Publ Eur Dial Transpl Assoc - Eur Ren Assoc* (2015) **30**:169–177. doi:10.1093/ndt/gfu105
64. Matejovic M, Ince C, Chawla LS, Blantz R, Molitoris BA, Rosner MH, Okusa MD, Kellum JA, Ronco C. Renal Hemodynamics in AKI: In Search of New Treatment Targets. *J Am Soc Nephrol* (2016) **27**:49–58. doi:10.1681/ASN.2015030234
65. Just A. Mechanisms of renal blood flow autoregulation: dynamics and contributions. *Am J Physiol Regul Integr Comp Physiol* (2007) **292**:R1-17. doi:10.1152/ajpregu.00332.2006
66. Salmasi V, Maheshwari K, Yang D, Mascha EJ, Singh A, Sessler DI, Kurz A. Relationship between Intraoperative Hypotension, Defined by Either Reduction from Baseline or

- Absolute Thresholds, and Acute Kidney and Myocardial Injury after Noncardiac Surgery: A Retrospective Cohort Analysis. *Anesthesiology* (2017) **126**:47–65. doi:10.1097/ALN.0000000000001432
67. El Sabbahy M, Vaidya VS. Ischemic kidney injury and mechanisms of tissue repair. *Wiley Interdiscip Rev Syst Biol Med* (2011) **3**:606–618. doi:10.1002/wsbm.133
68. Molitoris BA. Therapeutic translation in acute kidney injury: the epithelial/endothelial axis. *J Clin Invest* (2014) **124**:2355–2363. doi:10.1172/JCI72269
69. Sutton TA, Mang HE, Campos SB, Sandoval RM, Yoder MC, Molitoris BA. Injury of the renal microvascular endothelium alters barrier function after ischemia. *Am J Physiol Renal Physiol* (2003) **285**:F191-8. doi:10.1152/ajprenal.00042.2003
70. Molitoris BA, Sandoval RM. Kidney endothelial dysfunction: ischemia, localized infections and sepsis. *Contrib Nephrol* (2011) **174**:108–118. doi:10.1159/000329248
71. Rabb H, Griffin MD, McKay DB, Swaminathan S, Pickkers P, Rosner MH, Kellum JA, Ronco C. Inflammation in AKI: Current Understanding, Key Questions, and Knowledge Gaps. *J Am Soc Nephrol* (2016) **27**:371–379. doi:10.1681/ASN.2015030261
72. Jang HR, Rabb H. Immune cells in experimental acute kidney injury. *Nat Rev Nephrol* (2015) **11**:88–101. doi:10.1038/nrneph.2014.180
73. van der Vliet JA, Warlé MC. The need to reduce cold ischemia time in kidney transplantation. *Curr Opin Organ Transplant* (2013) **18**:174–178. doi:10.1097/MOT.0b013e32835e2a08
74. Newton K, Dugger DL, Maltzman A, Greve JM, Hedehus M, Martin-McNulty B, Carano RAD, Cao TC, van Bruggen N, Bernstein L, et al. RIPK3 deficiency or catalytically inactive RIPK1 provides greater benefit than MLKL deficiency in mouse models of inflammation and tissue injury. *Cell Death Differ* (2016) **23**:1565–1576. doi:10.1038/cdd.2016.46
75. Müller T, Dewitz C, Schmitz J, Schröder AS, Bräsen JH, Stockwell BR, Murphy JM, Kunzendorf U, Krautwald S. Necroptosis and ferroptosis are alternative cell death pathways that operate in acute kidney failure. *Cell Mol Life Sci* (2017) **74**:3631–3645. doi:10.1007/s00018-017-2547-4
76. Jorgensen I, Rayamajhi M, Miao EA. Programmed cell death as a defence against infection. *Nat Rev Immunol* (2017) **17**:151–164. doi:10.1038/nri.2016.147

77. Sureshbabu A, Patino E, Ma KC, Laursen K, Finkelsztein EJ, Akchurin O, Muthukumar T, Rytter SW, Gudas L, Choi AMK, et al. RIPK3 promotes sepsis-induced acute kidney injury via mitochondrial dysfunction. *JCI insight* (2018) **3**: doi:10.1172/jci.insight.98411
78. Zhang L, Jiang F, Chen Y, Luo J, Liu S, Zhang B, Ye Z, Wang W, Liang X, Shi W. Necrostatin-1 attenuates ischemia injury induced cell death in rat tubular cell line NRK-52E through decreased Drp1 expression. *Int J Mol Sci* (2013) **14**:24742–24754. doi:10.3390/ijms141224742
79. Linkermann A, Bräsen JH, Himmerkus N, Liu S, Huber TB, Kunzendorf U, Krautwald S. Rip1 (Receptor-interacting protein kinase 1) mediates necroptosis and contributes to renal ischemia/reperfusion injury. *Kidney Int* (2012) **81**:751–761. doi:10.1038/ki.2011.450
80. Hildebrand JM, Tanzer MC, Lucet IS, Young SN, Spall SK, Sharma P, Pierotti C, Garnier J-M, Dobson RCJ, Webb AI, et al. Activation of the pseudokinase MLKL unleashes the four-helix bundle domain to induce membrane localization and necroptotic cell death. *Proc Natl Acad Sci U S A* (2014) **111**:15072–15077. doi:10.1073/pnas.1408987111
81. Sun L, Wang H, Wang Z, He S, Chen S, Liao D, Wang L, Yan J, Liu W, Lei X, et al. Mixed lineage kinase domain-like protein mediates necrosis signaling downstream of RIP3 kinase. *Cell* (2012) **148**:213–227. doi:10.1016/j.cell.2011.11.031
82. Mandal P, Berger SB, Pillay S, Moriwaki K, Huang C, Guo H, Lich JD, Finger J, Kasparcova V, Votta B, et al. RIP3 induces apoptosis independent of pronecrotic kinase activity. *Mol Cell* (2014) **56**:481–495. doi:10.1016/j.molcel.2014.10.021
83. Tanzer MC, Tripaydonis A, Webb AI, Young SN, Varghese LN, Hall C, Alexander WS, Hildebrand JM, Silke J, Murphy JM. Necroptosis signalling is tuned by phosphorylation of MLKL residues outside the pseudokinase domain activation loop. *Biochem J* (2015) **471**:255–265. doi:10.1042/BJ20150678
84. Tonnus W, Linkermann A. The in vivo evidence for regulated necrosis. *Immunol Rev* (2017) **277**:128–149. doi:10.1111/imr.12551
85. Conos SA, Chen KW, De Nardo D, Hara H, Whitehead L, Núñez G, Masters SL, Murphy JM, Schroder K, Vaux DL, et al. Active MLKL triggers the NLRP3 inflammasome in a cell-

- intrinsic manner. *Proc Natl Acad Sci U S A* (2017) **114**:E961–E969.
doi:10.1073/pnas.1613305114
86. Krysko D V, Garg AD, Kaczmarek A, Krysko O, Agostinis P, Vandenabeele P. Immunogenic cell death and DAMPs in cancer therapy. *Nat Rev Cancer* (2012) **12**:860–875. doi:10.1038/nrc3380
87. Linkermann A, Stockwell BR, Krautwald S, Anders H-J. Regulated cell death and inflammation: an auto-amplification loop causes organ failure. *Nat Rev Immunol* (2014) **14**:759–767. doi:10.1038/nri3743
88. Martin-Sanchez D, Ruiz-Andres O, Poveda J, Carrasco S, Cannata-Ortiz P, Sanchez-Niño MD, Ruiz Ortega M, Egido J, Linkermann A, Ortiz A, et al. Ferroptosis, but Not Necroptosis, Is Important in Nephrotoxic Folic Acid–Induced AKI. *J Am Soc Nephrol* (2017) **28**:218–229. doi:10.1681/ASN.2015121376
89. Martin-Sanchez D, Fontecha-Barriuso M, Carrasco S, Sanchez-Niño MD, Mässenhausen A von, Linkermann A, Cannata-Ortiz P, Ruiz-Ortega M, Egido J, Ortiz A, et al. TWEAK and RIPK1 mediate a second wave of cell death during AKI. *Proc Natl Acad Sci* (2018) **115**:4182–4187. doi:10.1073/pnas.1716578115
90. Singbartl K, Green SA, Ley K. Blocking P-selectin protects from ischemia/reperfusion-induced acute renal failure. *FASEB J Off Publ Fed Am Soc Exp Biol* (2000) **14**:48–54. doi:10.1096/fasebj.14.1.48
91. Kelly KJ, Molitoris BA. Acute renal failure in the new millennium: time to consider combination therapy. *Semin Nephrol* (2000) **20**:4–19.
92. Sharfuddin AA, Molitoris BA. Pathophysiology of ischemic acute kidney injury. *Nat Rev Nephrol* (2011) **7**:189–200. doi:10.1038/nrneph.2011.16
93. Niemann-Masanek U, Mueller A, Yard BA, Waldherr R, van der Woude FJ. B7-1 (CD80) and B7-2 (CD 86) expression in human tubular epithelial cells in vivo and in vitro. *Nephron* (2002) **92**:542–556. doi:10.1159/000064084
94. Schofield ZV, Woodruff TM, Halai R, Wu MC-L, Cooper MA. Neutrophils--a key component of ischemia-reperfusion injury. *Shock* (2013) **40**:463–470. doi:10.1097/SHK.0000000000000044
95. Kinsey GR, Li L, Okusa MD. Inflammation in acute kidney injury. *Nephron Exp Nephrol* (2008) **109**:e102-7. doi:10.1159/000142934

96. Frangogiannis NG. Chemokines in ischemia and reperfusion. *Thromb Haemost* (2007) **97**:738–747.
97. Kelly KJ, Williams WWJ, Colvin RB, Meehan SM, Springer TA, Gutierrez-Ramos JC, Bonventre J V. Intercellular adhesion molecule-1-deficient mice are protected against ischemic renal injury. *J Clin Invest* (1996) **97**:1056–1063. doi:10.1172/JCI118498
98. Thornton MA, Winn R, Alpers CE, Zager RA. An evaluation of the neutrophil as a mediator of in vivo renal ischemic-reperfusion injury. *Am J Pathol* (1989) **135**:509–515.
99. Raup-Konsavage WM, Wang Y, Wang WW, Feliers D, Ruan H, Reeves WB. Neutrophil peptidyl arginine deiminase-4 has a pivotal role in ischemia/reperfusion-induced acute kidney injury. *Kidney Int* (2018) **93**:365–374. doi:10.1016/j.kint.2017.08.014
100. Rabb H, Mendiola CC, Dietz J, Saba SR, Issekutz TB, Abanilla F, Bonventre J V, Ramirez G. Role of CD11a and CD11b in ischemic acute renal failure in rats. *Am J Physiol* (1994) **267**:F1052-8. doi:10.1152/ajprenal.1994.267.6.F1052
101. Maddock HL, Gardner NM, Khandoudi N, Bril A, Broadley KJ. Protection from myocardial stunning by ischaemia and hypoxia with the adenosine A3 receptor agonist, IB-MECA. *Eur J Pharmacol* (2003) **477**:235–245. doi:10.1016/j.ejphar.2003.08.024
102. Kezić A, Stajic N, Thaiss F. Innate Immune Response in Kidney Ischemia/Reperfusion Injury: Potential Target for Therapy. *J Immunol Res* (2017) **2017**:6305439. doi:10.1155/2017/6305439
103. Baek J-H. The Impact of Versatile Macrophage Functions on Acute Kidney Injury and Its Outcomes. *Front Physiol* (2019) **10**:1016. doi:10.3389/fphys.2019.01016
104. Lee S, Huen S, Nishio H, Nishio S, Lee HK, Choi B-S, Ruhrberg C, Cantley LG. Distinct macrophage phenotypes contribute to kidney injury and repair. *J Am Soc Nephrol* (2011) **22**:317–326. doi:10.1681/ASN.2009060615
105. Benetti E, Chiazza F, Patel NSA, Collino M. The NLRP3 Inflammasome as a novel player of the intercellular crosstalk in metabolic disorders. *Mediators Inflamm* (2013) **2013**:678627. doi:10.1155/2013/678627

106. Chang A, Ko K, Clark MR. The emerging role of the inflammasome in kidney diseases. *Curr Opin Nephrol Hypertens* (2014) **23**:204–210. doi:10.1097/01.mnh.0000444814.49755.90
107. Stienstra R, van Diepen JA, Tack CJ, Zaki MH, van de Veerdonk FL, Perera D, Neale GA, Hooiveld GJ, Hijmans A, Vroegrijk I, et al. Inflammasome is a central player in the induction of obesity and insulin resistance. *Proc Natl Acad Sci U S A* (2011) **108**:15324–15329. doi:10.1073/pnas.1100255108
108. Lee DW, Faubel S, Edelstein CL. Cytokines in acute kidney injury (AKI). *Clin Nephrol* (2011) **76**:165–173. doi:10.5414/cn106921
109. Berry M, Clatworthy MR. Immunotherapy for acute kidney injury. *Immunotherapy* (2012) **4**:323–334. doi:10.2217/imt.11.175
110. Iyer SS, Pulskens WP, Sadler JJ, Butter LM, Teske GJ, Ulland TK, Eisenbarth SC, Florquin S, Flavell RA, Leemans JC, et al. Necrotic cells trigger a sterile inflammatory response through the Nlrp3 inflammasome. *Proc Natl Acad Sci U S A* (2009) **106**:20388–20393. doi:10.1073/pnas.0908698106
111. Rusai K, Huang H, Sayed N, Strobl M, Roos M, Schmaderer C, Heemann U, Lutz J. Administration of interleukin-1 receptor antagonist ameliorates renal ischemia-reperfusion injury. *Transpl Int Off J Eur Soc Organ Transplant* (2008) **21**:572–580. doi:10.1111/j.1432-2277.2008.00651.x
112. Coca SG, Yalavarthy R, Concato J, Parikh CR. Biomarkers for the diagnosis and risk stratification of acute kidney injury: a systematic review. *Kidney Int* (2008) **73**:1008–1016. doi:10.1038/sj.ki.5002729
113. Coca SG, Yusuf B, Shlipak MG, Garg AX, Parikh CR. Long-term risk of mortality and other adverse outcomes after acute kidney injury: a systematic review and meta-analysis. *Am J kidney Dis Off J Natl Kidney Found* (2009) **53**:961–973. doi:10.1053/j.ajkd.2008.11.034
114. See EJ, Jayasinghe K, Glassford N, Bailey M, Johnson DW, Polkinghorne KR, Toussaint ND, Bellomo R. Long-term risk of adverse outcomes after acute kidney injury: a systematic review and meta-analysis of cohort studies using consensus definitions of exposure. *Kidney Int* (2019) **95**:160–172. doi:10.1016/j.kint.2018.08.036

115. Grams ME, Sang Y, Coresh J, Ballew S, Matsushita K, Molnar MZ, Szabo Z, Kalantar-Zadeh K, Kovesdy CP. Acute Kidney Injury After Major Surgery: A Retrospective Analysis of Veterans Health Administration Data. *Am J kidney Dis Off J Natl Kidney Found* (2016) **67**:872–880. doi:10.1053/j.ajkd.2015.07.022
116. Millán JL. Alkaline Phosphatases : Structure, substrate specificity and functional relatedness to other members of a large superfamily of enzymes. *Purinergic Signal* (2006) **2**:335–341. doi:10.1007/s11302-005-5435-6
117. van Veen SQ, van Vliet AK, Wulferink M, Brands R, Boermeester MA, van Gulik TM. Bovine intestinal alkaline phosphatase attenuates the inflammatory response in secondary peritonitis in mice. *Infect Immun* (2005) **73**:4309–4314. doi:10.1128/IAI.73.7.4309-4314.2005
118. Heemskerk S, Masereeuw R, Moesker O, Bouw MPWJM, van der Hoeven JG, Peters WHM, Russel FGM, Pickkers P. Alkaline phosphatase treatment improves renal function in severe sepsis or septic shock patients. *Crit Care Med* (2009) **37**:417–23, e1. doi:10.1097/CCM.0b013e31819598af
119. Pickkers P, Heemskerk S, Schouten J, Laterre P-F, Vincent J-L, Beishuizen A, Jorens PG, Spapen H, Bulitta M, Peters WHM, et al. Alkaline phosphatase for treatment of sepsis-induced acute kidney injury: a prospective randomized double-blind placebo-controlled trial. *Crit Care* (2012) **16**:R14. doi:10.1186/cc11159
120. Pickkers P, Mehta RL, Murray PT, Joannidis M, Molitoris BA, Kellum JA, Bachler M, Hoste EAJ, Hoiting O, Krell K, et al. Effect of Human Recombinant Alkaline Phosphatase on 7-Day Creatinine Clearance in Patients With Sepsis-Associated Acute Kidney Injury: A Randomized Clinical Trial. *JAMA* (2018) **320**:1998–2009. doi:10.1001/jama.2018.14283
121. Yoshida T, Yamashita M, Iwai M, Hayashi M. Endothelial Krüppel-Like Factor 4 Mediates the Protective Effect of Statins against Ischemic AKI. *J Am Soc Nephrol* (2016) **27**:1379–1388. doi:10.1681/ASN.2015040460
122. Molnar AO, Coca SG, Devereaux PJ, Jain AK, Kitchlu A, Luo J, Parikh CR, Paterson JM, Siddiqui N, Wald R, et al. Statin use associates with a lower incidence of acute kidney injury after major elective surgery. *J Am Soc Nephrol* (2011) **22**:939–946. doi:10.1681/ASN.2010050442

123. Quintavalle C, Fiore D, De Micco F, Visconti G, Focaccio A, Golia B, Ricciardelli B, Donnarumma E, Bianco A, Zabatta MA, et al. Impact of a high loading dose of atorvastatin on contrast-induced acute kidney injury. *Circulation* (2012) **126**:3008–3016. doi:10.1161/CIRCULATIONAHA.112.103317
124. Mehran R, Aymong ED, Nikolsky E, Lasic Z, Iakovou I, Fahy M, Mintz GS, Lansky AJ, Moses JW, Stone GW, et al. A simple risk score for prediction of contrast-induced nephropathy after percutaneous coronary intervention: development and initial validation. *J Am Coll Cardiol* (2004) **44**:1393–1399. doi:10.1016/j.jacc.2004.06.068
125. Miao Y, Zhong Y, Yan H, Li W, Wang B-Y, Jin J. Alprostadil plays a protective role in contrast-induced nephropathy in the elderly. *Int Urol Nephrol* (2013) **45**:1179–1185. doi:10.1007/s11255-013-0484-1
126. Liu W-J, Zhang B-C, Guo R, Wei Y-D, Li W-M, Xu Y-W. Renoprotective effect of alprostadil in combination with statins in patients with mild to moderate renal failure undergoing coronary angiography. *Chin Med J (Engl)* (2013) **126**:3475–3480.
127. Vallon V, Osswald H. Adenosine receptors and the kidney. *Handb Exp Pharmacol* (2009)443–470. doi:10.1007/978-3-540-89615-9_15
128. Bianco JA, Appelbaum FR, Nemunaitis J, Almgren J, Andrews F, Kettner P, Shields A, Singer JW. Phase I-II trial of pentoxifylline for the prevention of transplant-related toxicities following bone marrow transplantation. *Blood* (1991) **78**:1205–1211.
129. Clift RA, Bianco JA, Appelbaum FR, Buckner CD, Singer JW, Bakke L, Bensinger WI, Bowden RA, McDonald GB, Schubert M. A randomized controlled trial of pentoxifylline for the prevention of regimen-related toxicities in patients undergoing allogeneic marrow transplantation. *Blood* (1993) **82**:2025–2030.
130. Hsu RK, McCulloch CE, Dudley RA, Lo LJ, Hsu C. Temporal changes in incidence of dialysis-requiring AKI. *J Am Soc Nephrol* (2013) **24**:37–42. doi:10.1681/ASN.2012080800
131. Li S, Gokden N, Okusa MD, Bhatt R, Portilla D. Anti-inflammatory effect of fibrate protects from cisplatin-induced ARF. *Am J Physiol Renal Physiol* (2005) **289**:F469–80. doi:10.1152/ajprenal.00038.2005

132. Kinsey GR, Sharma R, Huang L, Li L, Vergis AL, Ye H, Ju S-T, Okusa MD. Regulatory T cells suppress innate immunity in kidney ischemia-reperfusion injury. *J Am Soc Nephrol* (2009) **20**:1744–1753. doi:10.1681/ASN.2008111160
133. Tögel FE, Westenfelder C. Mesenchymal stem cells: a new therapeutic tool for AKI. *Nat Rev Nephrol* (2010) **6**:179–183. doi:10.1038/nrneph.2009.229
134. Sciascia S, Cuadrado MJ, Khamashta M, Roccatello D. Renal involvement in antiphospholipid syndrome. *Nat Rev Nephrol* (2014) **10**:279–289. doi:10.1038/nrneph.2014.38
135. Kagaya S, Yoshie O, Fukami H, Sato H, Saito A, Takeuchi Y, Matsuda K, Nagasawa T. Renal infarct volume and renal function decline in acute and chronic phases. *Clin Exp Nephrol* (2017) **21**:1030–1034. doi:10.1007/s10157-017-1399-4
136. Bae EJ, Hwang K, Jang HN, Kim MJ, Jeon D-H, Kim H-J, Cho HS, Chang S-H, Park DJ. A retrospective study of short- and long-term effects on renal function after acute renal infarction. *Ren Fail* (2014) **36**:1385–1389. doi:10.3109/0886022X.2014.947514
137. Bourgault M, Grimbert P, Verret C, Pourrat J, Herody M, Halimi JM, Karras A, Amoura Z, Jourde-Chiche N, Izzedine H, et al. Acute renal infarction: a case series. *Clin J Am Soc Nephrol* (2013) **8**:392–398. doi:10.2215/CJN.05570612
138. Bolderman R, Oyen R, Verrijcken A, Knockaert D, Vanderschueren S. Idiopathic renal infarction. *Am J Med* (2006) **119**:356.e9–12. doi:10.1016/j.amjmed.2005.06.049
139. Lin W-L, Seak C-J, Wu J-Y, Weng Y-M, Chen H-C. Risk factors for development of chronic kidney disease following renal infarction: retrospective evaluation of emergency room patients from a single center. *PLoS One* (2014) **9**:e98880. doi:10.1371/journal.pone.0098880
140. Frost L, Engholm G, Johnsen S, Møller H, Henneberg EW, Husted S. Incident thromboembolism in the aorta and the renal, mesenteric, pelvic, and extremity arteries after discharge from the hospital with a diagnosis of atrial fibrillation. *Arch Intern Med* (2001) **161**:272–276. doi:10.1001/archinte.161.2.272
141. Antopolsky M, Simanovsky N, Stalnikowicz R, Salameh S, Hiller N. Renal infarction in the ED: 10-year experience and review of the literature. *Am J Emerg Med* (2012) **30**:1055–1060. doi:10.1016/j.ajem.2011.06.041

142. Hazanov N, Somin M, Attali M, Beilinson N, Thaler M, Mouallem M, Maor Y, Zaks N, Malnick S. Acute renal embolism. Forty-four cases of renal infarction in patients with atrial fibrillation. *Medicine (Baltimore)* (2004) **83**:292–299.
doi:10.1097/01.md.0000141097.08000.99
143. Oh YK, Yang CW, Kim Y-L, Kang S-W, Park CW, Kim YS, Lee EY, Han BG, Lee SH, Kim S-H, et al. Clinical Characteristics and Outcomes of Renal Infarction. *Am J kidney Dis Off J Natl Kidney Found* (2016) **67**:243–250. doi:10.1053/j.ajkd.2015.09.019
144. Zhou X-J, Liu L-J, Chen M, Zhou F-D. Asynchronous Bilateral Renal Infarction and Thrombophilia With Associated Gene Mutations in a 43-Year-Old Man: A Case Report. *Medicine (Baltimore)* (2016) **95**:e3258. doi:10.1097/MD.0000000000003258
145. Altın C, Sakalioğlu O, Gezmiş E, Müderrisoğlu H. A novel oral anticoagulant, dabigatran, in acute renal infarction. *Anatol J Cardiol* (2015) **15**:158–159.
doi:10.5152/akd.2015.5837
146. Yun W-S. Long-term follow-up results of acute renal embolism after anticoagulation therapy. *Ann Vasc Surg* (2015) **29**:491–495. doi:10.1016/j.avsg.2014.09.028
147. Marschner JA, Schäfer H, Holderied A, Anders H-J. Optimizing Mouse Surgery with Online Rectal Temperature Monitoring and Preoperative Heat Supply. Effects on Post-Ischemic Acute Kidney Injury. *PLoS One* (2016) **11**:e0149489.
doi:10.1371/journal.pone.0149489
148. Joshi CN, Jain SK, Murthy PSR. An optimized triphenyltetrazolium chloride method for identification of cerebral infarcts. *Brain Res Brain Res Protoc* (2004) **13**:11–17.
doi:10.1016/j.brainresprot.2003.12.001
149. Schreiber A, Shulhevich Y, Geraci S, Hesser J, Stsepankou D, Neudecker S, Koenig S, Heinrich R, Hoecklin F, Pill J, et al. Transcutaneous measurement of renal function in conscious mice. *Am J Physiol Renal Physiol* (2012) **303**:F783-8.
doi:10.1152/ajprenal.00279.2012
150. Friedemann J, Heinrich R, Shulhevich Y, Raedle M, William-Olsson L, Pill J, Schock-Kusch D. Improved kinetic model for the transcutaneous measurement of glomerular filtration rate in experimental animals. *Kidney Int* (2016) **90**:1377–1385.
doi:10.1016/j.kint.2016.07.024

151. Ehling J, Bábíčková J, Gremse F, Klinkhammer BM, Baetke S, Knuechel R, Kiessling F, Floege J, Lammers T, Boor P. Quantitative Micro-Computed Tomography Imaging of Vascular Dysfunction in Progressive Kidney Diseases. *J Am Soc Nephrol* (2016) **27**:520–532. doi:10.1681/ASN.2015020204
152. Gremse F, Stärk M, Ehling J, Menzel JR, Lammers T, Kiessling F. Imalytics Preclinical: Interactive Analysis of Biomedical Volume Data. *Theranostics* (2016) **6**:328–341. doi:10.7150/thno.13624
153. Trietsch SJ, Naumovska E, Kurek D, Setyawati MC, Vormann MK, Wilschut KJ, Lanz HL, Nicolas A, Ng CP, Joore J, et al. Membrane-free culture and real-time barrier integrity assessment of perfused intestinal epithelium tubes. *Nat Commun* (2017) **8**:262. doi:10.1038/s41467-017-00259-3
154. Zimmermann S, Zarse K, Schulz TJ, Siems K, Müller-Kuhrt L, Birringer M, Ristow M. A cell-based high-throughput assay system reveals modulation of oxidative and nonoxidative glucose metabolism due to commonly used organic solvents. *Horm Metab Res = Horm und Stoffwechselforsch = Horm Metab* (2008) **40**:29–37. doi:10.1055/s-2007-1004542
155. Chernysh IN, Nagaswami C, Kosolapova S, Peshkova AD, Cuker A, Cines DB, Cambor CL, Litvinov RI, Weisel JW. The distinctive structure and composition of arterial and venous thrombi and pulmonary emboli. *Sci Rep* (2020) **10**:5112. doi:10.1038/s41598-020-59526-x
156. Yau JW, Teoh H, Verma S. Endothelial cell control of thrombosis. *BMC Cardiovasc Disord* (2015) **15**:130. doi:10.1186/s12872-015-0124-z
157. Tomaiuolo M, Brass LF, Stalker TJ. Regulation of Platelet Activation and Coagulation and Its Role in Vascular Injury and Arterial Thrombosis. *Interv Cardiol Clin* (2017) **6**:1–12. doi:10.1016/j.iccl.2016.08.001
158. Mezger M, Nording H, Sauter R, Graf T, Heim C, von Bubnoff N, Ensminger SM, Langer HF. Platelets and Immune Responses During Thromboinflammation. *Front Immunol* (2019) **10**:1731. doi:10.3389/fimmu.2019.01731
159. Lippi G, Franchini M, Targher G. Arterial thrombus formation in cardiovascular disease. *Nat Rev Cardiol* (2011) **8**:502–512. doi:10.1038/nrcardio.2011.91

160. Furie B, Furie BC. Mechanisms of thrombus formation. *N Engl J Med* (2008) **359**:938–949. doi:10.1056/NEJMra0801082
161. Mochan E, Keler T. Plasmin degradation of cartilage proteoglycan. *Biochim Biophys Acta* (1984) **800**:312–315. doi:10.1016/0304-4165(84)90412-4
162. Zorio E, Gilabert-Estellés J, España F, Ramón LA, Cosín R, Estellés A. Fibrinolysis: the key to new pathogenetic mechanisms. *Curr Med Chem* (2008) **15**:923–929. doi:10.2174/092986708783955455
163. Jernberg T, Payne CD, Winters KJ, Darstein C, Brandt JT, Jakubowski JA, Naganuma H, Siegbahn A, Wallentin L. Prasugrel achieves greater inhibition of platelet aggregation and a lower rate of non-responders compared with clopidogrel in aspirin-treated patients with stable coronary artery disease. *Eur Heart J* (2006) **27**:1166–1173. doi:10.1093/eurheartj/ehi877
164. Albadawi H, Oklu R, Raacke Malley RE, O’Keefe RM, Uong TP, Cormier NR, Watkins MT. Effect of DNase I treatment and neutrophil depletion on acute limb ischemia-reperfusion injury in mice. *J Vasc Surg* (2016) **64**:484–493. doi:10.1016/j.jvs.2015.01.031
165. Carestia A, Kaufman T, Schattner M. Platelets: New bricks in the building of neutrophil extracellular traps. *Front Immunol* (2016) **7**: doi:10.3389/fimmu.2016.00271
166. Anders HJ, Suarez-Alvarez B, Grigorescu M, Foresto-Neto O, Steiger S, Desai J, Marschner JA, Honarpisheh M, Shi C, Jordan J, et al. The macrophage phenotype and inflammasome component NLRP3 contributes to nephrocalcinosis-related chronic kidney disease independent from IL-1–mediated tissue injury. *Kidney Int* (2018) **93**:753–760. doi:10.1016/j.kint.2017.09.022
167. Jiménez-Alcázar M, Rangaswamy C, Panda R, Bitterling J, Simsek YJ, Long AT, Bilyy R, Krenn V, Renné C, Renné T, et al. Host DNases prevent vascular occlusion by neutrophil extracellular traps. *Science (80-)* (2017) **358**:1202–1206. doi:10.1126/science.aam8897
168. Gould TJ, Vu TT, Swystun LL, Dwivedi DJ, Mai SHC, Weitz JI, Liaw PC. Neutrophil extracellular traps promote thrombin generation through platelet-dependent and platelet-independent mechanisms. *Arterioscler Thromb Vasc Biol* (2014) **34**:1977–1984. doi:10.1161/ATVBAHA.114.304114

169. Martinez de Lizarrondo S, Gakuba C, Herbig BA, Repesse Y, Ali C, Denis C V, Lenting PJ, Touze E, Diamond SL, Vivien D, et al. Potent Thrombolytic Effect of N-Acetylcysteine on Arterial Thrombi. *Circulation* (2017) **136**:646–660. doi:10.1161/CIRCULATIONAHA.117.027290
170. Anders HJ. Necroptosis in Acute Kidney Injury. *Nephron* (2018) **139**:342–348. doi:10.1159/000489940
171. Mulay SR, Honarpisheh MM, Foresto-Neto O, Shi C, Desai J, Zhao ZB, Marschner JA, Popper B, Buhl EM, Boor P, et al. Mitochondria permeability transition versus necroptosis in oxalate-induced AKI. *J Am Soc Nephrol* (2019) **30**: doi:10.1681/ASN.2018121218
172. Shi C, Kim T, Steiger S, Mulay SR, Klinkhammer BM, Bauerle T, Melica ME, Romagnani P, Mockel D, Baues M, et al. Crystal Clots as Therapeutic Target in Cholesterol Crystal Embolism. *Circ Res* (2020) doi:10.1161/CIRCRESAHA.119.315625
173. Nakazawa D, Desai J, Steiger S, Muller S, Devarapu SK, Mulay SR, Iwakura T, Anders H-J. Activated platelets induce MLKL-driven neutrophil necroptosis and release of neutrophil extracellular traps in venous thrombosis. *Cell death Discov* (2018) **4**:6. doi:10.1038/s41420-018-0073-2
174. Jaynes BJ, Warren BA. Cerebral atheroembolism. An animal model. *Stroke* (1982) **13**:312–318. doi:10.1161/01.str.13.3.312
175. Benjamin EJ, Blaha MJ, Chiuve SE, Cushman M, Das SR, Deo R, de Ferranti SD, Floyd J, Fornage M, Gillespie C, et al. Heart Disease and Stroke Statistics-2017 Update: A Report From the American Heart Association. *Circulation* (2017) **135**:e146–e603. doi:10.1161/CIR.0000000000000485
176. Angiolillo DJ, Capodanno D, Goto S. Platelet thrombin receptor antagonism and atherothrombosis. *Eur Heart J* (2010) **31**:17–28. doi:10.1093/eurheartj/ehp504
177. Larson RJ, Fisher ES. Should aspirin be continued in patients started on warfarin? *J Gen Intern Med* (2004) **19**:879–886. doi:10.1111/j.1525-1497.2004.30419.x
178. Brinkmann V, Reichard U, Goosmann C, Fauler B, Uhlemann Y, Weiss DS, Weinrauch Y, Zychlinsky A. Neutrophil extracellular traps kill bacteria. *Science* (2004) **303**:1532–1535. doi:10.1126/science.1092385

179. Granger V, Faille D, Marani V, Noel B, Gallais Y, Szely N, Flament H, Pallardy M, Chollet-Martin S, de Chaisemartin L. Human blood monocytes are able to form extracellular traps. *J Leukoc Biol* (2017) **102**:775–781. doi:10.1189/jlb.3MA0916-411R
180. Ueki S, Melo RCN, Ghiran I, Spencer LA, Dvorak AM, Weller PF. Eosinophil extracellular DNA trap cell death mediates lytic release of free secretion-competent eosinophil granules in humans. *Blood* (2013) **121**:2074–2083. doi:10.1182/blood-2012-05-432088
181. Mulay SR, Anders H-J. Crystallopathies. *N Engl J Med* (2016) **374**:2465–2476. doi:10.1056/NEJMra1601611
182. Longstaff C, Varju I, Sotonyi P, Szabo L, Krumrey M, Hoell A, Bota A, Varga Z, Komorowicz E, Kolev K. Mechanical stability and fibrinolytic resistance of clots containing fibrin, DNA, and histones. *J Biol Chem* (2013) **288**:6946–6956. doi:10.1074/jbc.M112.404301
183. Kannemeier C, Shibamiya A, Nakazawa F, Trusheim H, Ruppert C, Markart P, Song Y, Tzima E, Kennerknecht E, Niepmann M, et al. Extracellular RNA constitutes a natural procoagulant cofactor in blood coagulation. *Proc Natl Acad Sci* (2007) **104**:6388–6393. doi:10.1073/pnas.0608647104
184. Baccarelli AA, Byun H-M. Platelet mitochondrial DNA methylation: a potential new marker of cardiovascular disease. *Clin Epigenetics* (2015) **7**:44. doi:10.1186/s13148-015-0078-0
185. Boudreau LH, Duchez A-C, Cloutier N, Soulet D, Martin N, Bollinger J, Pare A, Rousseau M, Naika GS, Levesque T, et al. Platelets release mitochondria serving as substrate for bactericidal group IIA-secreted phospholipase A2 to promote inflammation. *Blood* (2014) **124**:2173–2183. doi:10.1182/blood-2014-05-573543
186. Libby P. Molecular and cellular mechanisms of the thrombotic complications of atherosclerosis. *J Lipid Res* (2009) **50 Suppl**:S352-7. doi:10.1194/jlr.R800099-JLR200
187. Chen L, Yang G. Recent advances in circadian rhythms in cardiovascular system. *Front Pharmacol* (2015) **6**:71. doi:10.3389/fphar.2015.00071
188. Feng D, Lazar MA. Clocks, metabolism, and the epigenome. *Mol Cell* (2012) **47**:158–167. doi:10.1016/j.molcel.2012.06.026

189. Scheiermann C, Kunisaki Y, Lucas D, Chow A, Jang J-E, Zhang D, Hashimoto D, Merad M, Frenette PS. Adrenergic nerves govern circadian leukocyte recruitment to tissues. *Immunity* (2012) **37**:290–301. doi:10.1016/j.immuni.2012.05.021
190. Muller JE, Stone PH, Turi ZG, Rutherford JD, Czeisler CA, Parker C, Poole WK, Passamani E, Roberts R, Robertson T. Circadian variation in the frequency of onset of acute myocardial infarction. *N Engl J Med* (1985) **313**:1315–1322. doi:10.1056/NEJM198511213132103
191. Schloss MJ, Horckmans M, Nitz K, Duchene J, Drechsler M, Bidzhekov K, Scheiermann C, Weber C, Soehnlein O, Steffens S. The time-of-day of myocardial infarction onset affects healing through oscillations in cardiac neutrophil recruitment. (2016) **8**:937–948.
192. Adrover JM, Del Fresno C, Crainiciuc G, Cuartero MI, Casanova-Acebes M, Weiss LA, Huerga-Encabo H, Silvestre-Roig C, Rossaint J, Cossío I, et al. A Neutrophil Timer Coordinates Immune Defense and Vascular Protection. *Immunity* (2019) **50**:390-402.e10. doi:10.1016/j.immuni.2019.01.002
193. Yamazaki S, Numano R, Abe M, Hida A, Takahashi R, Ueda M, Block GD, Sakaki Y, Menaker M, Tei H. Resetting central and peripheral circadian oscillators in transgenic rats. *Science* (2000) **288**:682–685. doi:10.1126/science.288.5466.682

7 Abbreviations

AKI	Acute kidney injury	NET	Neutrophil extracellular trap
ATP	Adenosine triphosphate	NF- κ B	Nuclear factor-kappa-light-enhancer of activated β -cells
α SMA	Alpha smooth muscle actin	NLRP	NOD-like receptor protein
BUN	Blood urea nitrogen	Nec-1s	Necrostatin-1s
CCE	Cholesterol crystal embolism	RIPK	Receptor-interactin protein kinase
CC	Cholesterol crystal	PAD4	Peptidylarginine deiminase 4
CKD	Chronic kidney disease	PAS	Periodic acid Schiff
DAMP	Danger associated molecular pattern	PAMP	Pattern associated molecular pattern
DAPI	4',6-diamidino-2-phenylindole	PGE1	Prostaglandin E1
ecDNA	Extracellular DNA	ROS	Reactive oxygen species
GEEnC	Glomerular endothelial cell	TLR	Toll-like receptor
GFR	Glomerular filtration rate	TTC	2,3,5-triphenyltetrazolium chloride
HUVEC	Human Umbilical Vein Endothelial Cell	TNF	Tumor necrosis factor
IL	Interleukin	TUNEL	Terminal Deoxytransferase Uridine Triphosphate Nick End Labeling
IRI	Ischemia-reperfusion injury	vWF	von Willebrand factor
MLKL	Mixed lineage kinase domain-like protein		
MPO	Myeloperoxidase		

8 Acknowledgment

There are many who have helped and inspired me during my doctoral study, I would like to convey my gratitude to all those people.

First and foremost, I take this opportunity to thank my mentor & guide Prof. Hans-Joachim Anders who gave me the opportunity to participate in this project. Thank you for guiding my way with a lot of patience, sharing your knowledge, and advising me with constructive suggestions to proceed through the doctoral program. Thus allowing me to know the incredibly interesting but also frustrating sides of it, waking a deep sense of passion for science, instilling the confidence in me, and your help with the transition to a new professional perspective. I would also like to thank Dr. Shrikant R. Mulay, Dr. Stefanie Steiger, Dr. Takamasa Iwakura, Dr. Julian for their constant encouragement of my research work and constructive suggestions throughout my stay at the research labs of the Renal Division at LMU. I also thank Prof. Paola Romagnani, University of Florence, Italy, and Prof. Peter. Boor, RWTH Aachen University Hospital, Germany for sharing their knowledge and cooperation to complete this thesis.

I would also like to thank my co-workers, Mohsen, Orestes Foresto-Neto, and Jyaysi who kindly taught me not only lab methods but also critical thinking, troubleshooting, and team spirit. To Dan Draganovici and Janina Mandelbaum also many thanks for the preparation of histological sections. I am also indebted to my other colleagues Qiuyue, Yutian, Manga, Tehyung, Lina, and others, thank you for your love and support. Thank you all for giving me the life long memories, all the fun, the friendship, the international dinners, and unconditional support. You wonderful people made my time in Anders's laboratory full of unforgettable memories.

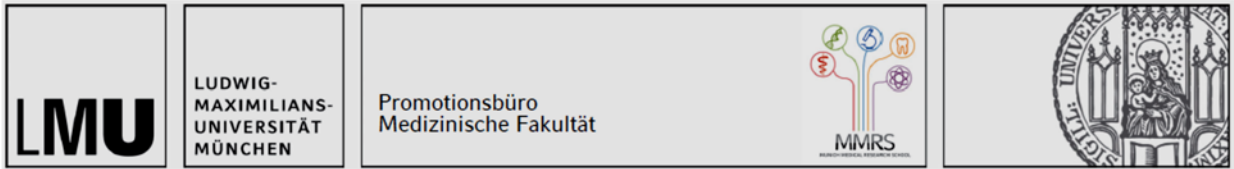
I owe my deepest gratitude to my family for their love, selfless support, and constant encouragement through good and bad times throughout my life.

I am grateful to everybody who has been part of my life and helped in some way or other, but if I failed to mention their names, thank you all.

I must express my immense gratitude to the animals, which have been sacrificed for the betterment of human beings.

Date:

Chongxu Shi



Affidavit

Shi Chongxu
Surname, first name

Munich
Street

Germany
Zip code, town, country

I hereby declare, that the submitted thesis entitled:

**Extracellular DNA contributes to cholesterol crystal embolism-induced
clot formation, acute kidney injury, and tissue infarction**

.....

is my own work. I have only used the sources indicated and have not made unauthorized use of services of a third party. Where the work of others has been quoted or reproduced, the source is always given.

I further declare that the submitted thesis or parts thereof have not been presented as part of an examination degree to any other university.

München, 21. April. 2021
place, date

Chongxu Shi
Signature doctoral candidate